DOCTOR OF PHILOSOPHY

Experimental studies of communications with chaotic semiconductor lasers

Paul, Jonathan Seymour

Award date:
2003

Awarding institution:
University of Wales, Bangor

Experimental studies of communications with chaotic semiconductor lasers

PhD thesis submitted by:

Jonathan Seymour Paul

For the degree of Doctor of Philosophy of

The University of Wales

2003

To dad and in memory of mum

Acknowledgements

I would like to thank the many people who helped me during my PhD studies at Bangor University. To begin with I would like to thank my supervisor, Professor Alan Shore for all his advice and help. I would also thank Dr Min Lee and especially Dr Siva Sivaprakasam for help and advice with laboratory experiments. Much thanks go to Dr Paul Spencer and Dr Paul Rees for giving both advice and guidance.

Last but by no means least I would like to thank Nortel Networks, Harlow, UK for sponsorship and especially my Nortel supervisor, Dr Takis Hadjifotiou for advice regarding experiments and equipment.

Summary

This thesis experimentally investigates issues relevant to the use of semiconductor lasers for optical secure communications systems. The motivation behind this work is in exploiting chaotic dynamics to mask a message, transmit the message to a receiver and recover the message.

The method of chaos generation employed in experimentation is using external-cavity semiconductor lasers. Chaos synchronisation properties, an important consideration for secure chaotic communication systems are studied. A demonstration of message encoding and decoding, and a comparison of different receiver configurations is presented. The advantages on system security of selecting the external-cavity length to increase security is discussed. A demonstration of chaotic wavelength division multiplexing is presented.

Contents

Chapter 1

Introduction

1.0 General Introduction

This chapter provides a general introduction to the thesis together with a brief description of a secure optical communication system based on synchronised chaotic semiconductor lasers. The layout of the thesis is then described with brief introductions to each of the separate investigations performed in the subsequent chapters. This thesis is concerned with experiments using semiconductor lasers in secure chaotic communication systems.

The amount of information transmitted through communication systems is ever increasing. There is growing trend for using, amongst others, internet banking and internet shopping, requiring the transmission of sensitive personal details through a network of increasing complexity designed to have easy access. To this end, public cryptosystems based on software techniques have provided a platform for security. To make transmitted information secure such systems can use a short secret parameter (key) or encode the message directly. Cryptosystems are especially suitable for exchanging secure information over large complex networks. As computational power increases, heightening the potential of security attack on such systems, the key length may be increased and the extra computing power available ensures that the time delay for encrypting the data does not increase significantly. The drawback of public cryptosystems is the requirement of providing means to validate the key used, thus, preventing an eavesdropper from distributing a key to potential users of a network and gaining access to sensitive data.

Improving the security of an encrypted message can be achieved by additional encoding at the physical hardware layer and, in particular, by using chaotic carriers generated by components in the system. This method complements the security implemented at the software level. Ideal components to generate chaotic carriers are semiconductor lasers which can act as transmitters and receivers in optical

communication systems. They are inherently non-linear devices that under various operating conditions exhibit non-linear dynamical behaviour. The underlying concept in such a secure communication system is that two physically separated chaotic lasers can synchronise making available the same chaotic dynamics at both transmitter and receiver. Once synchronised, the chaos at the transmitter laser can be used as a carrier on which the message can be encrypted. Because the same chaos is available at the receiver laser, the message can be decrypted. The key to good message recovery is that the receiver laser synchronises to the chaotic carrier, but not the message. Therefore, by comparing the input to receiver laser (chaotic carrier + message) with its output (chaotic carrier), the message can be decrypted. The quality of the recovered message depends on the chaos synchronisation quality of transmitter and receiver lasers. In practice, similar lasers with close matching parameters and operating conditions are required for good message recovery. The basic ideas behind a chaotic optical communication scheme are shown in figure 1.1

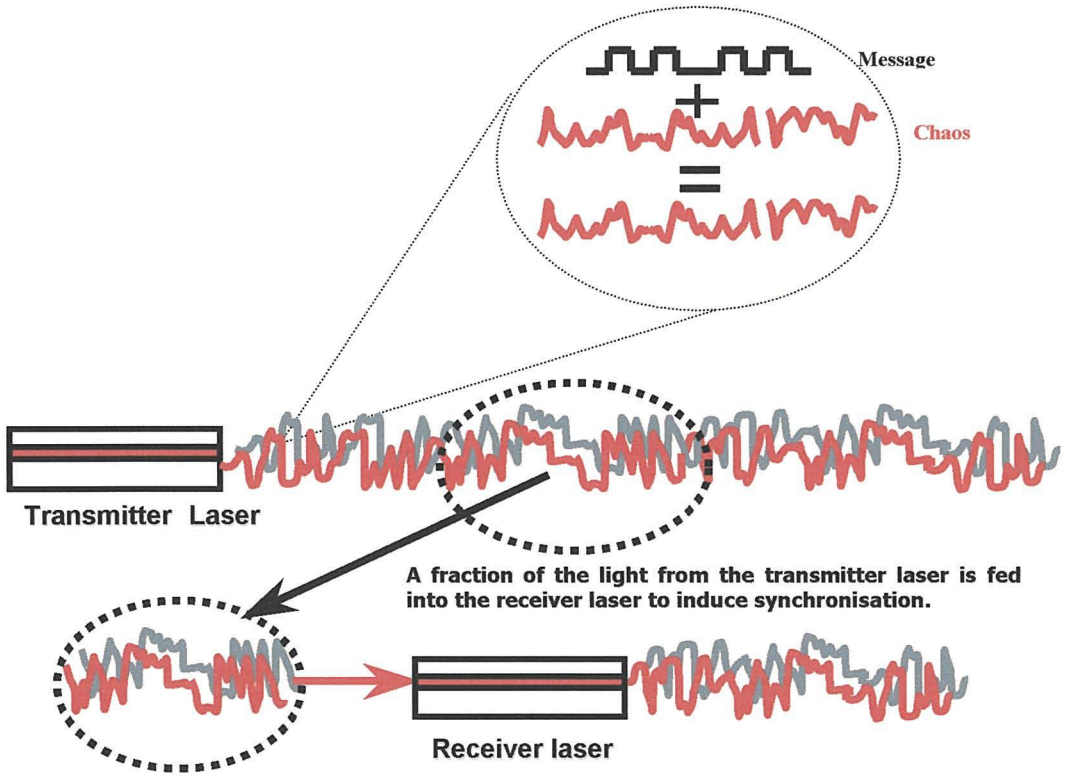

Figure 1.1: *The message is masked by the chaotic transmitter output. A fraction of the transmitter output is coupled to the receiver to induce synchronisation making the same chaos available at the receiver that is produced in the transmitter. Message recovery can be achieved by taking the difference of the receiver input and output*

Early work on chaotic secure communications [1] used an electrical circuit implementation of the Lorenz equations and showed the possibility for using the system as a communication scheme to transmit a small speech signal. The signal was hidden in the fluctuations of the x_T signal of the transmitter circuit. The receiver circuit generated its own synchronised x_R signal and by subtracting x_T-x_R the speech signal could be recovered. The main problem with this approach is that the circuits operate at low frequency and thus message bandwidth is limited to a few kHz. Moreover, as high speed communication networks increasingly utilise optics, a secure chaotic optical communication scheme based on optical chaos is highly desirable.

1.1 Optical communication systems

The portion of the electromagnetic spectrum that is used for non-optical communications (telephone, AM and FM radio, radar and satellite links etc), ranges from about 300 Hz to 90 GHz. The ever increasing demand for high bandwidth data communication led to research into the optical region, 50 nm (ultraviolet) to 100 μm (far infrared), with the visible spectrum being the 400 to 700 nm region. A great interest in communication at these frequencies was created in 1962 with the advent of the laser which made available a coherent optical source. The potential availability of wideband transmission offered by optical communications led to experiments carried out using atmospheric optical channels [2,3]. These experiments showed that tremendous cost would be incurred to develop all the necessary components and that limitations were imposed by rain, fog and snow etc.

Concurrent with the work on atmospheric optical channels were the investigations of optical fibres, providing a much more reliable and versatile optical channel. Initially the large losses, 1000dB/km observed in the best optical fibres made them impractical. Research on materials for optical transmission made dramatic progress reducing losses from 1000 dB/km to 20 dB/km. This, together with advances in lasers and photodetectors led to the first generation commercial optical fibre communication system in the early 1980's.

An optical communication system can be schematically represented by a transmitter semiconductor laser, coupled via optical fibre to a receiver semiconductor laser, as shown in figure 1.2

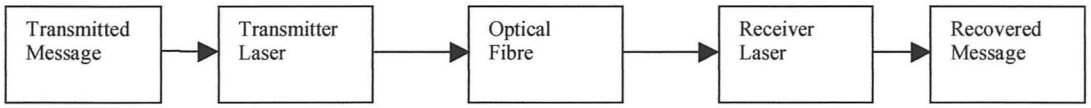

Figure 1.2: *Simple optical fibre communication system*

The desired information is used to modulate the transmitter laser, which may be achieved by modulation of the laser drive current, or by external modulation. The information is transmitted to the receive laser for recovery. In 1989 the development of diode-laser-pumped, ebrium doped fibre amplifiers (EDFA) led to the first long distance fibre transmission communication system. This development was followed in 1990 by the introduction of wavelength division multiplexing (WDM) using four wavelengths in the same fibre [4], thus increasing the bandwidth capability fourfold. The technology gained from WDM led to the development of dense wavelength division multiplexing (DWDM) with ten wavelengths in 1996. Current DWDM systems are capable of incorporating 160 channels over a single fibre. Future developments in laser and fibre technology will inevitably increase the available bandwidth and should offer fast access and high bandwidth data transmission for system users.

A secure chaotic optical communication system based on chaos synchronisation can also be schematically represented by the configuration shown in figure 1.1. However, the generation of the chaotic dynamics in the transmitter and receiver lasers and the decoding of the message requires additional components, thus the systems are of a slightly more complex nature.

1.2 Communicating with synchronised chaotic lasers

The first experimental demonstrations of the synchronisation of two chaotic lasers was performed using Nd: YAG [5] and CO_2 lasers [6-7]. In [5], the lasers were driven into chaos by periodic modulation of their pump beams. The first proposed scheme for encoding data within a chaotic carrier was made by Colet and Roy [8], and the first experimental demonstration of chaotic communication with an optical system (an erbium-doped fiber ring laser) was performed in 1998 by VanWiggeren and Roy [9-10]. In the last decade research from various groups, both theoretical and experimental, has focused on understanding the synchronisation phenomena in unidirectionally coupled lasers, its potential for use in secure communications, and its dependence on various laser parameters [11-15].

Two lasers are coupled unidirectionally if the dynamics of one laser (called the master or the transmitter) influences the dynamics of the other (called the slave or the receiver), and the master laser is isolated from the slave laser, such that the dynamics of the slave does not affect the dynamics of the master.

Mirasso, Colet and García-Fernández [11] were the first to show theoretically that chaotic semiconductor lasers with optical feedback, unidirectionally coupled, can be synchronized and used in encoded communications systems. In their scheme a message was encoded in the chaotic output of the transmitter laser, and it was transmitted to the receiver laser using an optical fiber. The receiver laser was assumed to operate under similar conditions as the transmitter laser. The message could be decoded by comparing the chaotic input and output of the receiver laser.

In 1999 Sivaprakasam and Shore were the first to demonstrate experimentally synchronisation [16] and in 2000 message encoding and decoding [17] using chaotic external-cavity semiconductor lasers. The work on synchronisation [16] identified an optimum coupling strength requirement between transmitter and receiver laser to achieve good quality robust synchronisation. The work on message encoding and decoding [17] transmitted and recovered a 9.5-kHz square wave message. The transmitter and receiver lasers were driven to chaos by external-cavity feedback and coupled together such that they synchronised. The message was added to the chaotic transmitter laser by direct amplitude modulation. Subsequent work on communicating with chaotic external-cavity semiconductor lasers has been directed

towards increasing the message bandwidth and improving the quality of the recovered message [18-20].

1.3 Thesis outline

Chapter 2 presents a description of the operating characteristics of, and chaos generation in, the semiconductor lasers employed in experiments in this thesis. The chapter includes a discussion on the following topics: the effects of external-cavity feedback, operating temperature and drive current on laser threshold current; the laser emission wavelength variations for changes in operational temperature and bias current; the effects optical feedback has on the modal operation and side mode suppression ratio; the transient from laser turn-on to fully developed chaos when the laser is subjected to external-cavity feedback; The regimes of operation of a semiconductor laser are also discussed.

Chapter 3 presents the various characteristics of chaos synchronisation encountered in semiconductor lasers. The chapter explores the following: the coupling strength required to achieve synchronisation; the effects of current, temperature and polarisation detuning on synchronisation quality; how multiple lasers can be configured in series whilst still achieving good synchronisation (cascaded synchronisation); inverse synchronisation, where the receiver laser output follows the transmitter laser output but its amplitude variations are inverted; nullified time of flight synchronisation investigates the phenomena where the receiver laser can synchronise to the transmitter laser without any time delay (the time delay that is normally introduced by the physical separation between the lasers). The work on nullified time of flight is based on publication [21] arising from the present research.

Chapter 4 presents the experimental methods employed to achieve secure chaotic communications. The chapter considers the following: the method employed for message encoding; message extraction at the receiver by chaos removal; message recovery quality comparison for closed-loop receiver (with external-cavity feedback) versus open-loop receiver (stand alone laser). The chapter is based on two publications [19-20] arising from the present research.

Chapter 5 presents the methods employed to enhance the security of the system. The chapter examines: optical modulation of the message (as compared to direct amplitude modulation of the transmitter laser bias current); the effects of external-cavity length on system security and how cavity length selection can enhance message masking; the encoding, transmission and recovery of a small-signal message. The chapter is based on a publication [22] arising from the present research.

Chapter 6 presents the methods employed in a chaotic wavelength division multiplexing scheme. The chapter explores the following aspects: crosstalk between channels; message encoding and decoding through two separate channels; a novel method of message recovery that has the potential to allow expansion of the scheme to incorporate many channels. The chapter is based on [23] arising from the present research.

Chapter 7 provides an overview of the main results of the thesis together with suggestions for future developments of this work.

1.4 References

[1] K. M. Cuomo, A. V. Oppenheim and S. H. Stogatz, "Synchronization of lorenz-based chaotic circuits with applications to communications," IEEE Trans. Circuits Syst. II, vol. **40**, pp. 626-633, 1993

[2] D. W. Berreman, "A lens or light guide using convectively distorted thermal gradients in gases," Bell Sys. Tech. J.,**43**, pp. 1469-1475, 1964

[3] R. Kompfner, "Optical communication," Science, **150**, pp. 149-155, 1965

[4] J. M. Gill, "Lasers: a forty year perspective," IEEE J. Sel. Top. Quant. Elec. **6**, pp. 1111-1115, 2000

[5] R. Roy and K. S. Thornburg, Jr., "Experimental synchronization of chaotic lasers," Phys. Rev. Lett. vol. **72**, pp. 2009-2012, 1994

[6] T. Sugawara, M. Tachikawa, T. Tsukamoto and T. Shimisu, "Observation of synchronization in laser chaos," Phys. Rev. Lett. vol. **72**, pp. 3502-3506, 1994

[7] Y. Liu, P. C. de Oliveira, M. B. Danailov, and J. R. Rios Leite, "Chaotic and periodic passive Q switching in coupled CO2 lasers with a saturable absorber," Phys. Rev. A vol. **50**, pp. 3464-3470, 1994

[8] P. Colet and R. Roy, "Digital communication with synchronized chaotic lasers," Opt. Lett., vol. **19**, pp. 2056-2058, 1994

[9] G.D. VanWiggeren and R. Roy, "Communication with chaotic lasers," Science vol. **279**, pp. 1198-1200, 1998

[10] G.D. VanWiggeren and R. Roy, "Optical communication with chaotic waveforms," Phys. Rev. Lett. vol. **81**, pp. 3547-3550, 1998

[11] C. R. Mirasso, P. Colet, P. Garcia Fernandez, "Synchronization of chaotic semiconductor lasers: Application to encoded communications," IEEE. Photon. Tech. Lett., vol. **8**, pp. 299–301, 1996

[12] V. Annovazzi-Lodi, S. Donati, and A. Scire, "Synchronization of chaotic injected-laser systems and its application to optical cryptography," IEEE J. Quantum Electron. vol. **32**, pp. 953-959, 1996.

[13] S. Sivaprakasam and K. A. Shore, "Signal masking for chaotic optical communication using external-cavity diode lasers," Opt. Lett. vol. **24**, pp. 1200-1202, 1999

[14] Y. Takiguchi, H. Fujino and J. Ohtsubo, "Experimental synchronization of chaotic oscillations in externally injected semiconductor lasers in a low-frequency fluctuations regime," Opt. Lett., **24**, pp. 1570-1572, 1999

[15] S. Sivaprakasam and K.A. Shore, "Message encoding and decoding using chaotic external-cavity diode lasers," IEEE. J. Quantum. Electron., vol. **36**, pp. 35-39, 2000

[16] S. Sivaprakasam and K. A. Shore, "Demonstration of optical synchronization of chaotic external-cavity laser diodes," Opt. Lett. vol. 24, pp. 466-468, 1999

[17] S. Sivaprakasam and K.A. Shore, "Message encoding and decoding using chaotic external-cavity diode lasers," IEEE. J. Quantum. Electron., vol. **36**, pp. 35-39, 2000

[18] I. Fischer, Y. Lui and P. Davis, "Synchronization of chaotic semiconductor laser dynamics on subnanosecond time scales and its potential for chaos communication," Phys. Rev. A, **62**, pp. 011801, 2000

[19] J. Paul, S. Sivaprakasam, P. S. Spencer, P. Rees and K. A. Shore, "GHz bandwidth message transmission using chaotic diode lasers," Elec. Lett., vol. **38**, pp. 28-29, 2001

[20] M. W. Lee, J. Paul, S. Sivaprakasam and K. A. Shore, "Comparison of closed-loop and open-loop feedback schemes of message decoding using chaotic laser diodes," Opt. Lett., vol **28**, 2003

[21] S. Sivaprakasam, J. Paul, P. S. Spencer, P. Rees, K. A. Shore, " Nullified time-of-flight lead-lag in synchronisation of chaotic external-cavity laser diodes," Optics Lett. Vol. **28**, pp. 1397-1399, 2003

[22] J. Paul, S. Sivaprakasam, P. S. Spencer and K. A. Shore, "Optically modulated chaotic communication scheme using external-cavity length as a key to security," J. Opt. Soc. Am. B, **20**, pp. 497-503 (2003)

[23] J. Paul, S. Sivaprakasam and K. A. Shore, "Dual-channel chaotic optical communications using external-cavity semiconductor lasers," accepted for publication to J. Opt. Soc. Am

Chapter 2

Semiconductor laser characteristics and chaos generation

2.0 Introduction

A strong stimulus for studying chaotic dynamics of semiconductor lasers is the opportunity for implementing all-optical secure communication systems that exploit the properties of chaotic dynamical systems. The generation of optical chaos in semiconductor laser systems may be achieved by current modulation, optical injection or optical feedback. Optical feedback is a popular technique and can be achieved by using a mirror that reflects some of the laser output back into the laser cavity. The distance from the laser to the mirror (the external-cavity length), the feedback strength and the feedback phase all affect the dynamics of the chaos produced in the laser.
Optical feedback is important in applications since it is often unavoidable (such as reflections from the surface of a CD, or from the end of an optical fibre). It is also interesting from the nonlinear dynamics point of view since optical feedback renders the laser capable of generating high-dimensional chaos. Following the pioneering work of Lang and Kobayashi [1] there have been, particularly in the last decade, intensive experimental and theoretical investigations of semiconductor lasers with optical feedback [2-6]. In this chapter a discussion is first offered of how external optical feedback affects the operation of laser diodes (threshold bias current and optical spectrum, wavelength emission), and then a description is given of the different dynamic regimes induced by optical feedback.

2.1 Threshold characteristics

The experimental research described in this thesis generally employ up to three single mode Fabry-Perot semiconductor lasers (Access Pacific, Model no. APL-830-40) in various configurations. Figure 2.1 shows schematically the experimental set-up used to determine the light-current characteristics of the lasers. The lasers can be operated

as stand alone lasers (solitary), without any optical feedback from the external-cavity mirror, or with optical feedback.

There are various methods which may be employed to determine the strength of the optical feedback from an external-cavity mirror.

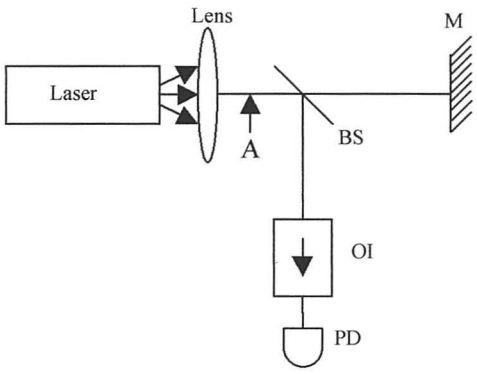

Figure 2.1: *Schematic diagram of experimental set-up to determine the semiconductor laser light-current characteristics. M – mirror, BS – beam splitter, OI optical isolator, PD – photodetector*

These include threshold reduction (the reduction in the laser threshold bias current caused by the external-cavity feedback), percentage feedback (the ratio of laser output power to that of the feedback power given as a percentage), external-cavity reflectivity (the ratio of the laser output power to that of the feedback power) and decibel level (found from the ratio of the laser output power to that of the feedback power).

Various problems are faced in determining an exact value for the optical feedback level. The direction of the feedback path cannot be guaranteed to be exactly perpendicular to the surface of the laser diode, thereby causing optical losses. The laser facet can produce optical losses due to imperfections. Also, the objective lens normally used to collimate the laser beam introduces some loss. For these reasons the optical feedback is given by measuring the return emission power to the laser at point "A" (figure 2.1), and calculating the feedback ratio. An attenuation allowance for the various factors given above is made and a final optical feedback level in dB is determined. Figure 2.2 shows the laser light-current characteristics without optical feedback from the external-cavity mirror M. A ramped laser bias current was applied from 0 to 32.7 mA. The temperature of each laser was stabilised to 22 ^{0}C. The laser

light emission is measured by the photodetector which converts the emission intensity into a voltage.

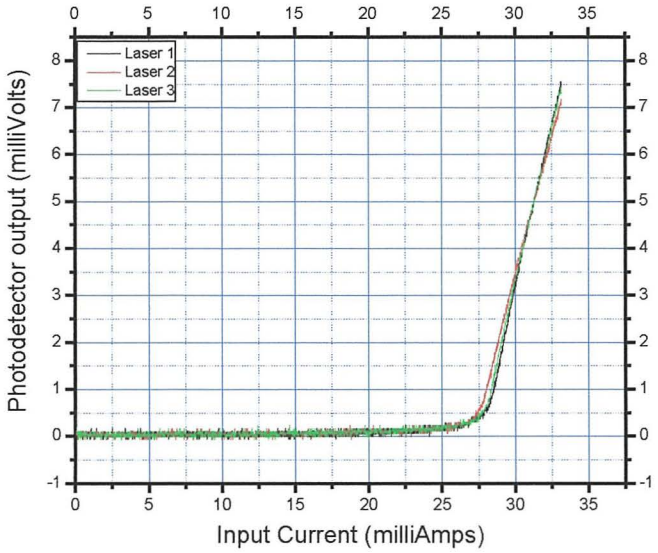

Figure 2.2: *Laser Light-current characteristic without optical feedback*

The threshold values and the light-current curve of the three lasers are very similar. From these curves the threshold currents of the three lasers at 22 ^{0}C are found as, 27.70 mA, 27.03 mA and 27.49 mA, for lasers 1, 2 and 3 respectively. When optical feedback (-25 dB) was applied to the three lasers by means of the external-cavity mirror the threshold bias current reduces considerably.

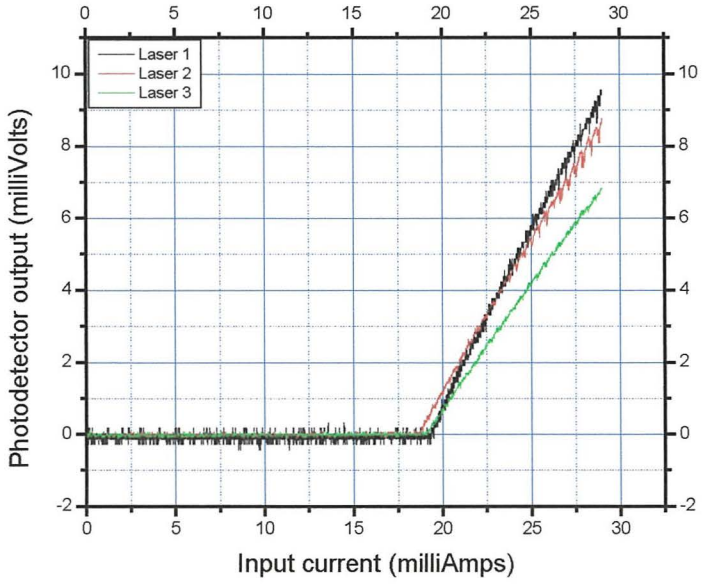

Figure 2.3: *Laser light-current characteristics with optical feedback (-25dB)*

The threshold bias current for the three lasers with optical feedback were found to be 19.09 mA, 18.39 mA and 18.87 mA, for laser1, 2 and 3 respectively.
It can be seen that with optical feedback the light-current curves of the three lasers differ more compared to the case without feedback indicating a sensitivity to optical feedback.

2.2 Wavelength Characteristics

The ability to predict the operational wavelength of semiconductor lasers is of utmost importance when laser chaos synchronisation is required. Figure 2.4 shows schematically the experimental set-up used to determine the wavelength of each laser.

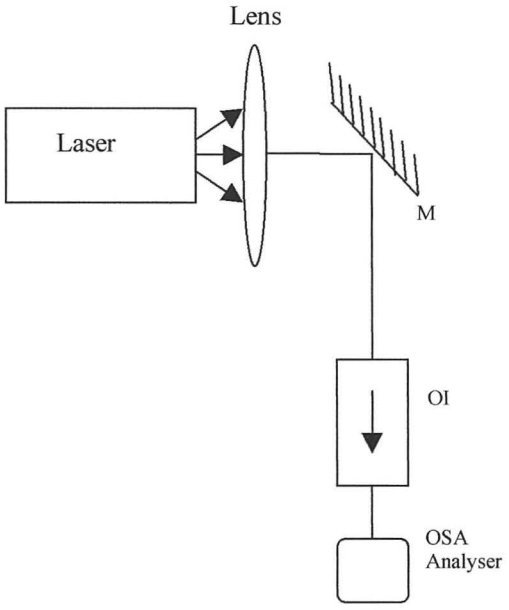

Figure 2.4: *Schematic diagram of experimental set-up to determine the semiconductor laser wavelength characteristics. M - mirror, OI - optical isolator, OSA - optical spectrum analyser*

The temperature of the lasers was varied from 18 ^{0}C to 37 ^{0}C. Recordings were made for the three different bias current levels of 33 mA, 36 mA and 39 mA. Figure 2.5 shows that laser 1 has a stable wavelength of 824 nm from 27 ^{0}C to 36 ^{0}C for current

ranges from 33 mA to 39 mA. Also at higher temperatures the effect of changes in current on the operational wavelength become less significant. Figure 2.6 shows the wavelength characteristics of laser 2.

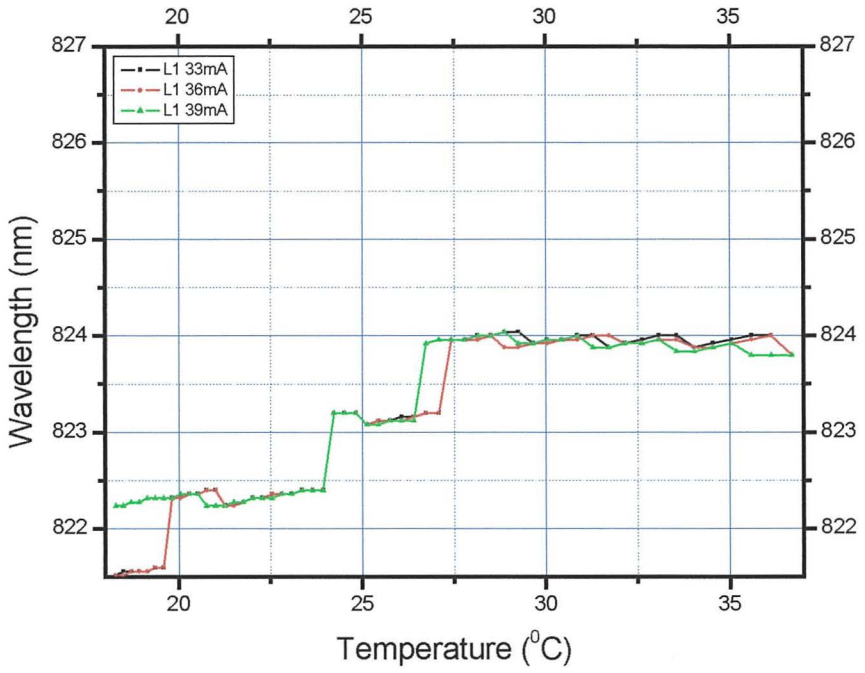

Figure 2.5: *Wavelength characteristics of laser 1*

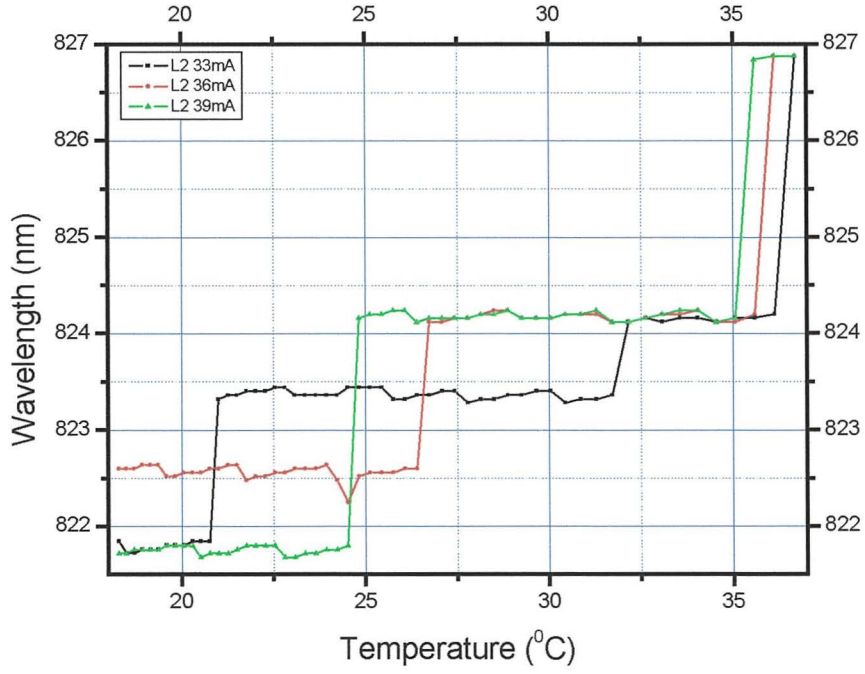

Figure 2.6: *Wavelength characteristics of laser 2*

It can been seen that laser 2 also operates at close to 824 nm from 27 ^{0}C to 35 ^{0}C for bias currents between 33mA and 36mA. Figure 2.7 shows that laser 3 operates close to 824 nm from 27.5 ^{0}C to 32^{0}C for bias current between 33 mA to 36 mA. As will be explained in chapter 3, it is essential that all three lasers have a range of bias current and temperature in which they operate as close to the same wavelength as possible.

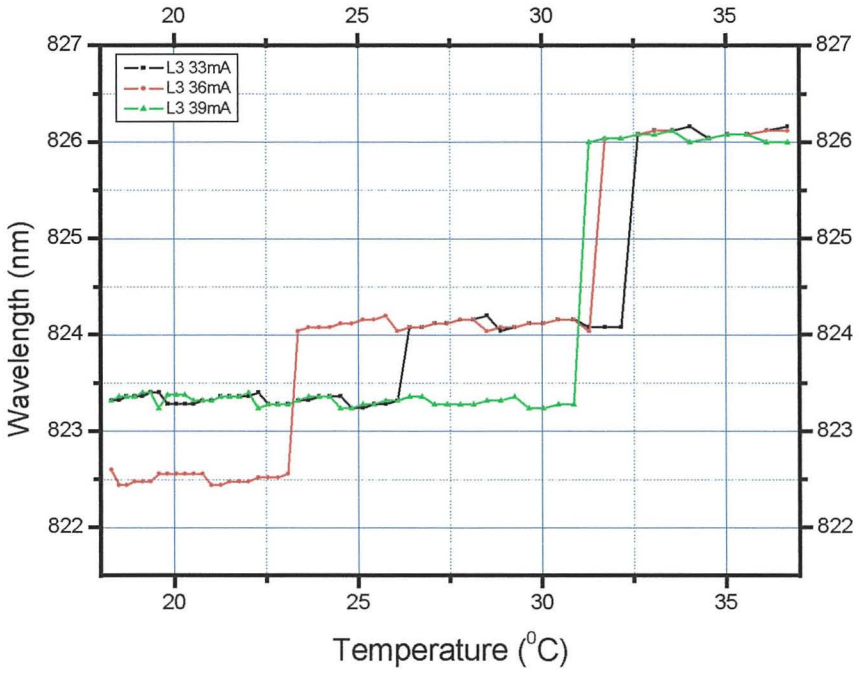

Figure 2.7: *Wavelength characteristics of laser 3*

Figure 2.8 shows that this can best be achieved by operating the lasers close to 824 nm and ensuring the lasers remain close to this wavelength by controlling the operating parameters accordingly. It has thus been shown that is possible to operate the three lasers at very similar wavelengths. It is of benefit to examine how changes in the drive current affect the operating wavelength of the laser being used. The laser was set to three different temperatures, 31.7 ^{0}C, 29.65 ^{0}C and 27.77 ^{0}C. At each of these temperatures the bias current of the laser was varied from 28 to 40 mA in 1 mA steps.

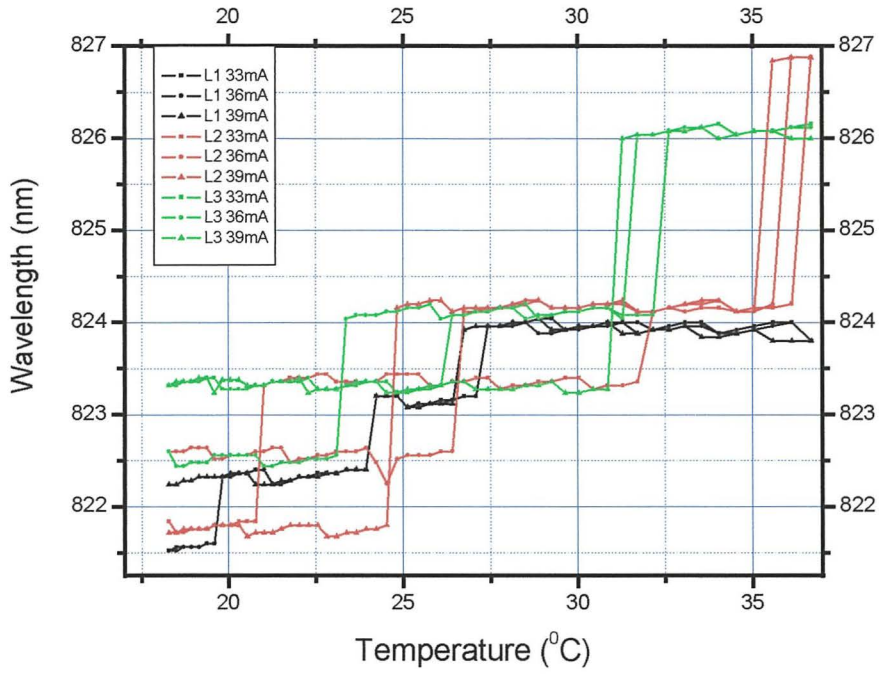

Figure 2.8: *Wavelength characteristics of laser 1, 2 and 3*

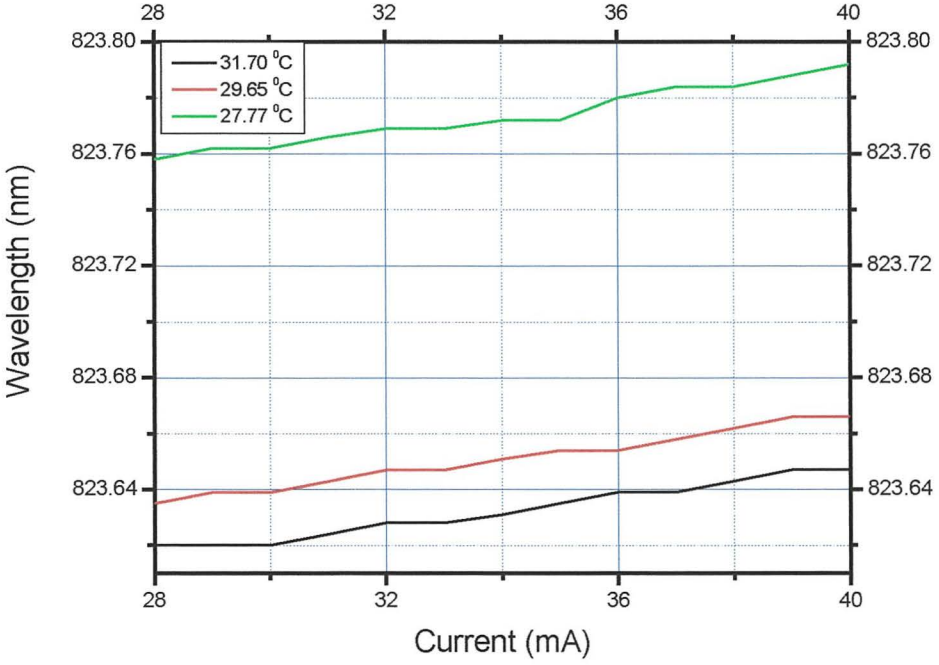

Figure 2.9: *Wavelength characteristics Vs current for temperatures of 31.7 ^{0}C, 29.65 ^{0}C and 27.77 ^{0}C*

As can be seen from figure 2.9, for a current change of 12 mA, the wavelength of the laser at 31.7 ^{0}C changes from 823.758 nm to 823.792. This is equivalent to a

frequency shift of 14.4 GHz. Likewise at 29.65 ^{0}C the laser frequency change is 14 GHz for a current change of 12 mA, and at 27.77 ^{0}C the frequency change is 12 GHz. This is equivalent to a 1GHz frequency shift per mA. In figure 2.8, laser 2 at 39 mA, shows that over a temperature change of 19 ^{0}C, the wavelength of the laser has changed from 822 nm to 827nm. This corresponds to a frequency change of 115 GHz per degree C. The current and temperature range used to gather data for figure 2.8 and figure 2.9 are typical of the operating range that is used in the experimentation. Therefore, to summarize, changes in the operating temperature have a more dramatic affect in the laser wavelength than changes in the bias current. This is because the refractive index of the laser waveguide changes with thermal variations and changes in the laser operating temperature have greater thermal effects on the laser than changes in laser bias current. Therefore, through out all the experiments in this thesis, the temperature of the lasers was strictly controlled (to a precision of 0.01 C).

2.3 Laser modes

Figure 2.10 shows that without feedback the laser operates as single mode with a side mode suppression ratio better than 25 dB. One of the important characteristics of semiconductor lasers is how the lasing mode structure changes with feedback.

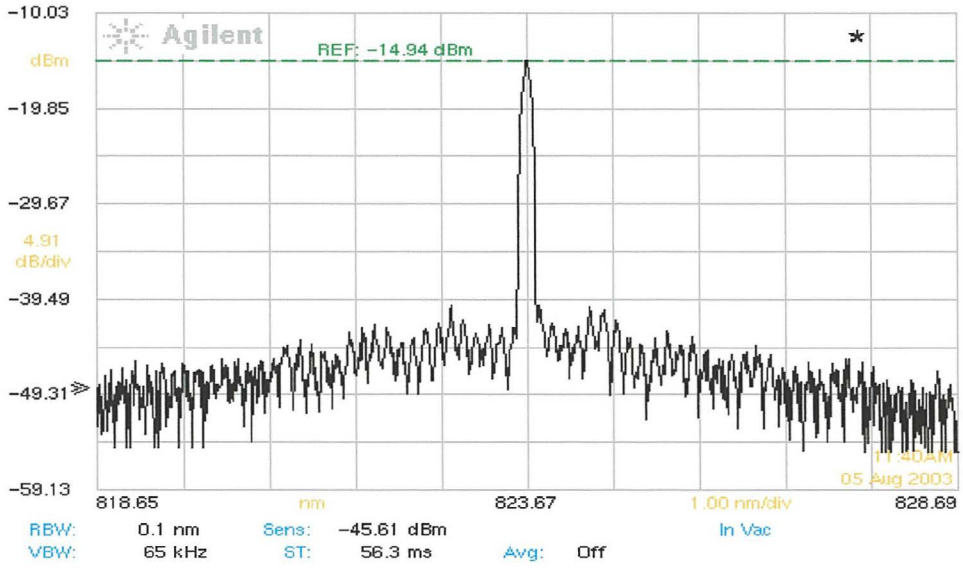

Figure 2.10: *Optical spectrum analyser output for laser operating at 32 mA with no optical feedback*

When optical feedback is introduced to the laser from an external-cavity mirror such that the laser output dynamics are chaotic, the laser is seen to operate on several longitudinal modes. Figure 2.11 shows that the laser is operating with three distinct modes, thus the laser has become multimode with moderate optical feedback (about -25 dB).

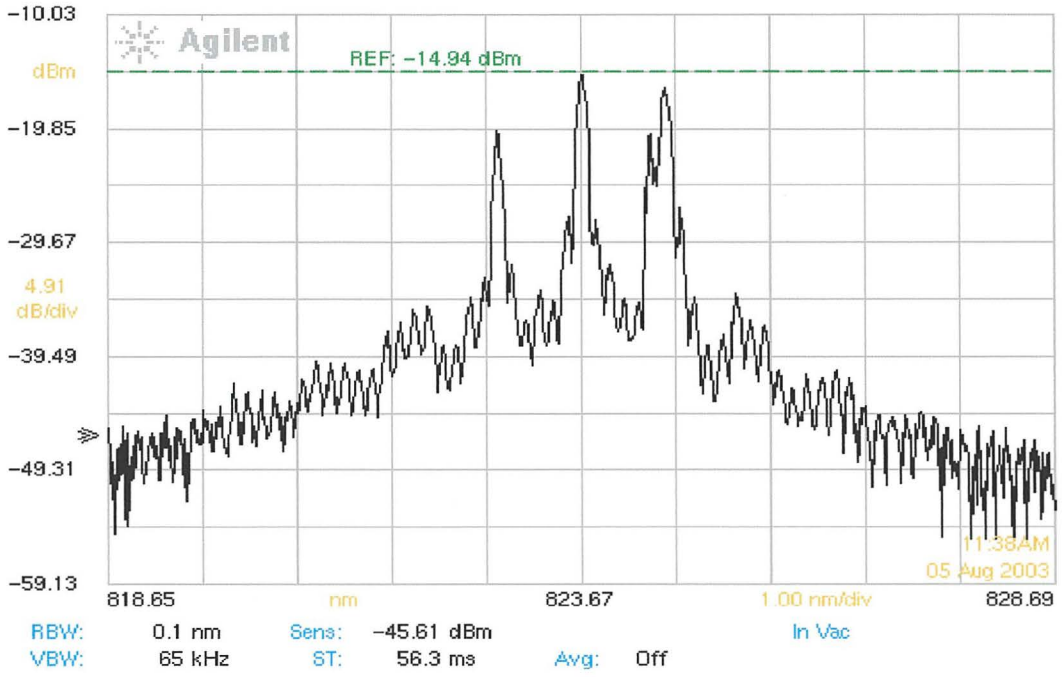

Figure 2.11: *Optical spectrum analyser output for laser operating at 32 mA with –25 dB optical feedback, the external-cavity length is 60 cm*

2.4 Chaos generation

So far, an examination on the effects of temperature and current on the operating wavelengths of semiconductor lasers has been undertaken. When semiconductor lasers are subject to optical feedback their output dynamics often become chaotic. To examine how this occurs, the same experimental set-up as that shown in figure 2.1 was used except that a neutral density filter was added to the feedback path thus enabling the feedback strength to be controlled. The laser temperature is set to 28 ^{0}C

and the drive current to 33 mA. The external-cavity length is set to be 60 cm giving a round trip time of 4 ns.

In this work use has been made of commercially available laser diodes (Access Pacific, Model no. APL-830-40) which have large spontaneous emission noise and therefore a short coherence length. It is estimated that the coherence length of the solitary laser is a few centimetres. Therefore, for the external-cavity length used here, the optical feedback is mostly incoherent. This will be of significance in the different feedback-induced dynamical regimes.

The feedback level of the laser is set to –30 dB. The laser drive current is applied to the laser and a time trace, shown in figure 2.12, of the laser dynamics is taken in a time close to the application of the laser bias current.

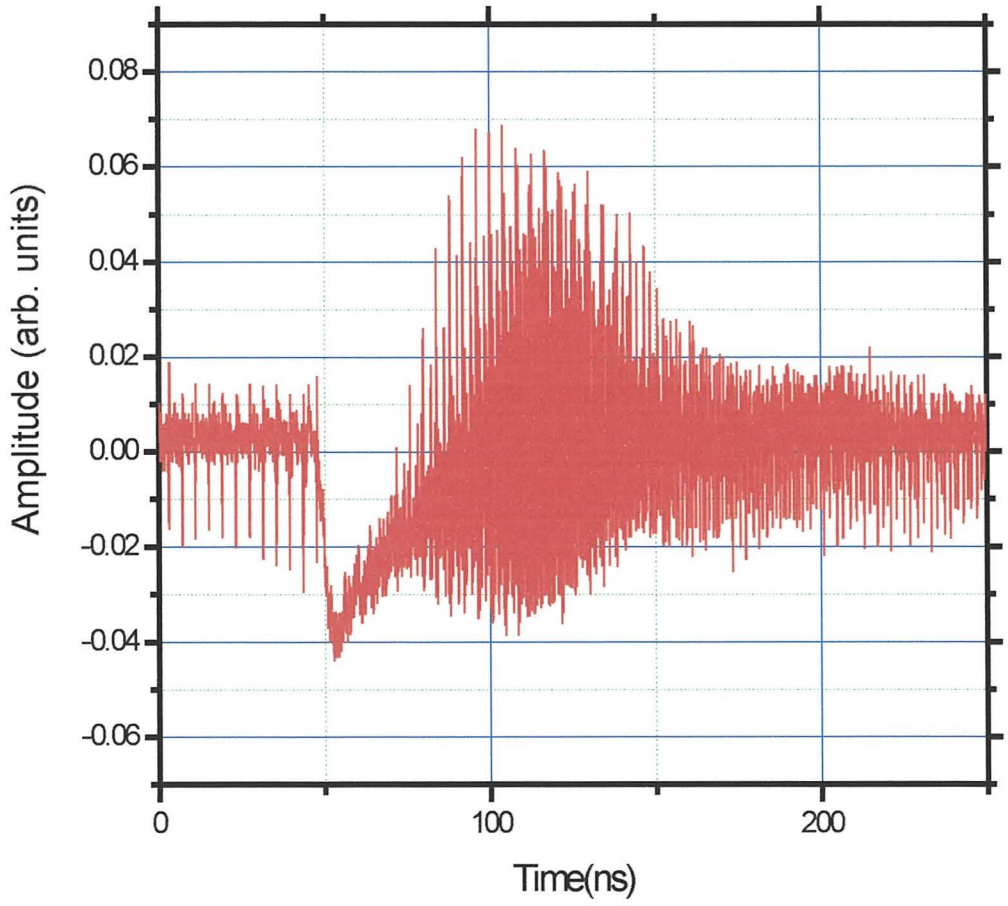

Figure 2.12: *Time trace of laser output for an external-cavity length of 60 cm. The time trace shows the laser output close to bias current application*

In the laser turn-on transient before fully developed chaos is established, a low-frequency fluctuations regime (LFF) is observed. In this regime the laser power drops abruptly, and then recovers gradually only to drop out again after a certain time. Figure 2.12 shows the first intensity dropout, which begins at about 50 ns. Prior to this, the affects of the external-cavity appear as an oscillation, whose period corresponds to the external-cavity length. For more clarity, figure 2.13 shows the output obtained from 0 to 40 ns

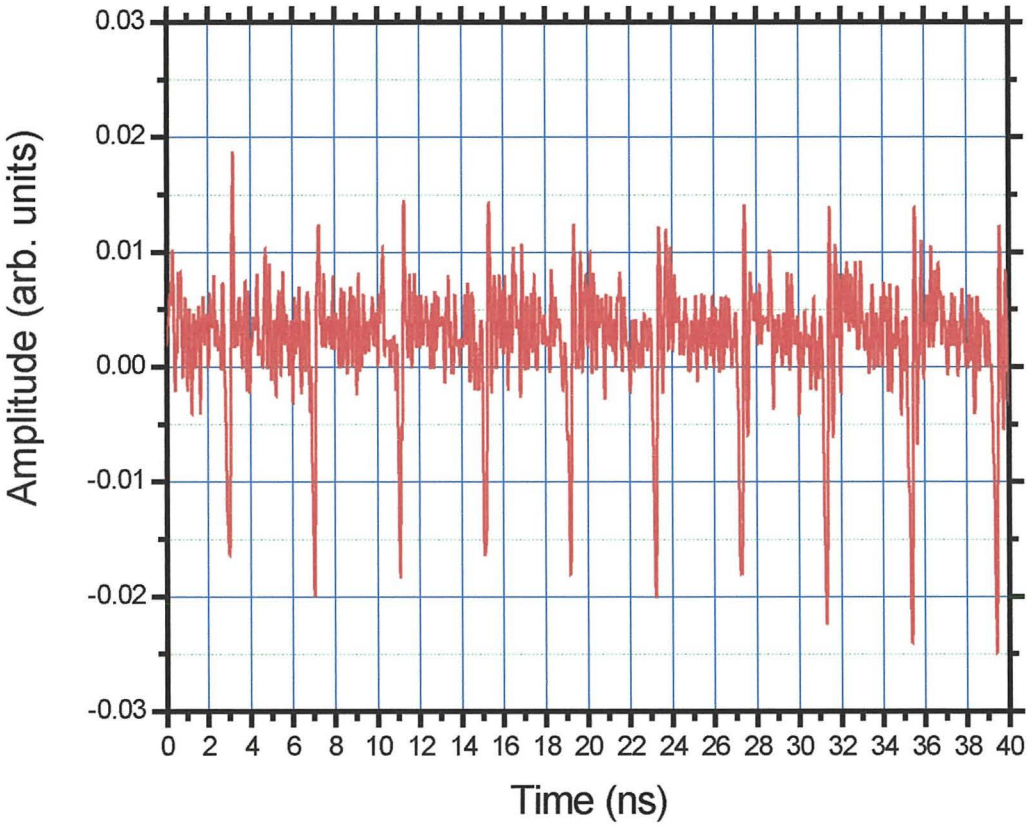

Figure 2.13: *Time trace of laser output for a cavity length of 60 cm. The trace shows the same data as figure 10, but focuses on the early part of the trace from 0 to 40 ns*

In figure 2.13 the periodic amplitude fluctuations that can be seen at approximately 3 ns, 7 ns, 11 ns etc, are caused by the external-cavity. The external-cavity length is 60 cm. Therefore, the return path for external-cavity feedback is 1.2 meters, whose 4 ns round-trip time is equivalent to an external-cavity free spectral range of 250 MHz. As

can be seen from figure 2.13, the period of the oscillation fluctuations is about 4 ns. It can be seen that this effect is caused by the external-cavity and can be altered according to the external-cavity length. In the laser output dynamics a few micro seconds later, it is seen that the laser output dynamics are LFF, as shown in figure 2.14.

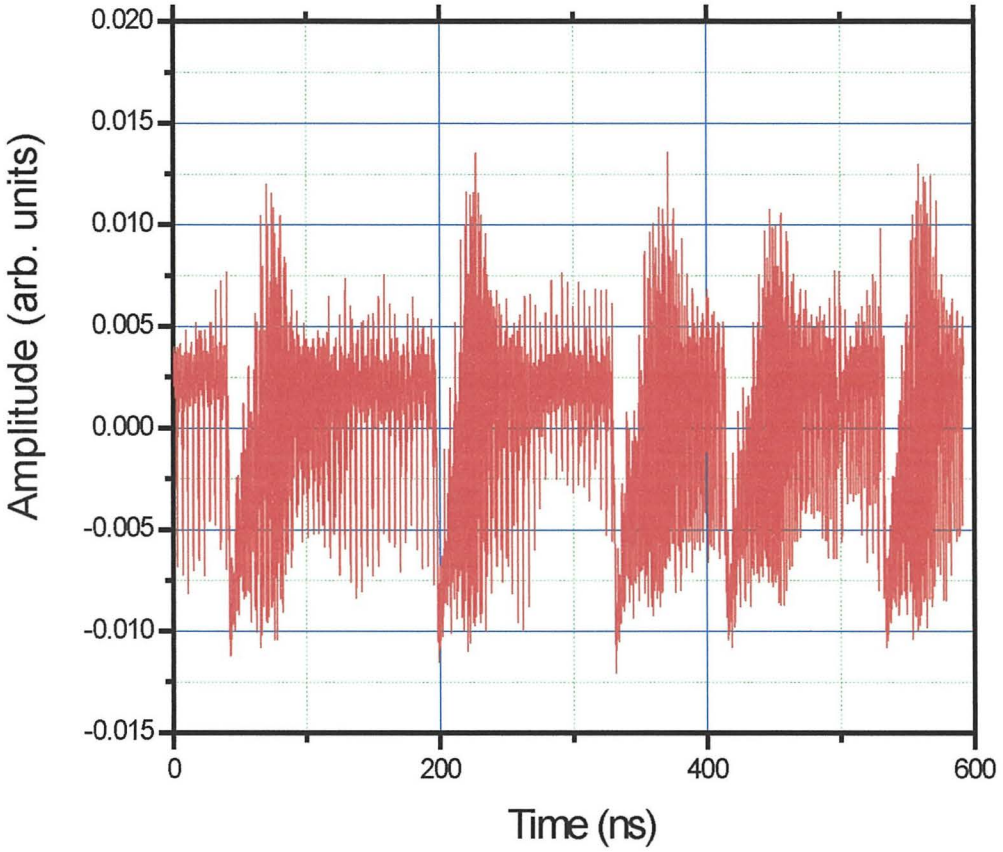

Figure 2.14: *Time trace of laser output for a cavity length of 60cm. The trace shows that the laser dynamics are LFF*

The time between the amplitude drop outs in the LFF is variable. In the FFT of the data collected to produce figure 2.14, it is seen that there is a strong relationship between the LFF and the external-cavity length. As can be seen from figure 2.15, the frequencies present in the power spectrum show that there are peaks at 250 MHz intervals. As expected, this is equal to the free spectral range of the external-cavity.

It can also be seen that there is a peak at low-frequency, which is related to the average time between dropouts.

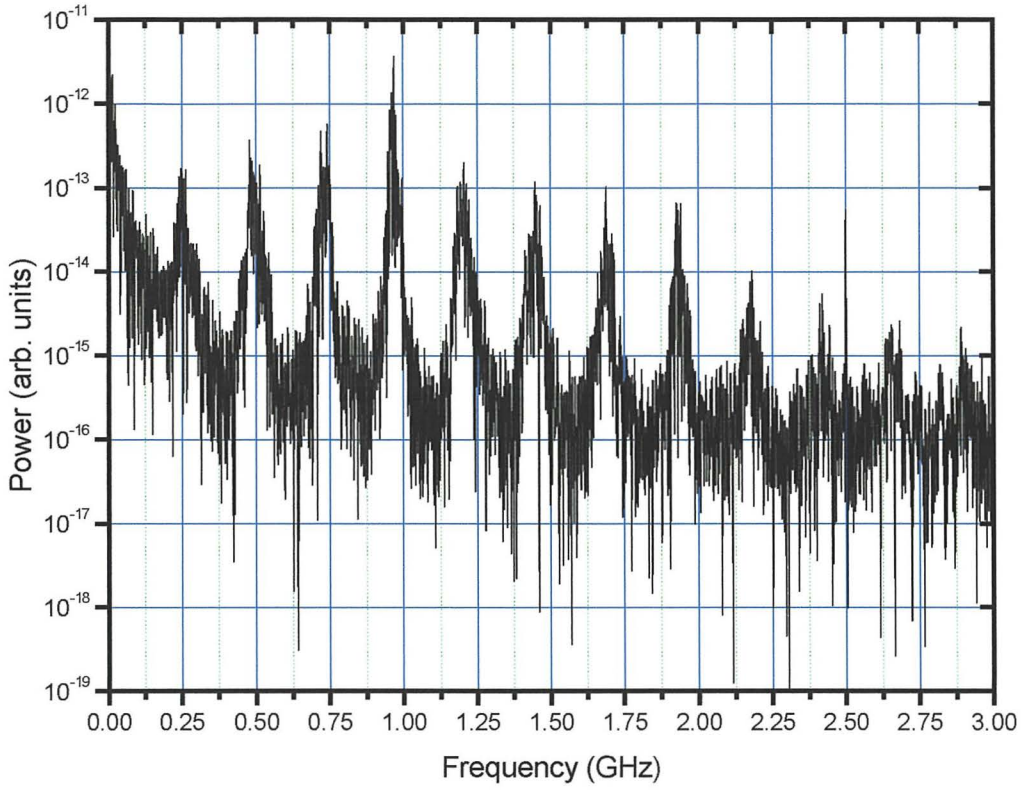

Figure 2.15: *FFT showing the power spectrum of the data used in figure 2.14*

It is well known that the LFF regime occurs for bias currents close to the solitary laser threshold [7,8]. If the injection current is well above threshold, LFF manifest themselves as a transient dynamics prior to fully developed chaos, often referred to as coherence collapse. The laser output dynamics a few micro seconds later than figure 2.14 show the laser has become chaotic and no intensity dropout can be clearly identified, only chaotic oscillations that look noisy are seen, as shown in figure 2.16. Once chaos had been established the laser was seen to behave consistently, the dynamics remaining robust (no obvious deviation in the amplitude or frequency of the laser output was observed over several hours.

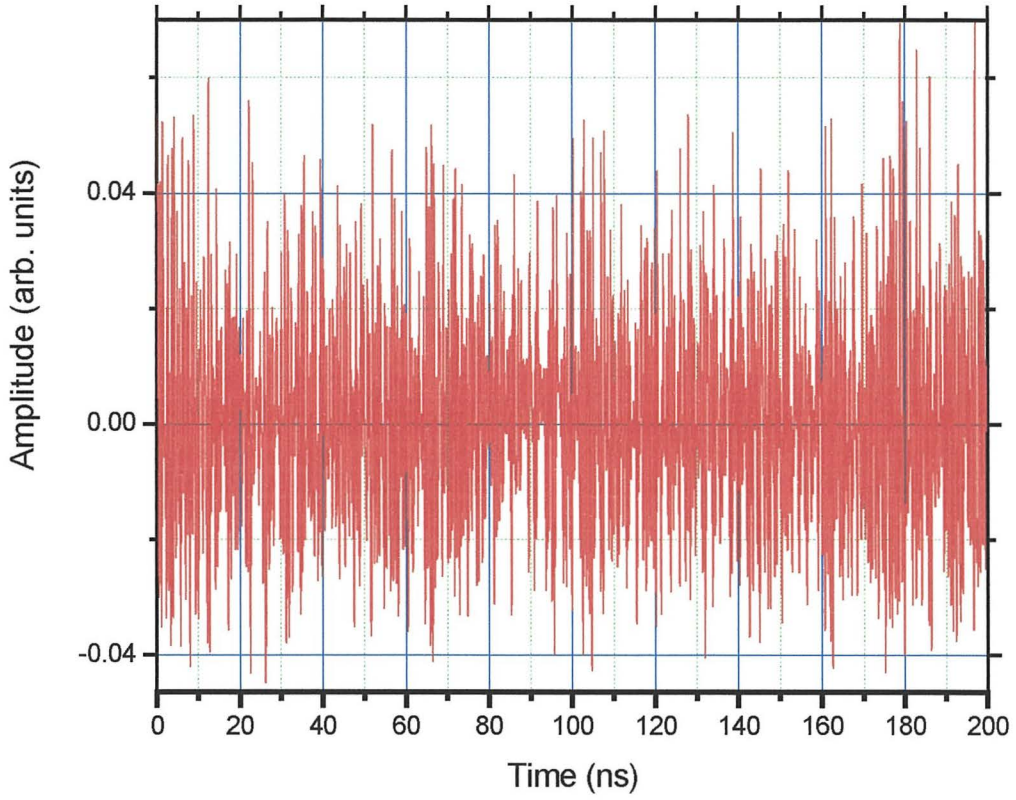

Figure 2.16: *Time trace of laser output for a cavity length of 60cm. The trace shows that the laser dynamics are chaotic*

As shown in figure 2.17, when the laser dynamics is chaotic the laser power spectrum does not exhibit the characteristics that were apparent when the output was LFF. In this case there are very small power increases at the frequencies determined by the free spectral range of the external-cavity. This is unlike figure 2.15 where the external-cavity free spectral range was plain to see. It can be seen that there is a general increase in power towards 1.5 GHz, and then the power of frequencies above this range decreases. Also, the peak at low-frequency (related to the mean time between dropouts) is not present.

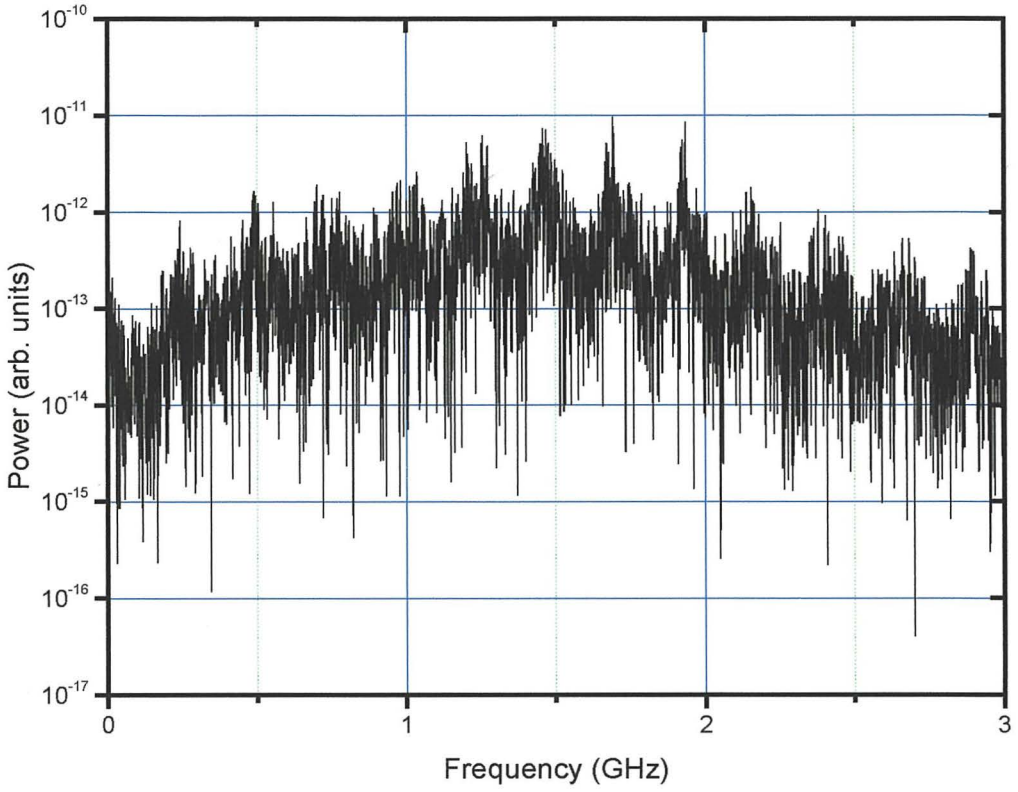

Figure 2.17: *FFT showing the power spectrum of the data used in figure 2.16*

2.5 Regimes of operation

Semiconductor lasers with optical feedback are found to operate in five distinct regimes [9], the regime of operation depending on the operational parameters of the laser. The laser can change its regime of operation with varying optical feedback strength.

Regime I at the lowest levels of feedback is identified by narrowing or broadening of the laser emission linewidth.

Regime II occurs as the feedback level increases and is identified by laser wavelength mode hopping.

Regime III is entered as the laser feedback level increase and is identified by the mode hopping being suppressed and the linewidth narrows.

Regime IV is seen when the feedback level reaches a value which causes the laser linewidth to broaden significantly and is termed coherence collapse [10].

Regime V is entered as the feedback reaches a level where the laser operates with a narrow linewidth.

To identify these regimes of operation in the lasers employed in the experiments use was made of the following set-up shown in figure 2.18.

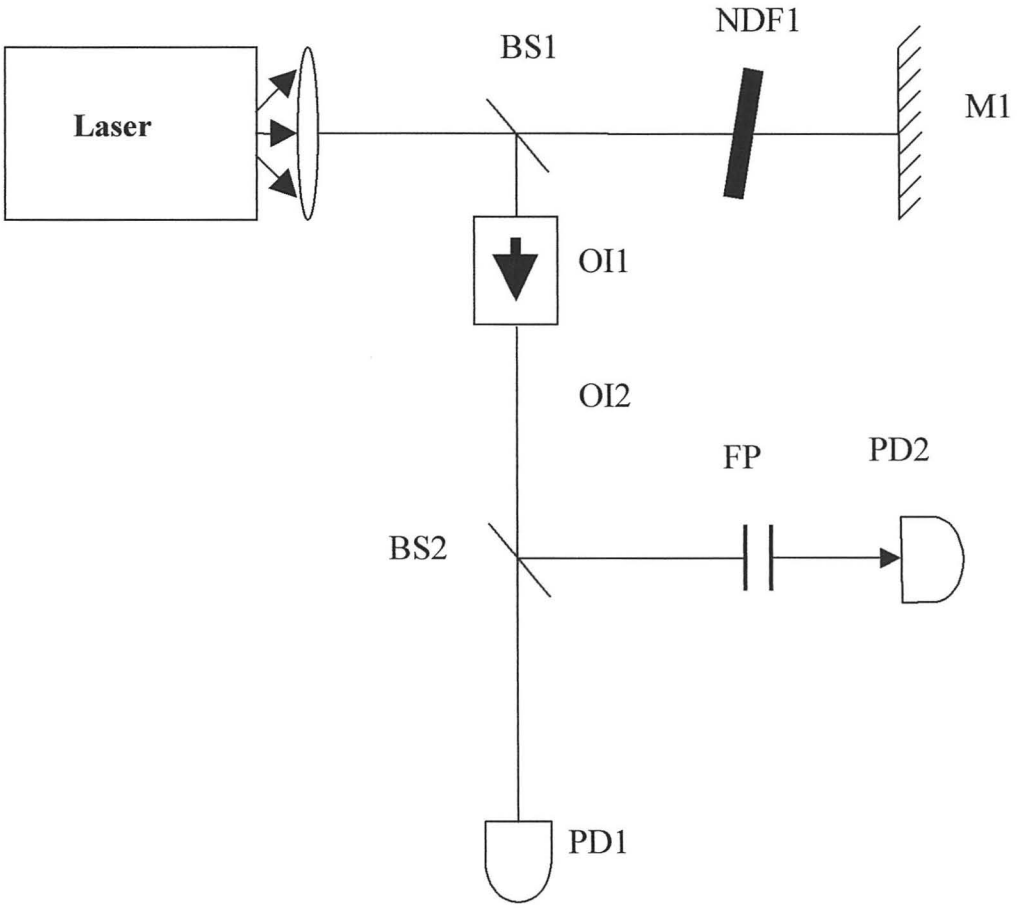

Figure 2.18: *Schematic diagram of experimental set-up to determine the regime of operation characteristics M1, mirror; OI, optical isolator; BS1 and BS2, beam splitters; NDF, neutral density filter; PD1 and PD2, photodetectors; FP, Fabry Perot Interferometer*

The laser operating current and temperature are 31.00 mA and 25.2 ^{0}C. Optical feedback to the laser is provided by mirror M1 with the strength of feedback being controlled by the neutral density filter (NDF). Beam splitter BS1 couples part of the

laser output via BS2 to photodetector PD1. BS2 couples part of the laser output to the Fabry Perot Interferometer (FP interferometer). The output from photodetector 1 is stored in a digital oscilloscope. The output from the Fabry Perot interferometer is coupled to photodetector 2 and is then stored in a digital oscilloscope. The external-cavity length is set to be 81cm. The NDF is altered in small increments to change the feedback level from –60 dB to –4 dB.

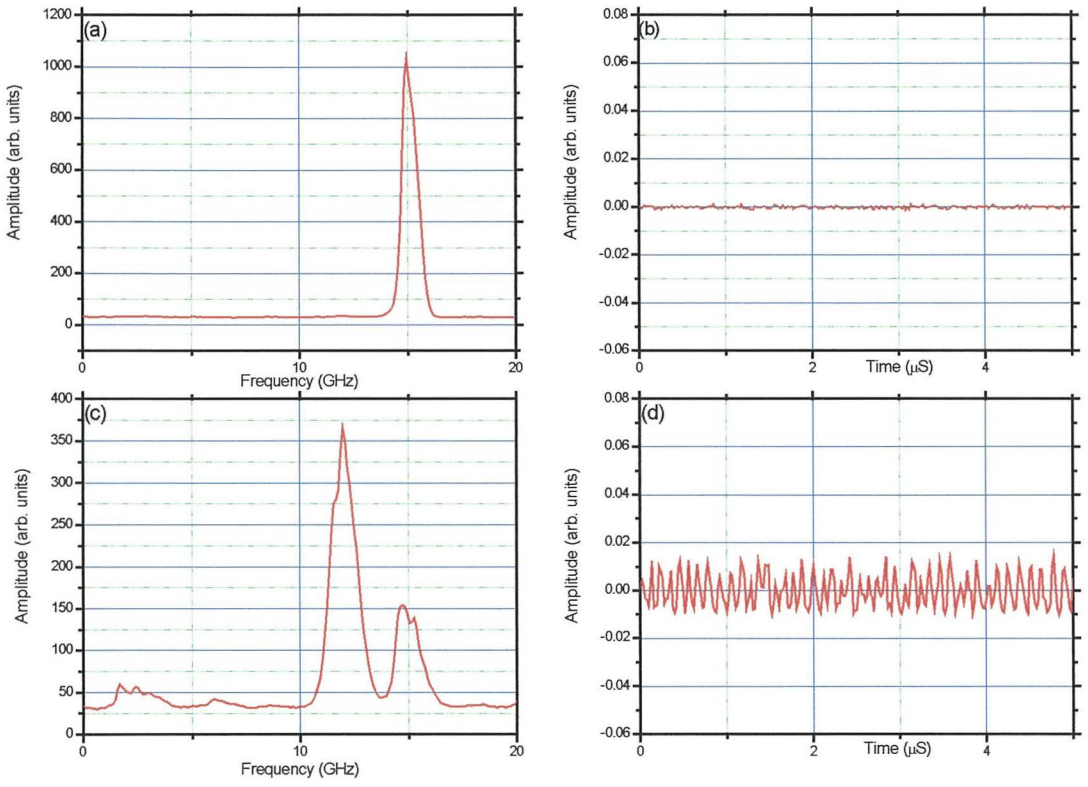

Figure 2.19: *Fabre Perot interferometer plots and time traces showing the laser with (a) and (b) no feedback, (c) and (d) – 40.46 dB*

As can be seen from figure 2.19 (a), with no feedback the laser has a narrow line width. The FP interferometer is set up for a free spectral range of 20 GHz such that linewidth broadening may be observed. However, the linewidth that can be seen from figure 2.19 (a) does not correspond to the 200 MHz that was quoted from the manufacturer on purchase. This is, however, expected as a 20 GHz FP interferometer free spectral range setting restricts the operational finesse of device. The time trace

shown in figure 2.19 (b) reveals that without feedback the laser intensity output is nearly constant. The FP interferometer output remained nearly constant for feedback level from zero to - 40.4 dB. When the feedback level reached - 40.46 dB the FP interferometer output showed that the laser started to mode hope, as can be seen from figure 2.19 (c). Figure 2.19 (d) shows that laser output intensity starts to fluctuate at this feedback level.

The feedback level was then increased and observation were made of any change in the FP interferometer output. Figure 2.20 shows the next change that was observed.

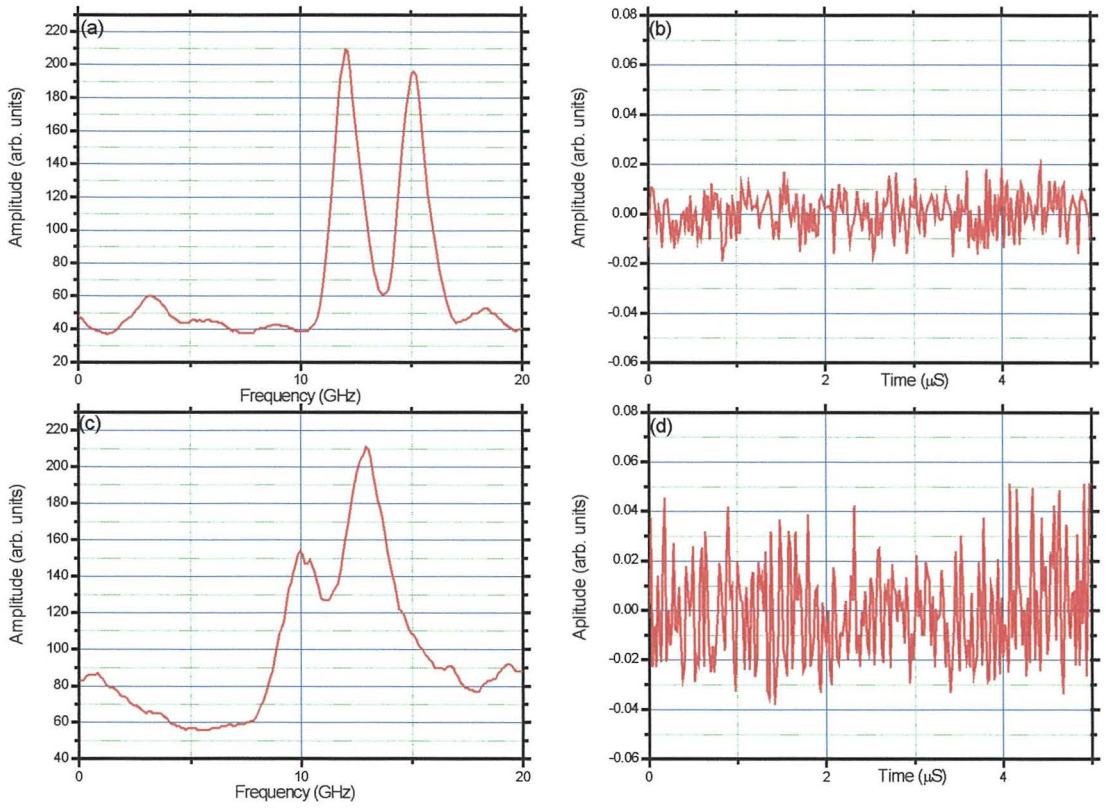

Figure 2.20: *Fabre Perot interferometer plots and time traces showing the laser with (a) and (b) – 33.6 dB feedback and (c) and (d) – 33.67 dB feedback*

The laser remained in the mode hopping regime for a feedback level of between - 40.46 dB and – 33.6 dB. Figure 2.20 (a) shows the FP interferometer output for a feed back level of - 33.6 dB with its associated time trace. As can be seen, the laser is

still operating in the mode hopping regime and the dynamics of the laser output intensity exhibits small fluctuations. As the feedback level was increased to – 33.67 dB the laser was seen to go through coherence collapse as shown in figure 2.20 (c). The laser linewidth increases dramatically and its associated time trace figure 2.20 (d) shows large intensity fluctuations. The regime of operation that is associated with coherence collapse is regime IV. As the external-cavity feedback is expected to be incoherent (small coherence length of the laser relative to the external-cavity length), it is not expected that regime III, requiring a coherent interaction between the field in the laser cavity and the field returning from the external-cavity mirror, would be entered. Therefore the laser has jumped from regime II to regime IV.

The laser feedback was now increased from – 33.67 dB to – 11.24 dB and any changes in the FP interferometer output were observed.

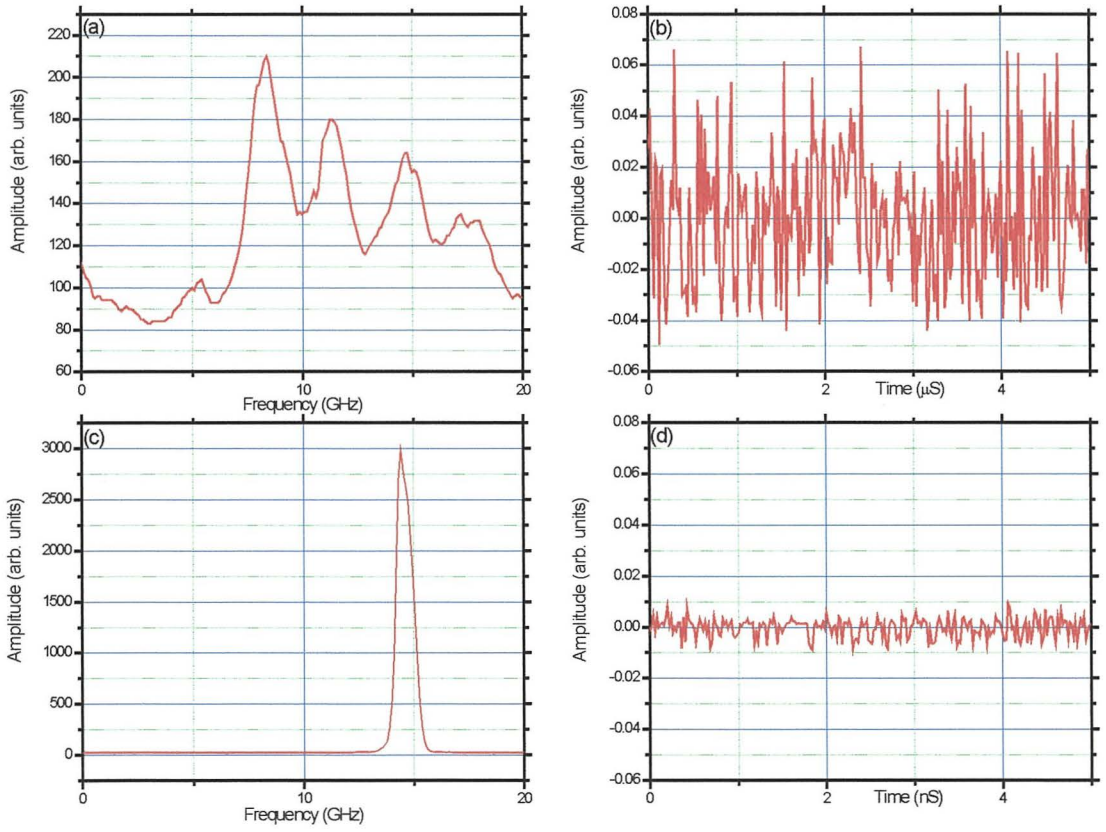

Figure 2.21: *Fabre Perot interferometer plots and time traces showing the laser with (a) and (b) –33.67 dB feedback and (c) and (d) – 11.24 dB feedback*

Figure 2.21 (a) shows that the laser is operating in regime IV and then enters regime V, figure 2.21 (c), as the feedback level reaches – 11.24 dB. Figure 2.21 (b) and (d) show that as the laser enters regime V the intensity fluctuations of the laser start to get suppressed. Figure 2.22 include the results from the above experiment showing the power levels at which transitions between regimes occur.

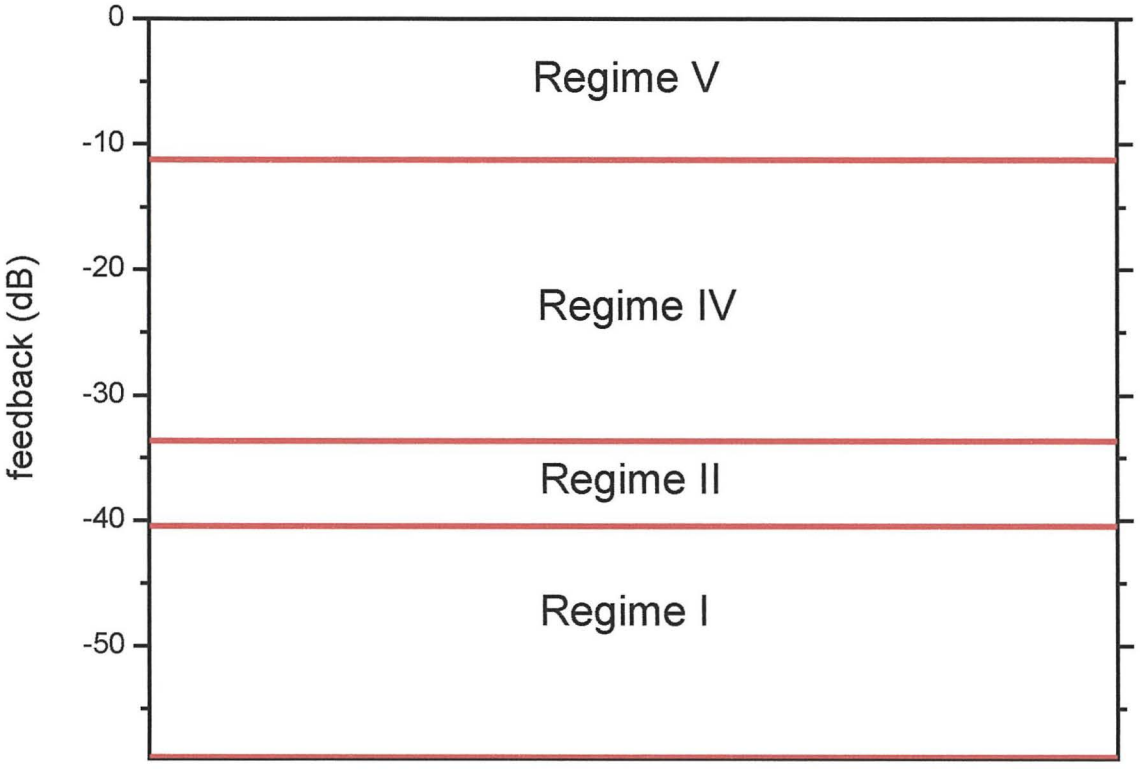

Figure 2.22: *Power levels at which transitions between regimes occur for an external-cavity length of 81 cm.*

Figure 2.22 gives a guide to the level of feedback that is required to enter into regime IV, but there maybe some variation since the transition is not smooth. If figure 2.19 (a) and figure 2.21 (a) are compared, it can be seen that the laser linewidth has increased by a factor of 15. The linewidth of the lasers used (without feedback, quoted by the manufactures) is 200 MHz. Therefore, in regime IV, it is observed that a dramatic increase of linewidth from few hundred MHz to a few GHz. There have been many studies on semiconductor lasers with optical feedback [9-10] that refer to

this increase as coherence collapse, i.e., the laser enters regime IV, and its dynamics becomes chaotic. As the dynamics become chaotic it is expected that new frequencies appear in the power spectrum of the laser, and this broadening gives the opportunity of hiding a message in the chaotic output of the laser, as will be discussed in chapter 4.

2.6 Conclusion

It has been shown that optical feedback modifies the threshold and wavelength of semiconductor lasers and induces a variety of different dynamic regimes. The feedback effects depend on the external-cavity length and feedback strength (the feedback is incoherent and thus no phase influence is expected). It has been shown that optical feedback can induce multimode behaviour in otherwise single mode lasers. Also, it was shown that the three lasers can operate at the same wavelength with similar threshold characteristics both with and without optical feedback and can be rendered chaotic with external-cavity optical feedback. The transient low-frequency-fluctuations turn-on dynamics to fully developed chaos (coherence collapse) was described in terms of the time-trace of the intensity fluctuations, and in terms of the time-resolved FFT power spectrum. The different dynamic regimes induced by optical feedback were characterised: Regime I occurs at the lowest feedback level and was characterised by a broadening of the laser emission linewidth. Regime II occurs at a larger feedback level and was identified by wavelength mode hopping. Regime III was not observed due to the fact that the feedback is mostly incoherent. Regime IV occurs for moderate feedback levels and was identified by a significant increase of the laser linewidth. Regime V was identified as single-mode narrow linewidth emission for strong feedback.

In the next chapter a study of the synchronisation of pairs of chaotic lasers is described. This includes some of the many types of synchronisation that the lasers can be made to exhibit.

2.7 References

[1] R. Lang and K. Kobayashi, "External optical feedback effects on semiconductor injection laser properties," IEEE, JQE. Vol. **16**, pp. 347-355, 1980

[2] J. Mork, B. Tromborg and J. Mark, "Chaos in Semiconductor lsaers with optical feedback: Theory and experiment," IEEE, JQE, Vol. **28,** pp. 93-108, 1992

[3] G. H. Van Tartwijk, A. M. Levine and D. Lenstra, "Sisyphus effects in semiconductor lasers with optical feedback," IEEE, J. Sel. Topics Quantum Electronin. Vol. **1** pp. 466-472, 1995

[4] V. Ahlers, U. Parlitz and W. Lauterborn, "Hyperchaotic dynamics and synchronisation of external-cavity semiconductor lasers," Phys. Rev. E, Vol. **58**, pp. 7208-7213, 1998

[5] D. W. Sukow, T. Heil, I. Fischer, A. Gavrielides, A. Hohl-Abichedid and W. Elsäβer, "Picosecond intensity statistics of semiconductor lasers operating in the low frequency fluctuation regime," Phys. Rev. E, Vol. **60**, pp. 667-673, 1999

[6] A. Uchida, Y. Liu, I. Fischer, P. Davis and T. Aida, "Chaotic antiphase dynamics and synchronisation in multimode semiconductor lasers," Phys. Rev. E, Vol. **64**, pp 23801-1-6, 2001

[7] G. H. M. Van Tartwijk and D. Lenstra, "Semiconductor lasers with optical injection and feedback," Quantum Semiclassical Optics, **7**, pp. 87-143, 1995

[8] G. H. M. Van Tartwijk and G.P. Agrawal, "laser instabilities: a modern perspective," prog. Quant electron, **22**, 43- 122, 1998

[9] R. W. Tkach and A. R. Chraplyvy, "Regimes of feedback effects in 1.5 μM distributed feedback lasers," Jour. Light. Tech., Vol. **LT4**, pp. 1655-1661, 1986

[10] D. Lenstra, B. H. Verbeek and A. J. Den Boef, "Coherence collapse in single mode semiconductor lasers due to optical feedback," IEEE J Quant. Elect., Vol. QE **21**, pp. 674-679, 1985

Chapter 3

Chaos Synchronisation

3.0 Introduction

Having described in the previous chapter the method of chaos generation employed in experimentation it is now desirable to explore the characteristics of chaos synchronisation that are observed in semiconductor laser diodes. The purpose of the present chapter is to introduce chaos synchronisation encountered in many different fields of study and the techniques used to test for the presence of synchronisation and the quality of synchronisation present.

In section 3.1 of this chapter a short outline of synchronisation of chaotic systems is given. Section 3.2 gives a brief description of chaos synchronisation of semiconductor lasers. Section 3.3 gives an experimental demonstration of the effects of coupling strength changes between transmitter and receiver lasers in a semiconductor unidirectional coupled system. The effects of temperature and current detuning on synchronisation quality is studied in section 3.4. More complex synchronisation starting with cascade synchronisation is examined in section 3.5. Section 3.6 deals with the characteristics of inverse synchronisation where the intensity of the receiver follows the transmitter but is inverted. The phenomenon of the receiver anticipating the dynamics of the transmitter is the subject of section 3.7. This allows the system being synchronised to have a nullified time-of-flight (the time delay in the system introduced by the physical distance between the transmitter and receiver lasers is nullified). Finally, conclusions drawn from the research carried out on synchronisation are given in section 3.8.

3.1 Synchronisation of chaotic systems

The synchronisation of chaotic systems is an area of study that is found in many research fields including, amongst others, biology, chemistry, physics, mathematics

and has been an area of particular interest in recent years, particularly in the area of chaotic secure communications. Synchronisation can take place in systems that are unidirectional or mutually coupled and can exhibit in-phase characteristics or inverted (inverse synchronisation). Chaos synchronisation can take place in a number of different ways and can be described as complete synchronisation, frequency synchronisation, phase synchronisation, lag synchronisation, anticipation synchronisation and generalised synchronisation. Synchronisation of chaotic systems can take place by the systems having a common motion in their properties due to coupling. Therefore, methods have been devised to determine the extent or quality of the synchronisation achieved.

Research in chaos synchronisation [1-3] and its application towards communication [4,5] advanced greatly in 1996. Mirasso, Colet and Garcia-Fernadez presented a theoretical model that showed that message encoding and decoding is possible if two chaotic semiconductor diode lasers are synchronised. The theory indicated that this could be achieved by introducing a small part of the output from one laser and injecting into the other [4]. Thus it was predicted that a message can be encoded into the chaotic carrier, transmitted to the receiver and decoded.

The first experimental demonstration of synchronisation of chaotic semiconductor lasers was achieved by Sivaprakasam and Shore in 1999 [6]. This demonstration used external-cavity semiconductor laser and demonstrated that an optimum coupling strength between transmitter and receiver lasers can lead to robust synchronisation.

3.2 Synchronisation of semiconductor lasers

Figure 3.1 shows the experimental arrangement used for synchronisation measurements. The experiment uses two single-mode Fabry-Perot lasers emitting at 825 nm, with a line width of 200 MHz (Access Pacific, Model no. APL-830-40). The side mode suppression ratio is -30dB. These lasers are driven by ultra low noise current sources (ILX-Lightwave, LDX-3620, noise level: $2pA/Hz^{1/2}$) and temperature controlled using thermo-electric controllers (ILXLightwave-LDT-5412) to a precision of 0.01 K. The laser output is collimated using antireflection-coated laser-diode objectives (NewPort-FLA17). The transmitter and receiver lasers are subject to

optical feedback from external mirrors, the feedback strength being controlled by continuously variable neutral-density filters. The cavity length is 60 cm in both cases. The optical isolators (OFR-IO-5-NIR-HP) ensure that the lasers are free from back reflection, the typical isolation is –41dB per isolator. Isolator IO1 and IO2 ensure that the transmitter is isolated from the receiver. The plane of polarisation of the laser is parallel to the plane of table. Each isolator introduces a change in the plane of polarisation by 45^0. A half wave plate (HWP) corrects this polarisation change introduced by IO1 and IO2.

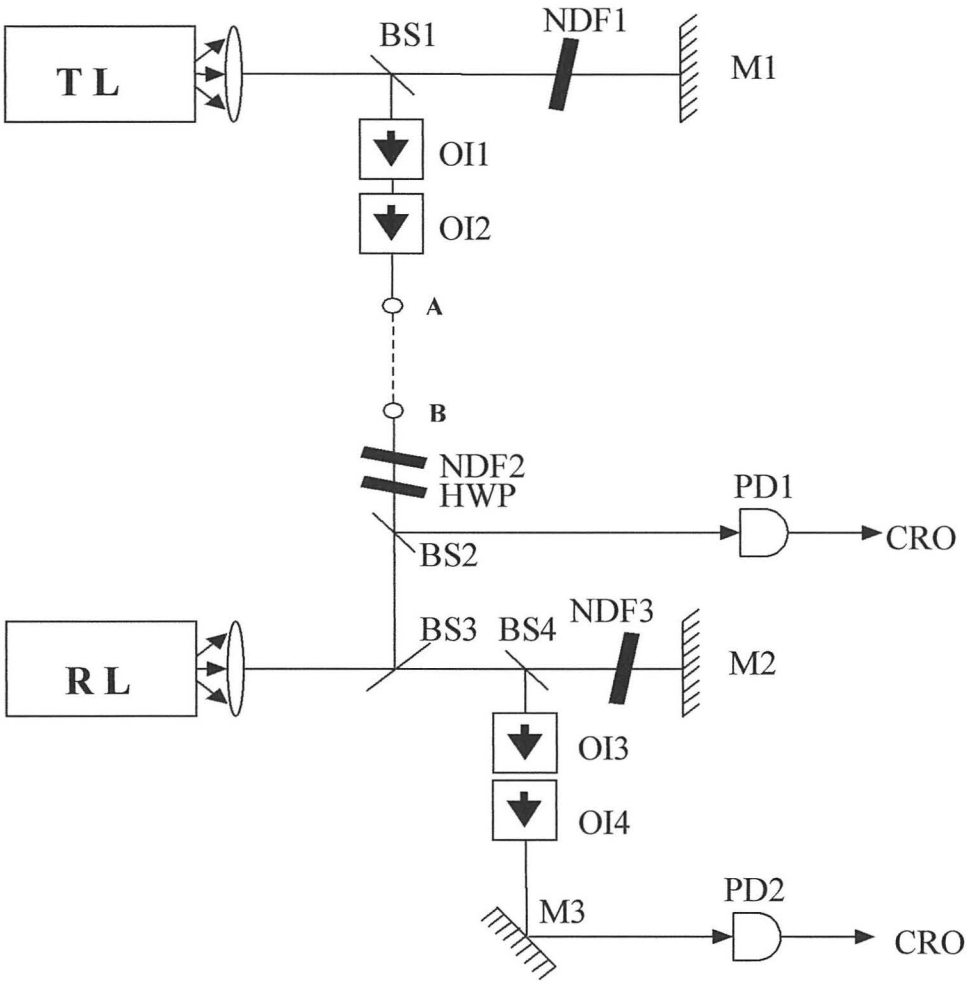

Figure 3.1: *Experimental arrangement used for synchronisation measurements. TL, Transmitter laser; RL, Receiver laser; BS1-BS4, beam splitters; NDF1-NDF3, neutral density filters; M1-M3, mirrors; OI1-OI4, optical isolators; HWP, half wave plate; PD1 and PD2, photodetectors; CRO, oscilloscope; A and B, transmission path*

This ensures that maximum coupling between transmitter and receiver laser is achieved and allows stable synchronisation of transmitter and receiver lasers. Two identical fast photodetectors (NewPort, model no. AD-70xr) of bandwidth 6 GHz are used for detection. The output of the transmitter is coupled to photodetector PD1 via beam splitter BS1 and BS2. Beam splitter BS3 acts as a coupling element between the transmitter and receiver. Beam splitter BS4 couples the receiver output to photodetector PD2.

3.3 Coupling strength

The transmitter and receiver lasers are driven to chaos by application of appropriate feedback from the external-cavity mirrors. The effective external cavity reflectivity for transmitter and receiver lasers are –30.8 dB and –31.1 dB respectively. The free-running threshold current (I_{th}) values are 27 mA for both the lasers. The temperature and current of the transmitter (27.53 ^{0}C, 30.31 mA) and receiver (25.82 ^{0}C, 29.23 mA) are so adjusted to ensure that they operate at the same wavelength. The photodetector outputs are stored in a digital storage oscilloscope (LeCroy LC564A 1GHz) and then acquired by a PC. The transmission path A to B is free space. The transmitter and receiver lasers are driven into chaos by application of appropriate feedback from the external-cavity mirror by adjustment of NDF1 and NDF3. The amount of the transmitter laser power that is coupled to the receiver laser (the coupling strength) is controlled by NDF3. NDF3 is adjusted through a range of coupling strengths to identify the optimum level.

The data collected via PD1 and PD2 is used to plot time traces of the transmitter and receiver lasers. The data from the transmitter laser is shifted in time to compensate for the time of flight from transmitter to receiver. Figure 3.2 shows the time traces for the transmitter and receiver for a coupling strength of 2 % (2% of the transmitter output power is coupled via BS1 and BS3 into the external-cavity of the receiver laser). The receiver laser time trace closely follows that of the transmitter. The quality of synchronisation is determined by plotting the transmitter laser output, at a given time, against that of the receiver laser, at the same time, to obtain a synchronisation diagram.

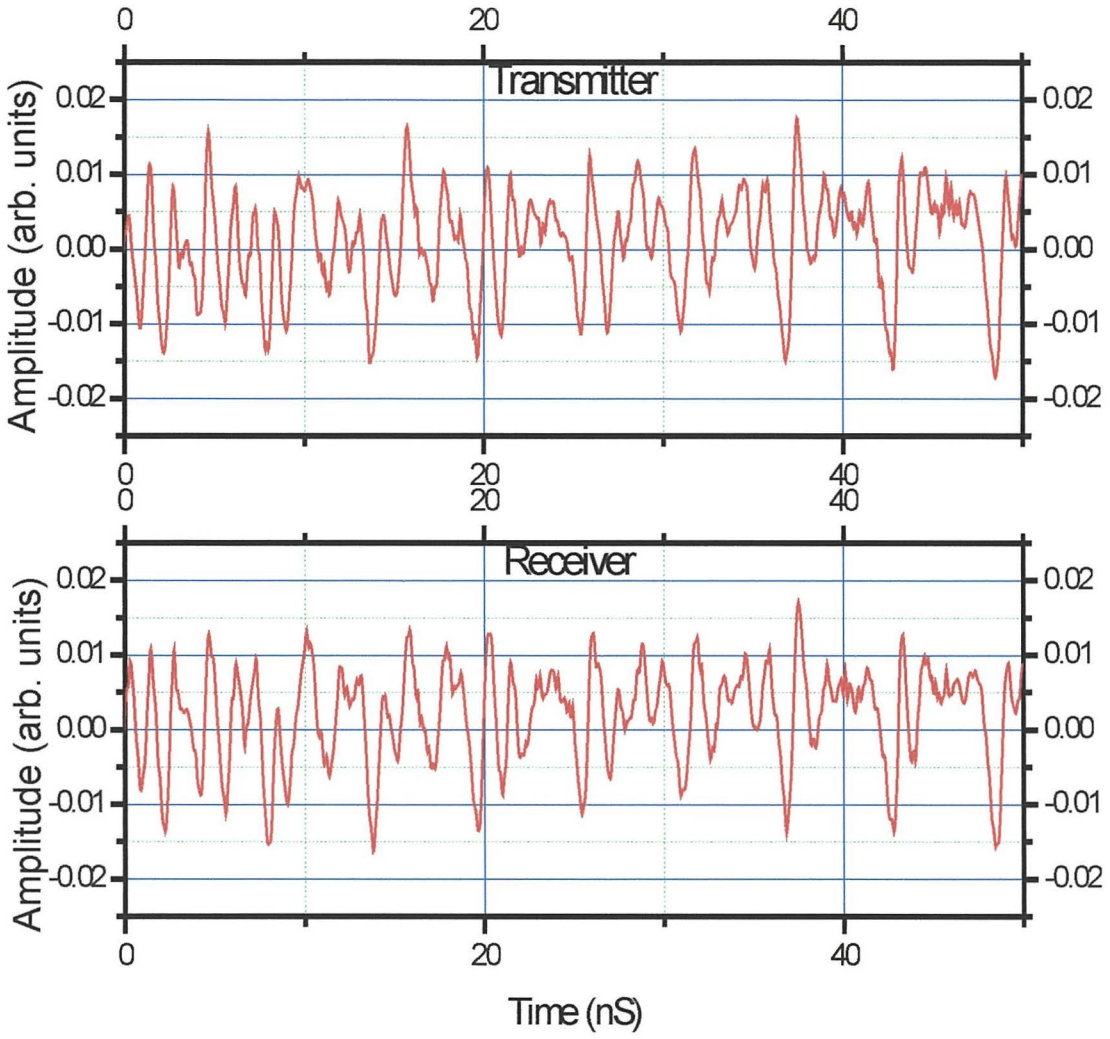

Figure 3.2: *Time traces of transmitter and receiver lasers for a coupling strength of 2 %*

The time-of-flight of the system (the time taken for the output of the transmitter to reach the receiver) is also taken into account for the purpose of producing synchronisation diagrams.

If the synchronisation is extremely poor and the receiver does not show any tendency to follow the transmitter the resulting synchronisation diagram shows a random distribution of points, such as that shown in figure 3.3 (a). In the case that synchronisation is exact a diagram such as figure 3.3 (b) showing a straight line with unity slope would be obtained. However, this quality of synchronisation is not

observed in experimentation. Thus, a good synchronisation diagram would be such as figure 3.4.

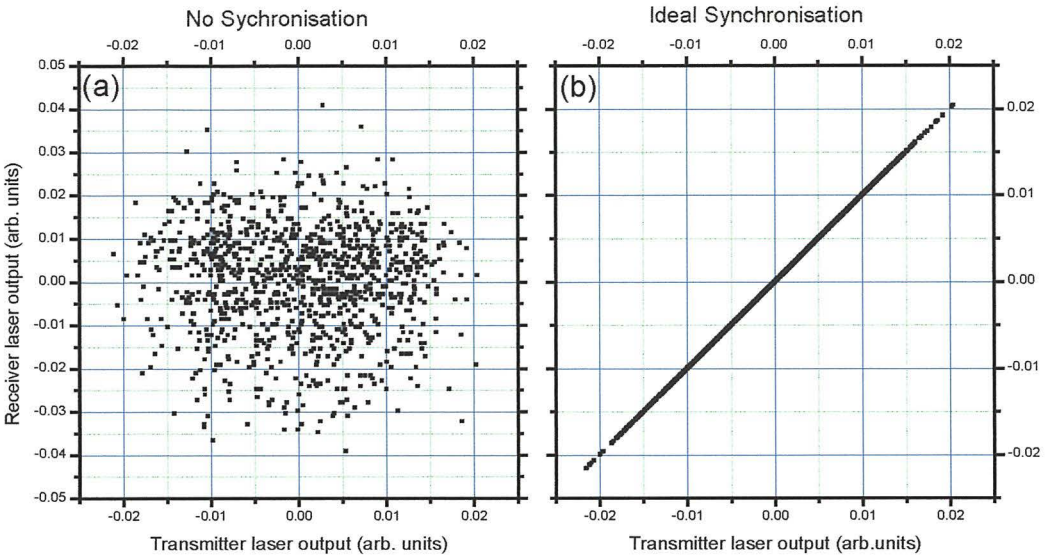

Figure 3.3: *Synchronisation diagram showing; (a) no synchronisation and (b) ideal synchronisation of two time traces*

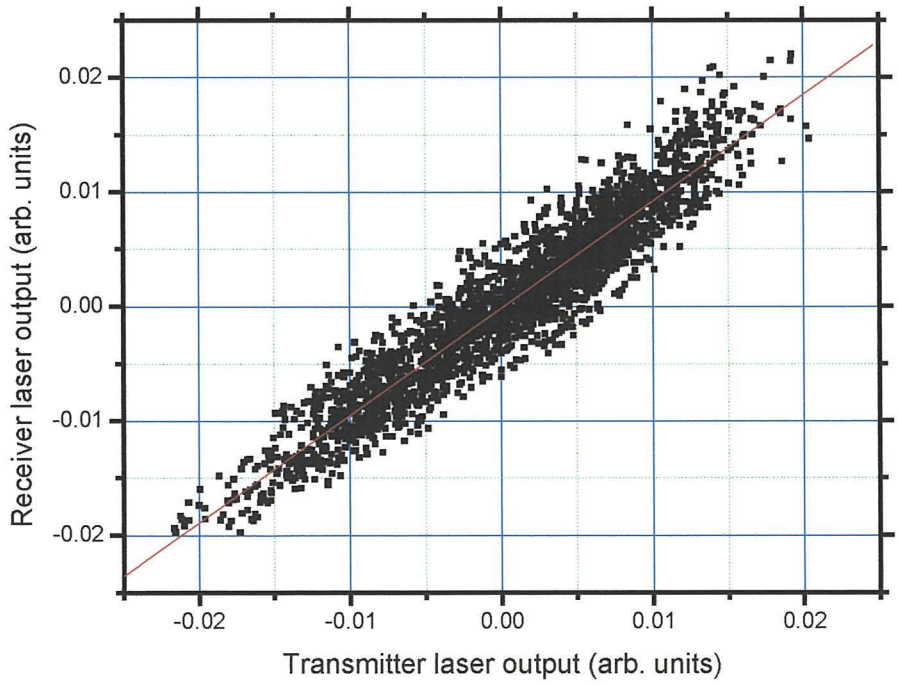

Figure 3.4: *Synchronisation Diagram of transmitter and receiver laser for a coupling strength of 2%*

The time traces shown in figure 3.2 for a coupling strength between transmitter and receiver lasers of 2% were used to construct the synchronisation diagram shown in figure 3.4. The straight line shown in figure 3.4 is obtained by a linear regression of the data points in the diagram. The linear regression is used to calculate the slope of the synchronisation diagram, the error in the slope and the correlation coefficient (percentage variation in the receiver that is accountable by variation in the transmitter) between transmitter and receiver. The correlation coefficient is used to calculated the covariance (which is the square of the correlation coefficient) of transmitter and receiver. NDF2 was varied such that the coupling between transmitter and receiver varied from 0.65% to 7%. The transmitter and receiver time traces were recorded at different levels of coupling and were used to calculate the transmitter receiver covariance and changes in the slope of the synchronisation diagram. The covariance between transmitter and receiver is shown in figure 3.5.

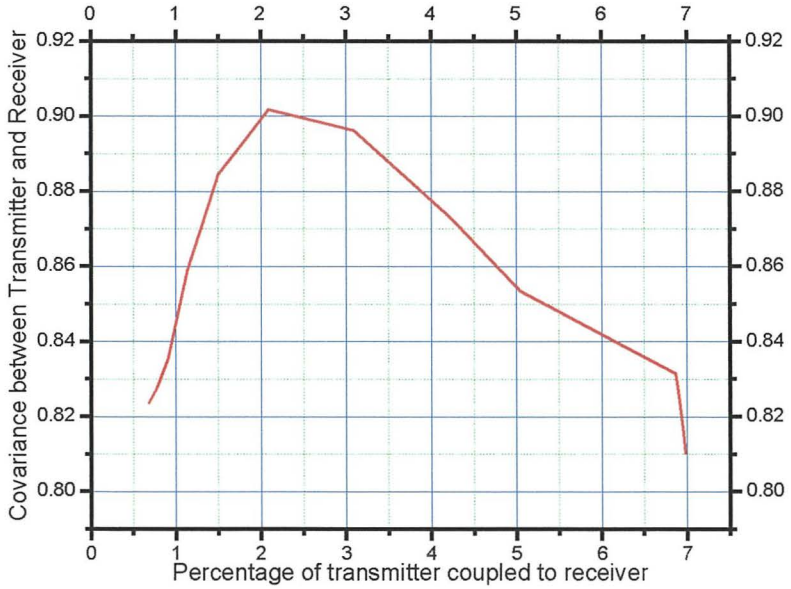

Figure 3.5: *Covariance between transmitter and receiver for variations in coupling strength between transmitter and receiver*

It can be seen from figure 3.5 that there is an optimum coupling strength of 2.1% that achieves the best covariance between transmitter and receiver lasers. Below the optimum level, the transmitter power introduced into the receiver laser is too low to

affect the receiver dynamics. When the coupling strength is increased beyond the optimum level, the receiver laser power starts to saturate and thus the synchronisation quality deteriorates. The slope of the straight line fit is shown in figure 3.36. The ideal slope is unity (indicating that the transmitter and receiver laser output are of equal amplitude) which occurs for coupling strengths of about 1% and 5 %.

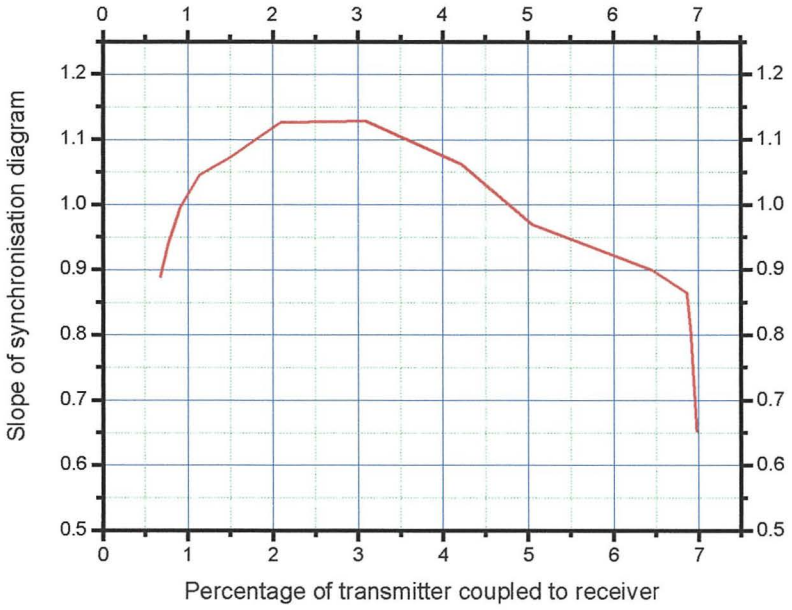

Figure 3.6: *Slope of synchronisation diagrams for variations in the coupling strength between transmitter and receiver*

To sum up, Figures 3.5 and 3.6 show that the best synchronisation between transmitter and receiver laser is achieved for a transmitter, receiver coupling strength of between 2% and 3%.

3.4 Detuning

Once good synchronisation has been obtained between the transmitter and receiver lasers, it is of benefit to examine the system parameters that may affect the quality of synchronisation. These parameters include the operating temperature of the lasers, the laser bias current and the polarisation of the laser beam. The experimental set-up is the same as that shown in figure 3.1. Good synchronisation is achieved, and then

each of the three parameters is varied in turn and the affect on the covariance of the synchronisation between transmitter and receiver lasers is observed. Firstly the temperature of the receiver laser is varied from 32.725 ^{0}C to 33.025 ^{0}C. The outputs from photodetector PD1 and PD2 were recorded. The transmitter laser was time corrected to allow for the lag in the receiver and synchronisation plots of transmitter and receiver were made. The synchronisation plots were then used to calculate the covariance between transmitter and receiver lasers as shown in figure 3.7.

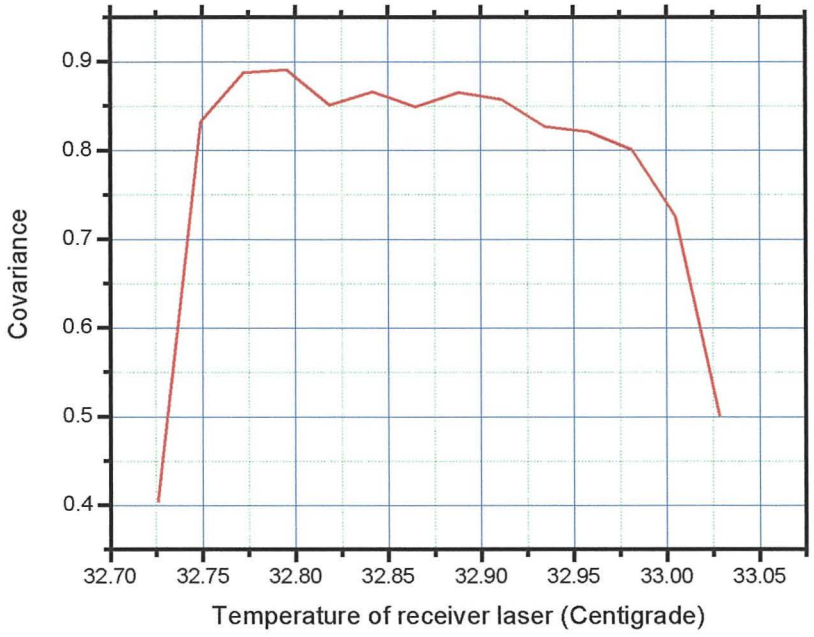

Figure 3.7: *Covariance between transmitter and receiver for variations in receiver laser temperature*

It can be seen from figure 3.7 that when the temperature of the laser lies between 32.975 ^{0}C and 32.75 ^{0}C, synchronisation quality is good. Either side of this temperature the quality of the synchronisation deteriorates rapidly with temperature variation. This leaves a window of operation for good synchronisation of only 0.225 ^{0}C. Next the effects on synchronisation quality by changes in the drive current of the receiver laser were examined. The receiver lasers drive current was varied from 24 to 40 mA and the covariance between transmitter and receiver laser was calculated as shown in figure 3.8. As can be seen, good synchronisation is achieved between the transmitter and receiver laser for receiver laser drive currents from 27.5 mA to 31 mA.

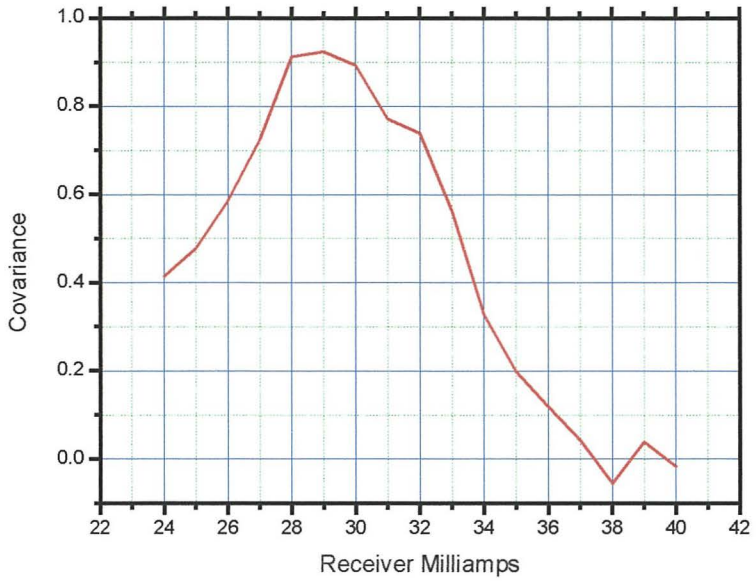

Figure 3.8: *Covariance between transmitter and receiver for variations in receiver laser drive current*

The half wave plate shown in figure 3.1 was varied through 360^0. The effects on the quality of transmitter to receiver synchronisation quality in terms of the covariance were calculated. As can be seen from figure 3.9 the best quality of synchronisation occurs when the transmitter and receiver lasers outputs have the same plane of polarisation.

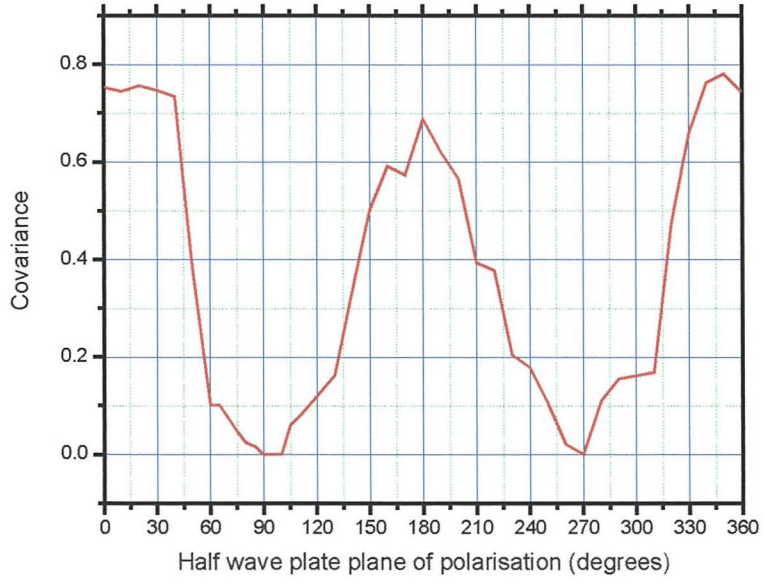

Figure 3.9: *Covariance between transmitter and receiver for variations in transmitter to receiver laser beam polarisation*

The optical isolators OI1 and OI2 in figure 3.1 introduce a change of polarisation in the transmitter laser beam of 45^0 each. When the receiver lasers plane of polarisation is at 90^0 to that of the transmitter synchronisation is lost completely.
Therefore, without the half wave plate to correct for this change in polarisation, synchronisation of transmitter and receiver laser would be of poor quality with one optical isolator in the set-up and hard to achieve with two optical isolators.

3.5 Cascade Synchronisation

Consideration has so far been given to the chaotic synchronisation of two lasers, one being the transmitter and one the receiver. However, there may be requirements for more complex configurations, for example to increase transmission distances, whilst making available the same chaos at the receiving end as that generated at the transmitter. One possible way to achieve this is by using cascade synchronisation. Cascade synchronisation of external-cavity laser diodes was first demonstrated in 2001 [7]. The experimental set-up is similar to that shown in figure 3.1, however there is a second receiver laser as shown in figure 3.10. The transmitter, receiver 1 and receiver 2 lasers are driven to chaos by external-cavity feedback from mirrors M1, M2 and M3 respectively. The optical isolators OI1 and OI2 ensure that the transmitter to receiver 1 coupling is unidirectional. Likewise OI3 and OI4 ensure that the receiver 1 to receiver 2 coupling is unidirectional. The temperature and current of the three lasers is adjusted such that they operate at the same wavelength. Coupling attenuator CA1 is adjusted to achieve synchronisation between transmitter laser and receiver laser 1 and coupling attenuator CA2 is adjusted so that receiver laser 1 and receiver laser 2 synchronise. Photodetectors PD1, PD2 and PD3 measure the output from the transmitter, receiver 1 and receiver 2 lasers respectively and are stored in a digital oscilloscope. The outputs of the transmitter laser, receiver laser 1 and receiver laser 2 were time corrected for the time of flight and used to plot the time traces shown in figure 3.11

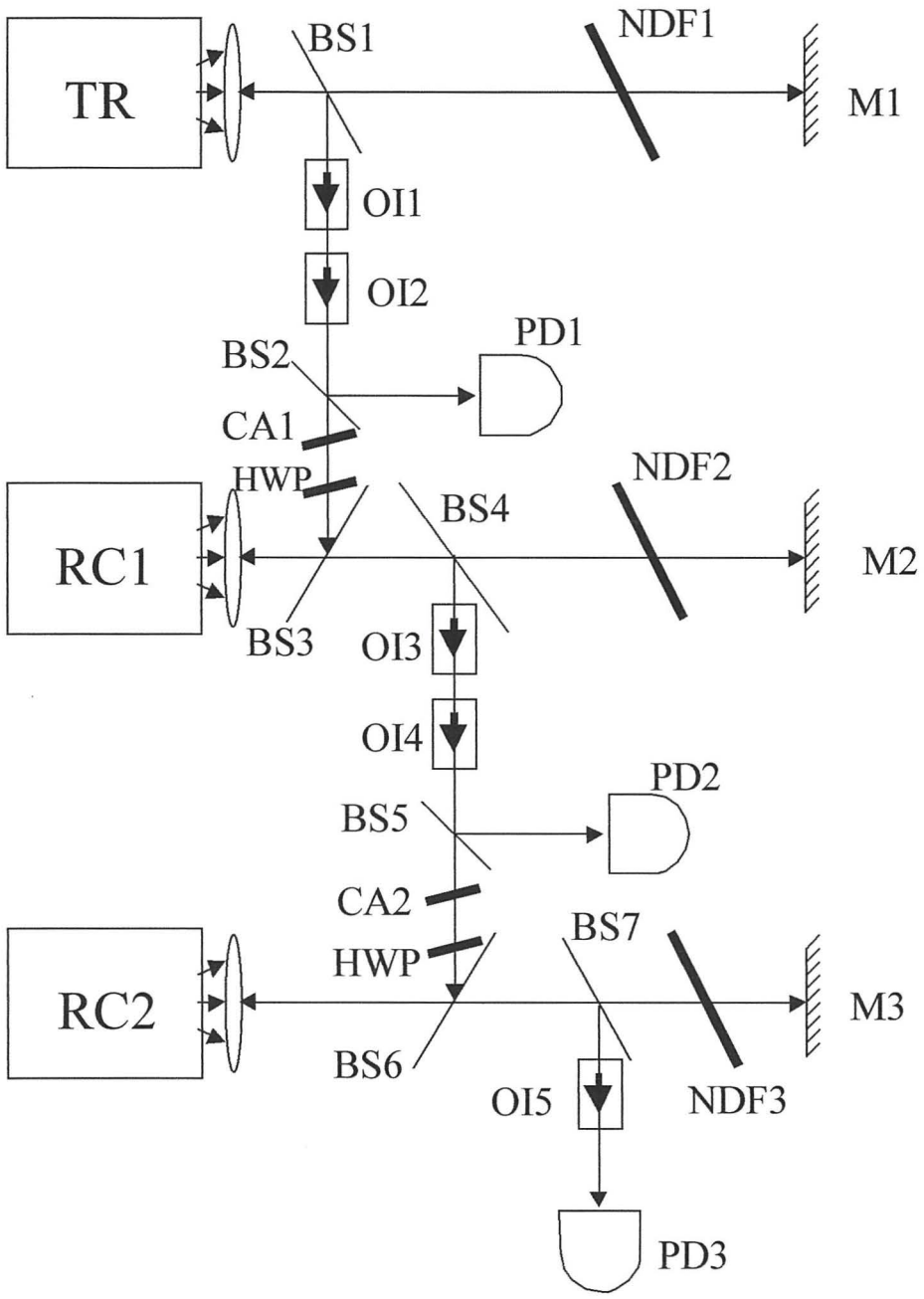

Figure 3.10: *Experimental arrangement used for synchronisation measurements. TR, Transmitter laser; RC1 and RC2, Receiver lasers; BS1-BS4, beam splitters; NDF1-NDF3, neutral density filters; M1-M3, mirrors; OI1-OI5, optical isolators; HWP, half wave plate; CA1 and CA2, coupling attenuators; PD1 – PD3, photodetectors; CRO, oscilloscope*

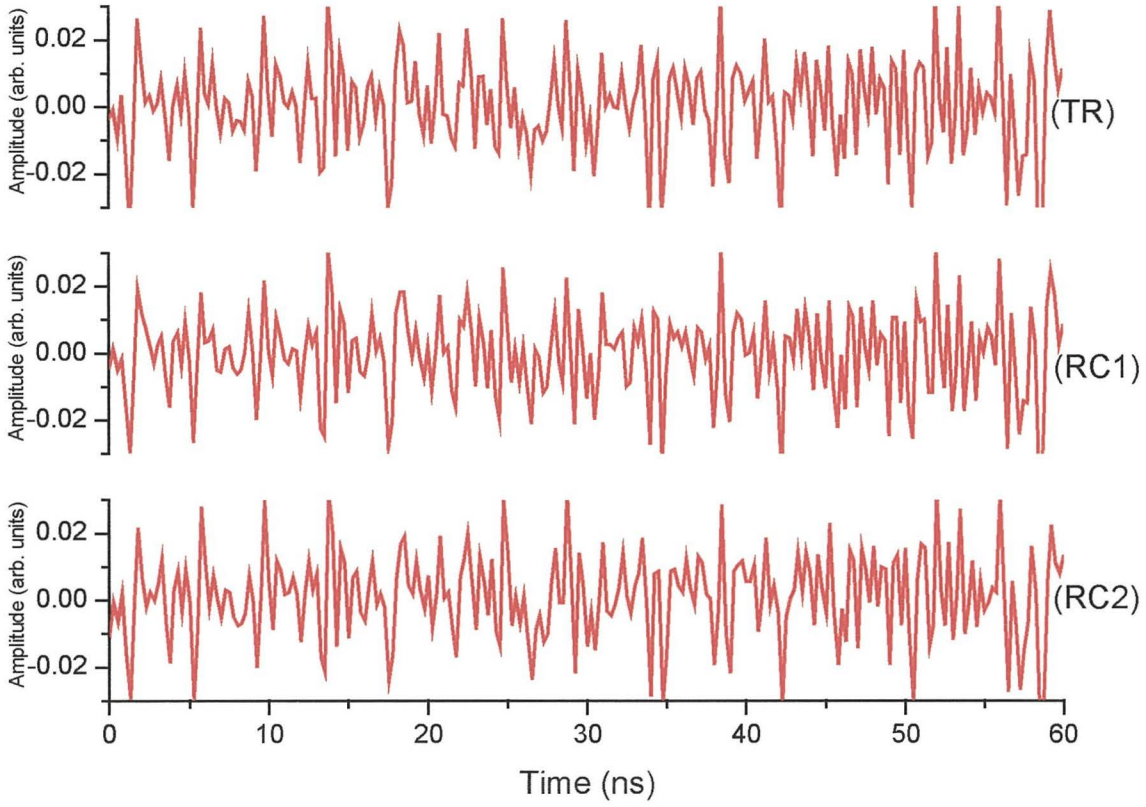

Figure 3.11: *Time traces of transmitter laser (TR), receiver laser 1 (RC 1) and receiver laser 2 (RC 2)*

The time corrected time traces in figure 3.11 show that the chaos in both receiver laser 1 and receiver laser 2 closely follows the chaos of the transmitter laser. To confirm this the data used to generate the time traces in figure 3.11 was used to produce the synchronisation diagram shown in figure 3.12. Figure 3.12 (a) shows the synchronisation between transmitter and receiver laser. It can be seen that good quality synchronisation is achieved. Figure 3.12 shows the synchronisation between the transmitter and receiver lasers. Here it can be seen that the chaos of the receiver laser 2 is well synchronised to that of the chaos produced in the transmitter. Also from figure 3.12 (c), it can be seen that the receiver laser 2 is well synchronised to the receiver laser 1. Thus it is seen that cascade synchronisation is achievable with little loss of quality of the chaotic signal produced at the receiving lasers.

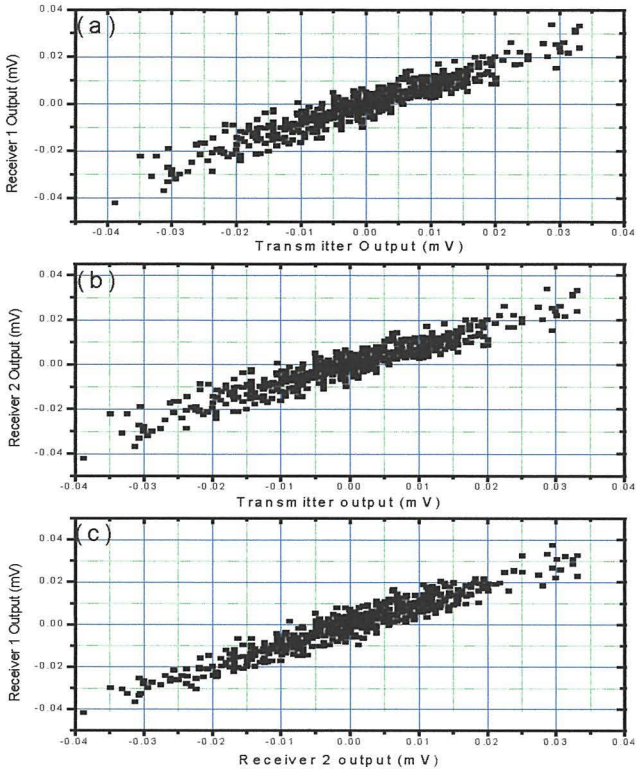

Figure 3.12: *Synchronisation Diagrams. (a) transmitter laser Vs receiver laser1, (b) transmitter laser Vs receiver laser 2 and (c) receiver laser 2 Vs receiver laser 1*

3.6 Inverse synchronisation

Inverse synchronisation of diode lasers was first demonstrated experimentally in 2001 [8]. The receiver laser emission wavelength is detuned from the transmitter, therefore there is very little coupling into the receiver lasing mode. Thus the dominant effect is nonresonant amplification. This causes a reduction in the carrier density of the receiver laser through the loss of electron-hole pairs. This effect is enhanced as the transmitter laser output increases, leading to inverse synchronisation.

The experimental set-up is the same as that shown in figure 3.1. To observe the inverse synchronisation phenomenon the lasers are operated in the low-frequency fluctuation (LFF) regime. When the lasers are operated in the LFF regime [9] rather than in the fully chaotic regime, inverse synchronisation is evident, whilst it is less evident in the fully chaotic regime. Inverse synchronisation is achieved by wavelength detuning either the transmitter or receiver laser. In this case the receiver

laser is detuned. The wavelength detuning is achieved by varying the bias current of the laser. A 1mA change in laser bias current changes the laser emission wavelength by 1GHz. The transmitter and receiver lasers were driven to LFF by application of external-cavity feedback. The two laser were synchronised as described above. The receiver laser is detuned by reducing its bias by 8 mA, in 1 mA steps. This is equivalent to a receiver laser emission wavelength shift of 8 GHz, in 1 GHz steps. The output from photodetectors PD1 and PD2 (New focus, 1621) were stored in the oscilloscope. The data for the receiver laser is time corrected to allow for the lag in the system (the time delay introduced by the physical distance between the transmitter laser, receiver laser 1 and receiver laser 2). Transmitter and receiver time traces of laser output intensity for detuning of 0 mA and 8 mA are shown in figure 3.13.

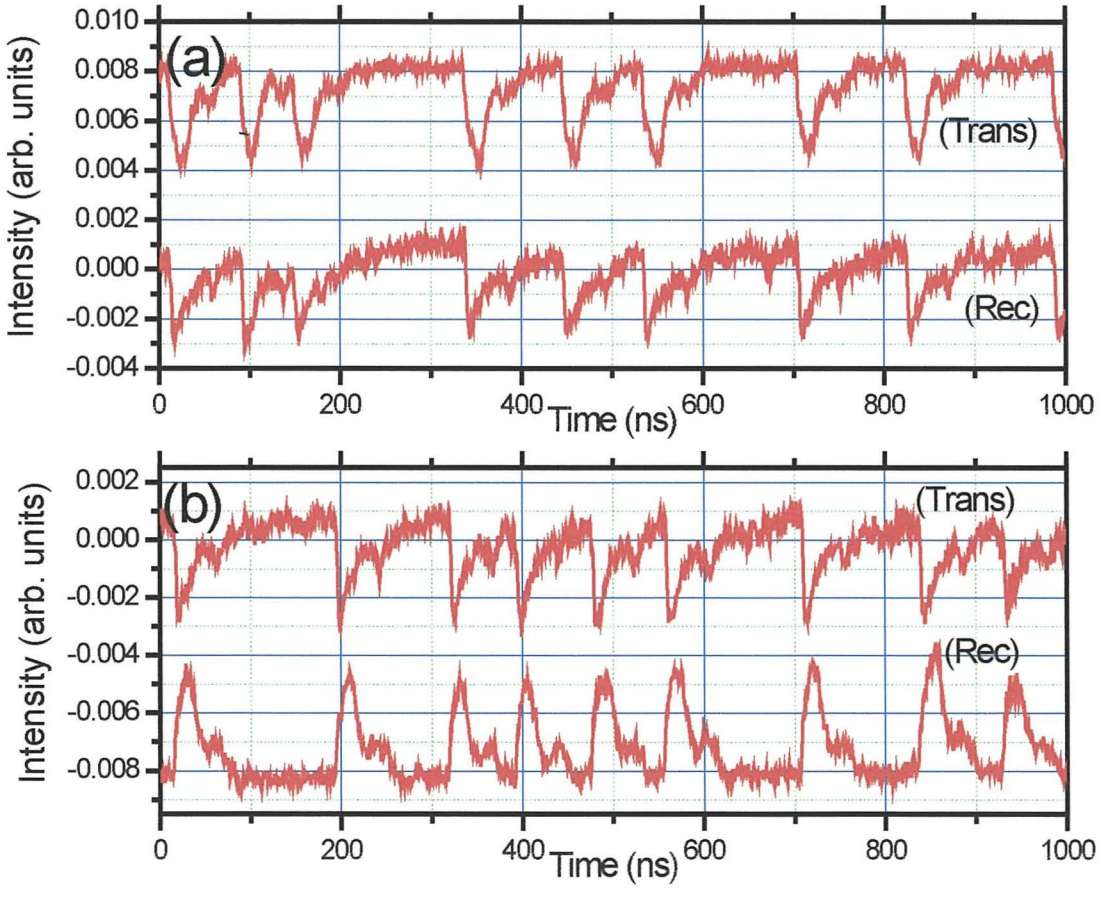

Figure 3.13: *Time traces of transmitter laser (Trans), receiver laser (Rec) for (a) no detuning and (b) 8 GHz detuning of the receiver laser*

It is seen from figure 3.13 (a) that when no detuning occurs, good synchronisation of the LFF is achieved. When the receiver laser is detuned by 8 mA equivalent to an emission wavelength shift of 8 GHz, the receiver laser can be seen to be inverse synchronised to the transmitter. In the inverse synchronisation regime (figure 3.13b), the receiver laser follows the transmitter but is inverted. As the receiver laser drive current is reduced, the synchronisation quality deteriorates to a minimum at about 4.5 mA. The receiver laser becomes inverse synchronised to the transmitter and the synchronisation quality starts to improve. However the slope of the synchronisation diagram becomes negative. The synchronisation diagrams are shown in figure 3.14.

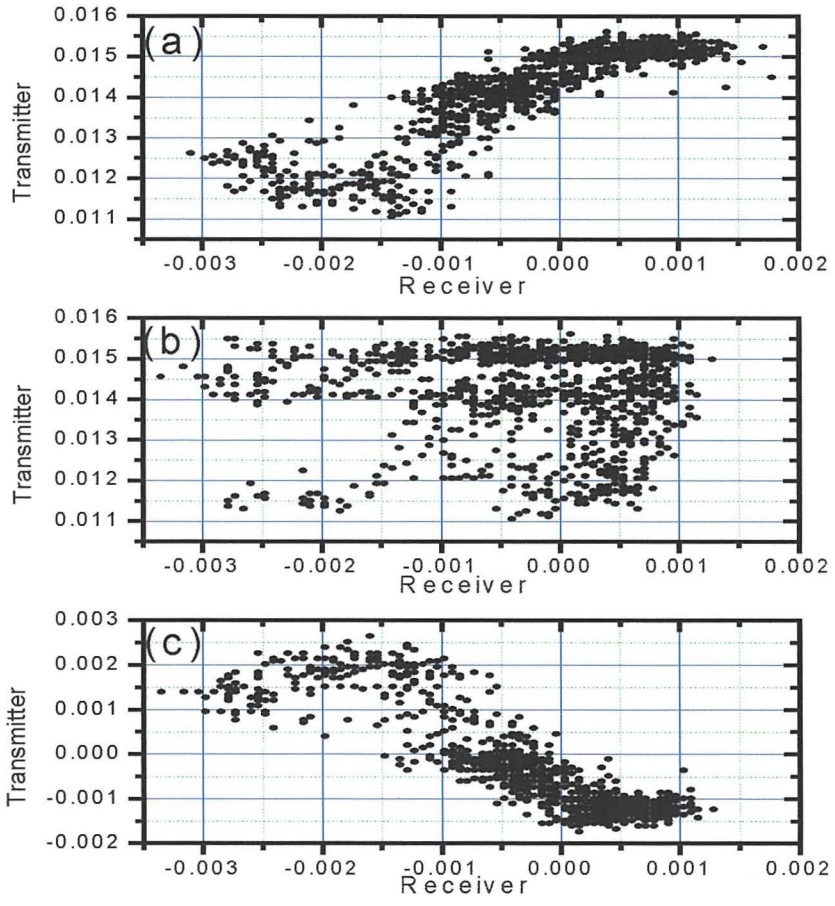

Figure 3.14: *Synchronisation Diagram of transmitter laser Vs receiver laser detuning of, (a) 0 GHz, (b) 4GHz and (c) 8 GHz*

Figure 3.14 (a) is for zero detuning of the receiver laser. As can be seen from 3.14 (a), the synchronisation quality is not as good as some of the previous synchronisation

diagram in this chapter. This is because the lasers are operating in the LFF regime. Figure 3.14 (b) shows that synchronisation has been lost and 3.14 (c) shows that at a receiver detuning level of 8 GHz, the slope of the synchronisation diagram has become negative and hence inverse synchronisation is achieved.

3.7 Nullified time of flight synchronisation

This section contains experimental results obtained with the present research concerning means for nullifying the effects of time-of-flight between transmitter and receiver. So far in this chapter all the types of synchronisation shown have had a lag between the transmitter and receiver. This is where the receiver laser follows behind the transmitter by a time that is governed by the distance between the transmitter and receiver lasers. This lag time τ_F is the time-of-flight of the light from the transmitter to the receiver, and in all previous examples of synchronisation in this chapter the synchronisation diagram and time traces have been time corrected to remove the time-of flight delay of the system.

In 2000 numerical and analytical work [10] identified a regime of operation where two coupled scalar differential equations in a unidirectional delayed coupled system may exhibit anticipation. In the anticipation regime, the receiver dynamics of the system lead the transmitter dynamics. Also numerical work in 2001 [11] identified a regime of anticipating synchronisation in chaotic external-cavity semiconductor lasers using unidirectional coupling between transmitter and receiver lasers. Later the same year the first experimental demonstration of anticipation synchronisation in chaotic semiconductor lasers with optical feedback [12] was achieved. However, this experiment employed mutually coupled transmitter and receiver lasers. The experimental work used two semiconductor lasers as transmitter and receiver. The anticipation time, the amount of time the receiver laser leads the transmitter was found to be equal to the flight time of the system. More recently, as part of the present research, a demonstration has been reported of an experiment configuration where the effect of the time-of-flight is nullified. This section is based on reference [13].

The idea of nullified time of flight synchronisation is to achieve a system where the transmitter and receiver are synchronised with no time lag or lead between them. The experimental set-up is shown in figure 3.15. The transmitter and mediator laser are mutually coupled since there is no isolator between them. The transmitter is subjected

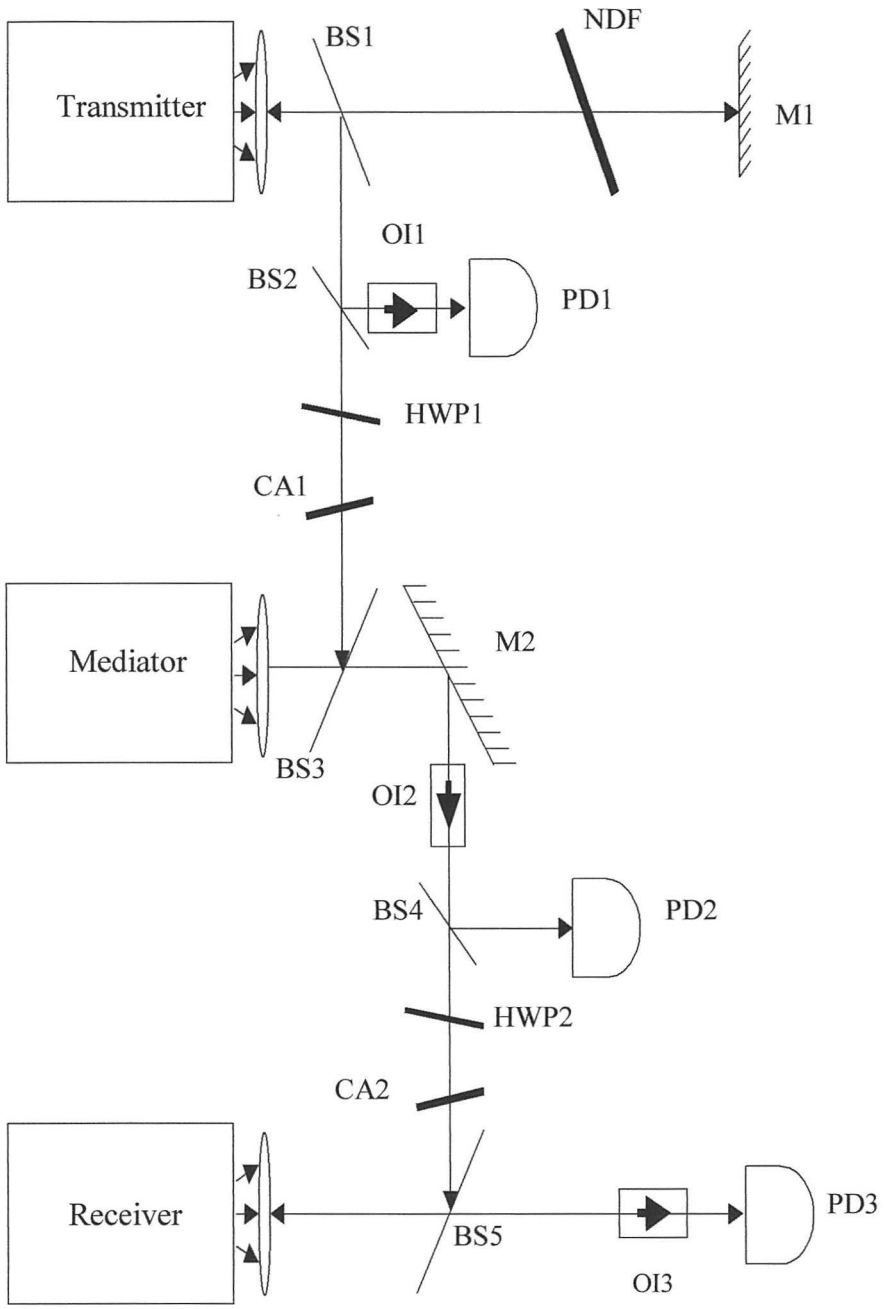

Figure 3.15: *Schematic diagram of the experiment. BS1-BS5 : Beam splitters, M1-M2: Mirrors, OI1-OI3: Optical isolators, HWP1-HWP2 : Half wave plates, CA1-CA2: Coupling attenuators and PD1-PD3: Photodetectors*

to optical feedback from an external mirror M1 and the feedback strength is controlled using a continuously variable neutral density filter NDF. The external cavity round trip time (τ) is 10 ns. Optical isolator (OI2) ensures unidirectional coupling between the mediator and receiver laser. PD1, PD2 and PD3 are identical fast photodetectors (NewFocus -1621) with a response time of 2 ns. The optical output of the transmitter is coupled to the photodetector PD1 by the beamsplitters BS1 and BS2. Beamsplitter BS3 acts as coupling element between the transmitter and mediator. Mirror (M2) and beam-splitter (BS5) couples the mediator laser output to the photodetector PD2. Beamsplitter BS5 acts as the coupling element between the mediator and receiver. Photodetector outputs are stored in a digital storage oscilloscope . The half wave plates are used to ensure identical polarisation between the lasers. The time of flight between the transmitter laser and mediator laser is 4.5 ns and the time of flight between the mediator laser and receiver laser is also set at 4.5 ns. The transmitter laser is driven into low-frequency fluctuations (LFF). A fraction of the transmitter laser output is coupled to the mediator laser. The coupling attenuator (CA1) is used to control the light coupled between the lasers. The coupling coefficient between the lasers is 0.5% - this is the percentage of the transmitter output power coupled to the mediator and vice versa. This coupling coefficient is low enough to ensure that the mediator laser's facet reflectivity does not induce any significant dynamics in the transmitter output. The operating temperature and current of the transmitter (27.66°C, 1.2 I_{th}) and mediator (25.85°C, 1.168 I_{th}) are optimised such that the mediator laser dynamics anticipates the transmitter laser dynamics [12]. Figure 3.16 (a) and figure 3.16 (b) shows the time evolution of the transmitter and mediator laser. In figure 3.16(a) and 3.16(b), it can be seen close to the 620 ns, 735 ns and 925 ns the mediator laser falls and revives ahead of the transmitter laser. Hence the mediator laser is leading the transmitter laser by a time known as anticipation time (τ_A) [11, 12], which is measured using the oscilloscope and is found to be 4.5 ns. This measured value of the anticipation time is equal to the time of flight (τ_F). The mediator laser output is plotted against the transmitter laser output to obtain synchronisation plots. The time delay between the transmitter and mediator laser has been taken into account to plot the synchronisation diagram shown in figure 3.17. Figure 3.17(a) shows the synchronisation diagram between the transmitter and mediator.

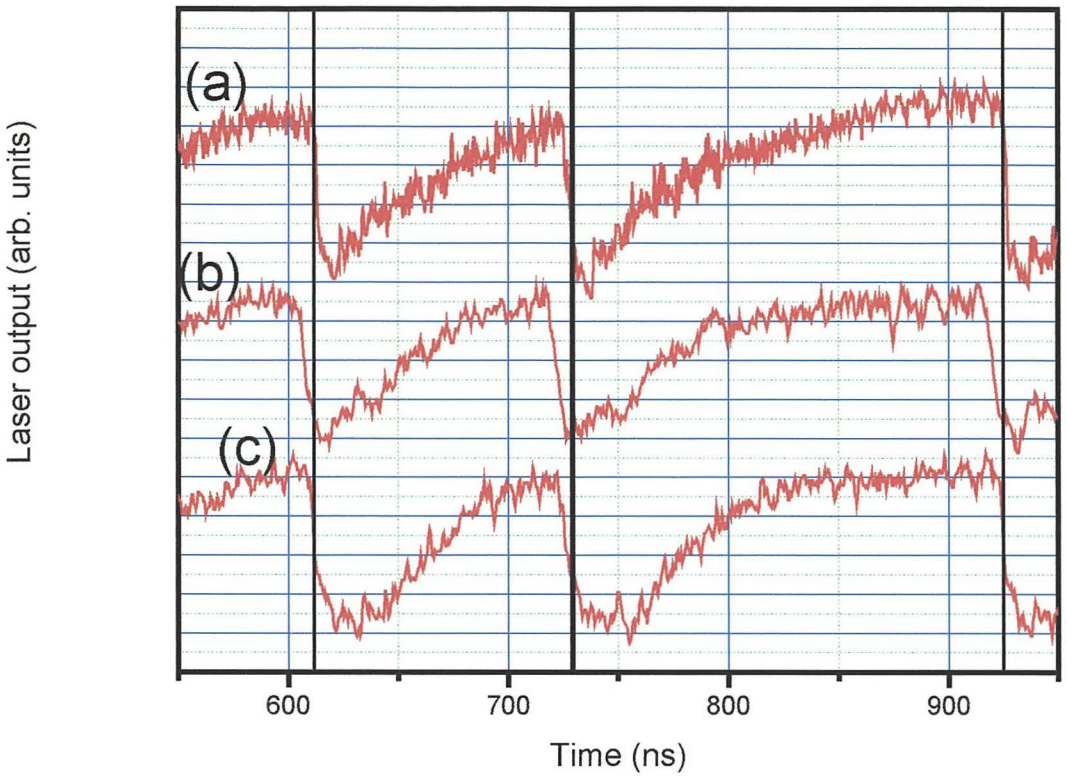

Figure 3.16: *Time traces of (a) transmitter, (b) mediator and (c) receiver laser outputs. The transmitter and mediator lasers' time traces are shifted vertically for clarity. The vertical lines at 620 ns, 735 ns and 925 ns enable comparison of the time evolution of the three lasers and demonstrate that the mediator laser is ahead of the other two lasers*

A fraction (0.9%) of the mediator laser output is coupled uni-directionally to the receiver laser. The receiver laser operating temperature and current (26.83°C, 1.04 I_{th}) are optimised so as to obtain synchronisation in their output intensities. The time trace of the receiver laser is shown in figure 3.16(c). In figure 3.16(b) and 3.16(c), it can be seen close to the 620 ns, 735 ns and 925 ns, the receiver laser falls and revives behind the transmitter laser. Hence the receiver laser is lagging behind the mediator laser by a time known as lag time (τ_L) [12-13], which is measured to be 4.5 ns using the oscilloscope. This measured value of the lag time is equal to the time of flight (τ_F) between the mediator and receiver laser. The receiver laser output is plotted against the mediator laser output to obtain synchronisation diagram and is shown in figure 3.17 (b). The time delay between the receiver and mediator laser has been taken into account to plot the synchronisation diagram.

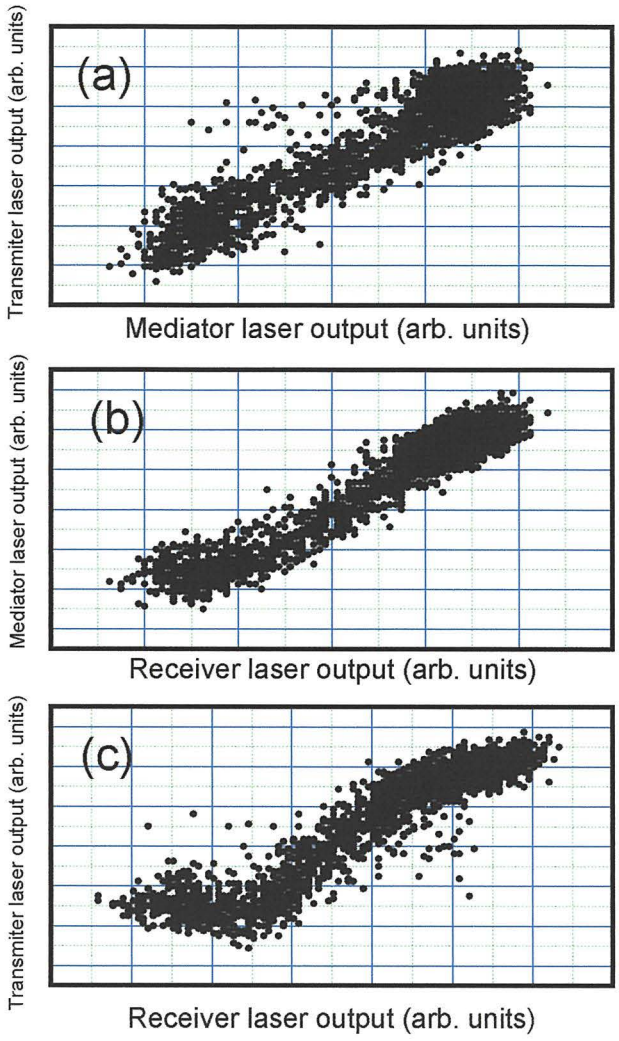

Figure 3.17: *Synchronisation diagrams: (a) transmitter laser Vs mediator laser output, (b) mediator laser Vs receiver laser output and (c) transmitter laser Vs receiver laser output. The synchronisation between the mediator and receiver laser is superior to that of the other two cases*

A comparison of the time evolution of the transmitter and receiver lasers (guided by the vertical lines in figure 3.16) reveals that the transmitter and receiver lasers neither lead nor lag each other - but they evolve together in time. This lead-lag null situation is achieved by effective utilisation of the anticipating and lag synchronisation configurations. The transmitter - mediator pair (pair-1) is operated in 'anticipating' configuration and the mediator - receiver pair (pair-2) is operated in 'lag' configuration. The most important parameter to match is the time of flight in both the pairs. A larger time of flight in pair-1 compared to that of pair-2, would result in the

receiver laser leading the transmitter laser. On the contrary, if the time of flight in pair-1 is smaller, it would result in the receiver laser lagging behind the transmitter laser.

The synchronisation diagram between the transmitter and receiver is shown is figure 3.17 (c). A further study is made by varying the mediator laser bias current from 1.04 to 1.28 I_{th} and the synchronisation diagram is plotted between the transmitter and mediator (red) and, between the mediator and receiver (black) at every step of the mediator laser bias current. These synchronisation diagrams are least square fitted to a straight line to obtain the slope-1 (red) and slope-2 (black). Figure 3.18 shows the dependence of the slope-1 and slope-2 on the mediator bias current.

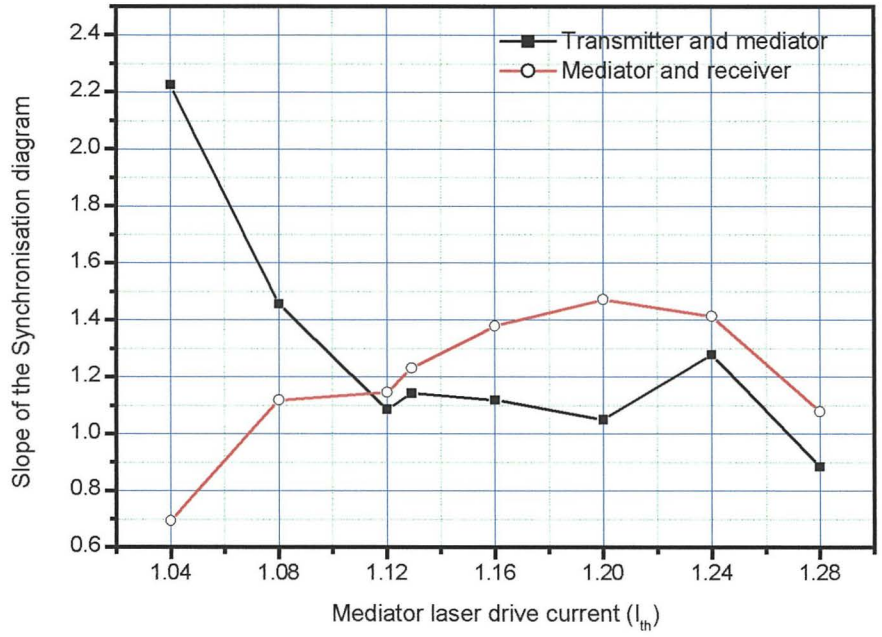

Figure 3.18: *Dependence of the slope of the synchronisation diagram for the transmitter and mediator lasers (■) and for the mediator and receiver lasers (○) with respect to the change in the mediator laser bias current. (I_{th} is 25 mA)*

Slope-1 shows a high value for low mediator bias levels and stabilises at around 1.12 I_{th} of the mediator laser. Slope-2 shows a low value for low mediator bias levels and stabilises at around the same mediator bias level as that of slope-1. At high mediator bias levels (1.28 I_{th}) both the slope-1 and slope-2 shows degradation. Varying the bias

level of the mediator laser effects changes in its output intensity and emission wavelength and hence affects the slope of the synchronisation diagrams.
In conclusion, it has been demonstrated that there is a means for synchronising two chaotic diode lasers such that their output intensities evolve together in time without lead or lag between them. Measurements of the slope of the synchronisation diagrams for the lasers show that all the three lasers are synchronised for a particular region of mediator laser bias current.

3.8 Conclusion

In this chapter it has been shown experimentally that it is possible to synchronise external-cavity semiconductor lasers. It was shown that there are many operational parameters that affect the quality of synchronisation, such as the coupling strength, which was controlled with a coupling attenuator, and the detuning between the lasers, which was varied through the lasers drive currents and the lasers operating temperatures. Also, it has been shown that there are several types of synchronisation that chaotic semiconductor lasers can experience: unidirectional synchronisation, mutual synchronisation, cascade synchronisation, and inverse synchronisation. It has been shown that under certain operating conditions the receiver lasers dynamics may lead the dynamics of the transmitter laser, thereby anticipating the transmitter. This occurs when the lasers are mutually coupled and the transmitter laser is subjected to its own external-cavity feedback. A demonstration of cascade synchronisation has shown that three diode lasers may be chaotically synchronised in a cascade configuration. A particular configuration of the cascade scheme lead to nullified time of flight synchronisation, in which the intensities of the transmitter and receiver lasers synchronise with no lag-time between them, due to a mediator laser that anticipates the transmitter.

3.9 References

[1] U. Parlitz, L. Junge, W. Lauterborn and L. Kocarev, "Experimental observation of phase synchronisation," Phys. Rev. E., Vol. **54**, pp. 2115-2117, 1996

[2] T. Stojanovski, L. Kocarev and U. Parlitz, "Driving and synchronising by chaotic impulses," Phys. Rev. E., Vol. **76**, pp. 2128-2131, 1996

[3] T. L. Carroll, J. F. Heagy and L. M. Pecora, "Transforming signals with chaotic synchronisation," Phys. Rev. E., Vol. **54**, pp. 4676-4680, 1996

[4] C. R. Mirraso, P. Colet, and P. G. Ferbnandez, " Synchronisation of chaotic semiconductor lasers: Application to encoded communications," IEEE Photonics Technol. Lett., Vol. **8**, pp. 299-301, 1996

[5] U. Parlitz, L. Kocarev, T. Stojanovski and H. Preckel, "Encoding messages using chaotic synchronisation," Phys. Rev. E., Vol. **53**, pp. 4351-4361, 1996

[6] S. Sivaprakasam and K. A. Shore, "Demonstration of optical synchronisation of chaotic external-cavity laser diodes," Optics Lett. Vol. **24**, pp. 466-468, 1999

[7] S. Sivaprakasam and K. A. Shore, "Cascade synchronisation of external-cavity laser diodes," Optics Lett. Vol. **26**, pp. 253-255, 2001

[8] S. Sivaprakasam, I. Pierce, P. Rees, P. Spencer and K. A. Shore, "Inverse synchronisation in semiconductor laser diodes," Phys. Rev. A., Vol. **64**, 13805,1-8, 2001

[9] A. Gavrielides, T. C. Newell, V. Kovanis, R. G. Harrison, N. Swanston, D. J. Yu, and W. P. Lu, "Synchronous Sisyphus effect in diode lasers subject to optical feedback," Phys. Rev. A., **60**, pp. 1577-1581, 1999

[10] H. U. Voss, "Anticipating chaotic Synchronisation," Phys. Rev. E., Vol. **61**, pp. 5115-5119, 2000

[11] C. Masoller, "Anticipation in the synchronisation of chaotic semiconductor lasers with optical feedback," Phys. Rev. Lett., Vol. **86**, pp.2782-2785, 2001

[12] S. Sivaprakasam, E. M. Shahverdiev, P. S. Spencer and K. A. Shore, "Experimental demonstration of anticipating synchronisation in chaotic semiconductor lasers with optical feedback," Phys. Rev. Let. **87**, pp. 154101, 2001

[13] S. Sivaprakasam, J. Paul, P. S. Spencer, P. Rees, K. A. Shore, " Nullified time-of-flight lead-lag in synchronization of chaotic external-cavity laser diodes," Optics Lett. Vol. **28**, pp. 1397-1399, 2003

Chapter 4

Message encoding and decoding

4.0 Introduction

Having described the method used to synchronise chaotic lasers diodes, this chapter is devoted to the methods employed in encrypting a message into the chaotic dynamics of a transmitter laser, transmitting it to a receiver laser and recovering the message. Also consideration is given to the quality of the message recovery for a receiver operated in two distinctly different ways, one being an open loop receiver (a stand alone solitary laser) and the other being a closed loop receiver (a laser with external-cavity optical feedback).

Early work carried out on communication systems using chaos to hide a message employed electric circuits [1]. The work demonstrated experimentally that if two chaotic electric circuits are synchronised, a message may be transmitted and recovered in two ways. Firstly, the message is used to modulate a transmitter coefficient thus causing a synchronisation error at the receiver. Using the synchronisation error, the modulation can be detected. Secondly, a noise like masking signal (the generated chaos) is added to the message at the transmitter and at the receiver the chaotic masking is removed.

In laser systems, for encoding and decoding of messages, three types of synchronisation schemes have been proposed [2]: chaos modulation (CMO) [3-4], chaos masking (CMA) [5-6] and chaos shift keying (CSK) [7-8]. In the CMO scheme, the chaos is modulated by the message. In the CMA scheme, the message is simply added to the chaotic signal. The CSK scheme uses two separate states corresponding to a bit sequence. The message can be decoded depending on the synchronisation quality of the transmitter to the receiver.

The first demonstration of communication with chaotic lasers (CMO) [3] was performed in 1998 employing an erbium-doped fibre ring laser. The transmitter and receiver lasers where synchronised and a 10 MHz square wave message was embedded in the chaotic transmitter laser output, transmitted to the receiver laser and

recovered. Message recovery was achieved by subtracting the receiver output from the receiver input. In the same year wavelength modulation of a chaotic transmitter using a distributed feedback (DFB) semiconductor laser was demonstrated [4]. A message was used to wavelength modulate the chaotic transmitter, which is synchronised to the receiver and message recovery was achieved by subtraction of the receiver output from the receiver input.

The first demonstration of chaotic message encoding and decoding (CMA) using external-cavity semiconductor laser diodes was achieved in 2000 [5]. The transmitter and receiver lasers were driven into chaos by application of external-cavity feedback. Coupling between the transmitter and receiver lasers was adjusted such that the lasers synchronised. A 2.5 kHz square wave message was added to the chaotic transmitter by direct amplitude modulation and message recovery was achieved by subtraction of the receiver output from the receiver input. In this case the receiver laser synchronises to the chaotic output of the transmitter, but does not show the same level of synchronisation to the message. Therefore, the input to the receiver laser contains both the chaos and the message, whilst the output from the receiver laser contains the chaos and a much reduced amplitude message. By subtracting the output of the receiver laser from the input to the receiver laser the message may be recovered. However, the quality of message recovery depends on the synchronisation quality between the transmitter and receiver.

More recently, as part of the present research, an experimental demonstration of 1 GHz bandwidth chaotic message encoding and decoding using external-cavity semiconductor laser was reported [9]. Also a 2.5 Gbits/s message encoding and decoding through synchronisation of chaotic pulsing semiconductor lasers has been demonstrated [10].

Section 4.1, 4.2 and 4.3 of this chapter are based on [9]. That paper demonstrated the first GHz bandwidth message encoding and decoding using chaotic external-cavity semiconductor lasers. Section 4.1 describes the experimental set-up. The synchronisation of the lasers, along with message encoding is described in section 4.2. Section 4.3 describes the methods used for message recovery.

The basic concept of the experiment is shown in figure 4.1. As can be seen, the message is introduced electronically via the drive current of the transmitter laser. The transmitter laser is rendered chaotic by optical feedback. The masked message is transmitted to the receiver over the transmission path, which is free space. The

receiver laser synchronises to the chaos of the transmitter and its output is measured at photodetector B. The input to the receiver laser, measured at photodetector A contains both the chaos and the masked message, thus by subtracting the output from photodetector B from that of Photodector A, the message is recovered.

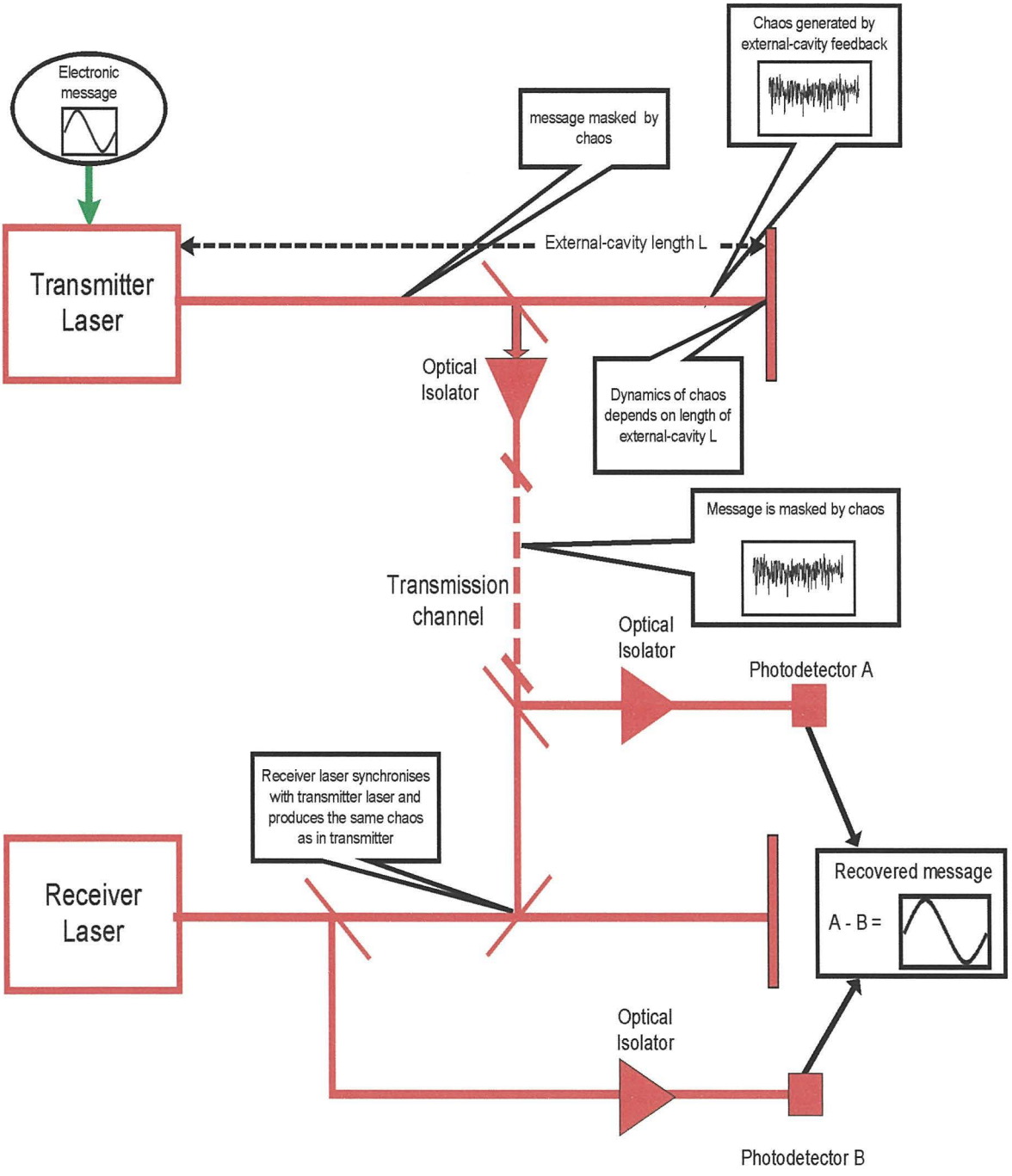

Figure 4.1: *Diagram showing the concept behind message encoding and decoding using external-cavity semiconductor lasers*

The concept behind this method of message masking is that the same chaotic dynamics are available at both transmitter laser and receiver laser i.e. that the transmitter and receiver lasers are synchronised. An eavesdropper intercepting the message in the transmission path will see what appears to be a random signal containing no message.

To achieve message recovery, the photodetector outputs are stored in a digital oscilloscope. The time of flight of the system is removed from photodetector A and both photodetector output are adjusted such that they are of similar amplitude. This ensures that when the subtraction of the photodetectors is completed, maximum message quality is achieved.

Section 4.4 of this chapter is based on [11]. That paper investigates the effects on quality of message recovery for two different receiver laser configurations. The first is with the receiver laser having optical feedback from an external-cavity mirror (closed-loop). The second is with a stand alone solitary receiver laser with no optical feedback (open-loop). Also, the method of message encoding is modified such that the message is optically injected into the external-cavity of the transmitter laser (optical modulation). The first demonstration of optical modulation in such a scheme [12] is discussed further in chapter 5.

4.1 Experimental Set-up for message masking and unmasking

The experimental arrangement use in [9] is shown schematically in figure 4.2. The transmitter and receiver lasers are subject to optical feedback from external mirrors (M1 and M2), the feedback strength being controlled by continuously variable neutral density filters (NDF1 and NDF2). The cavity length is 50 cm in both cases. The optical isolators (OFR-IO-5-NIR-HP) ensure that the lasers are free from back reflection and the typical isolation is –41dB per isolator. Isolator IO1 and IO2 ensure that the transmitter is isolated from the receiver. The plane of polarisation of the laser is parallel to the plane of the table. Each isolator introduces a change in the plane of polarisation by 45^0. A half wave plate (HWP) corrects this polarisation change introduced by IO1 and IO2. Two identical fast photo detectors (Newport, model no. Ad-70xr) of bandwidth 6GHz are used for detection. The output of the transmitter is coupled to photodetector PD1 via beam splitter BS1 and BS2.

Beam splitter BS3 acts as a coupling element between the transmitter and receiver. Beam splitter BS4 couples the receiver output to photodetector PD2. The photodetector outputs are stored in a digital storage oscilloscope (LeCroy LC564A 1GHz) and then acquired by a PC. The message is derived from a signal generator (Marconi Instruments - Model 2022) introduced by direct amplitude modulation of the laser drive current via a bias T connector (Mini-Circuits, model ZFBT-6GW) to the transmitter laser.

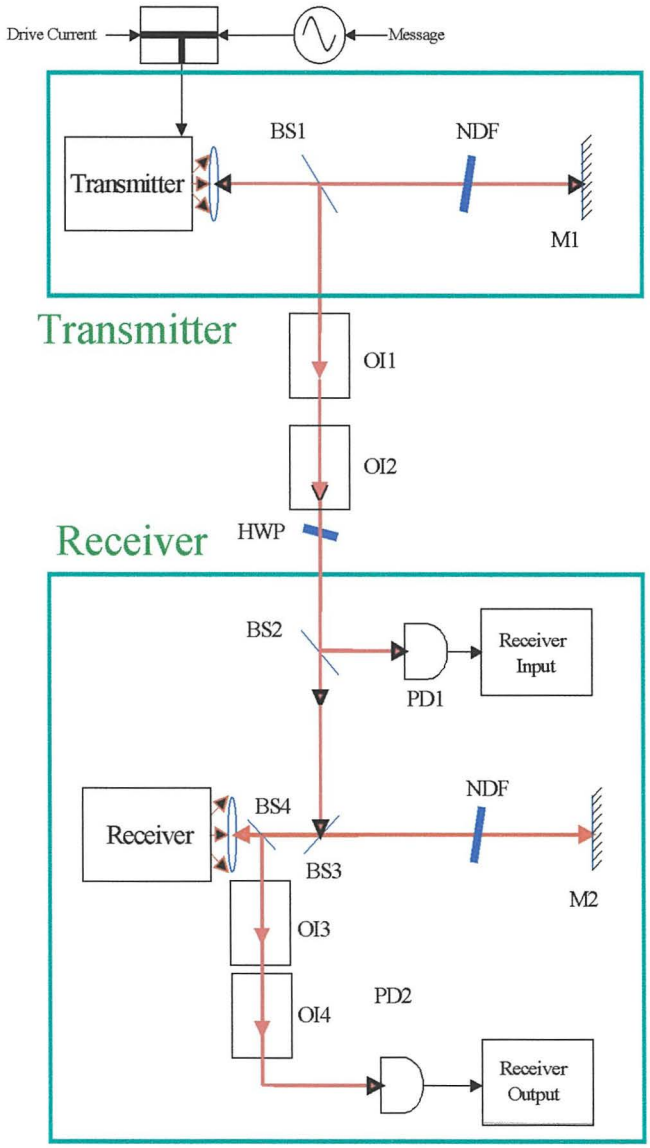

Figure 4.2: *Schematic representation of the experimental arrangement. BS1-BS4, beam splitters; PD1, PD2, photodetector; OI1-OI4, optical isolators; M1, M2, mirrors; NDF's, neutral density filters; HWP, half wave plate*

4.2 Synchronisation and encoding

The transmitter and receiver lasers are driven into chaos by application of appropriate feedback from the external-cavity mirrors. The optical feedback power for transmitter and receiver lasers are –39.1 dB and –39 dB respectively. The free-running threshold current (I_{th}) values are 27mA for both the lasers. The temperature and current of the transmitter (27.53 ^{0}C, 30.51mA) and receiver (25.82 ^{0}C, 27.23mA) are so adjusted to ensure that they operate at the same wavelength. A 1 GHz sine wave from the signal generator is used as the message and is coupled to the laser drive current using a bias T connector, achieving direct amplitude modulation of depth 0.1% of the chaotic transmitter laser output. A fraction (4.2%) of the transmitter optical output is fed to the receiver laser, which leads to synchronisation of the lasers. The receiver laser set-up is as identical as possible to the transmitter laser set-up, especially in terms of cavity length, feedback strength and operating current. The time traces of the transmitter and receiver output are shown in figure 4.3(a) and (b) respectively. The power spectra of the transmitter and receiver output are shown in figure 4.3(c) and 4.3(d) respectively.

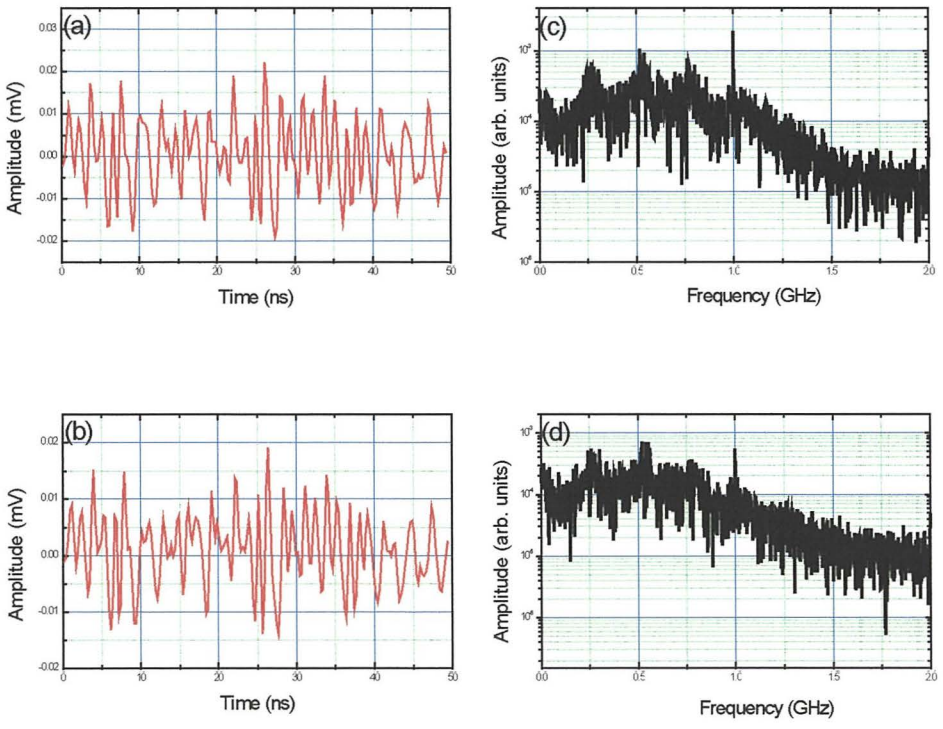

Figure 4.3: *(a) transmitter output, (b) receiver output, (c) power spectrum of the transmitter output, the strong peak shows the message component and (d) power spectrum of the receiver output, the strong peak shows the message component*

For the present experiment deliberate use has been made of a relatively strong message signal whose presence is clearly seen in figures 4.3(c) and 4.3(d). Figures 4.3(a) and 4.3(b) show that the receiver laser output follows the output of the transmitter as is confirmed by plotting the synchronisation diagram shown in figure 4.4.

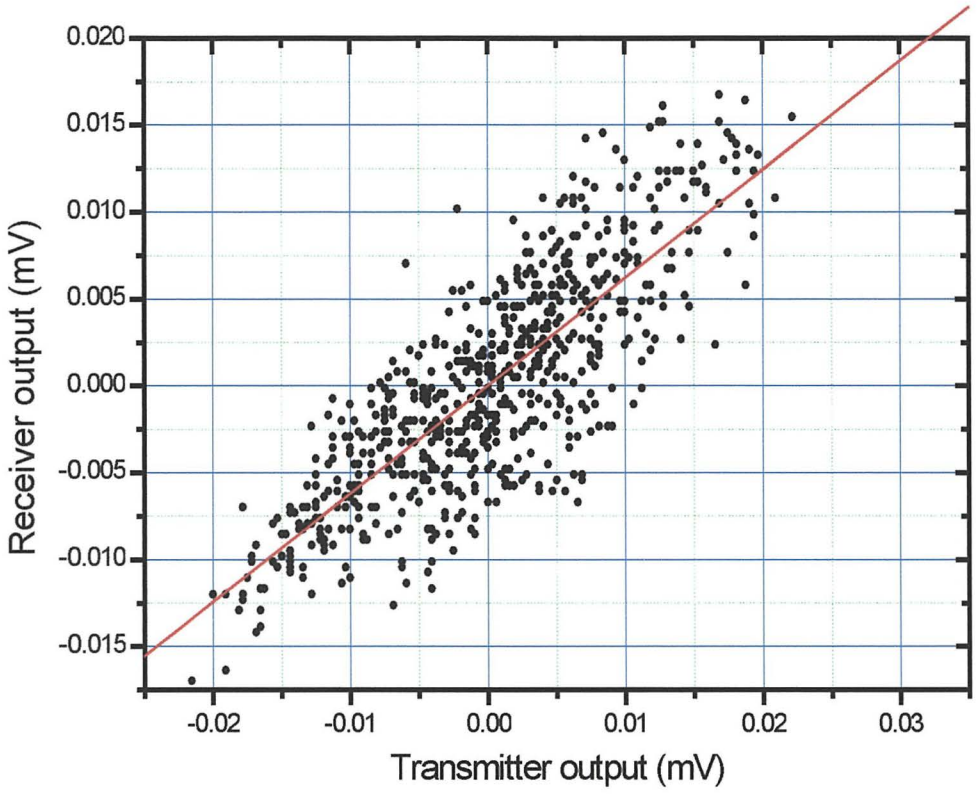

Figure 4.4: *Synchronization plot. Receiver output intensity is plotted against the transmitter intensity. The straight line shows the fitting of the synchronisation plot*

4.3 Decoding

A similar technique to that followed by Van Wiggeren and Roy [3] is used to decode the message. The message is recovered by taking the difference between the output intensities of the transmitter and receiver. The recovered message signal is shown in figure 4.5(a). The power spectrum of the decoded message is shown in figure 4.5(b), which confirms the recovery of the 1GHz message and the suppression of other frequency components.

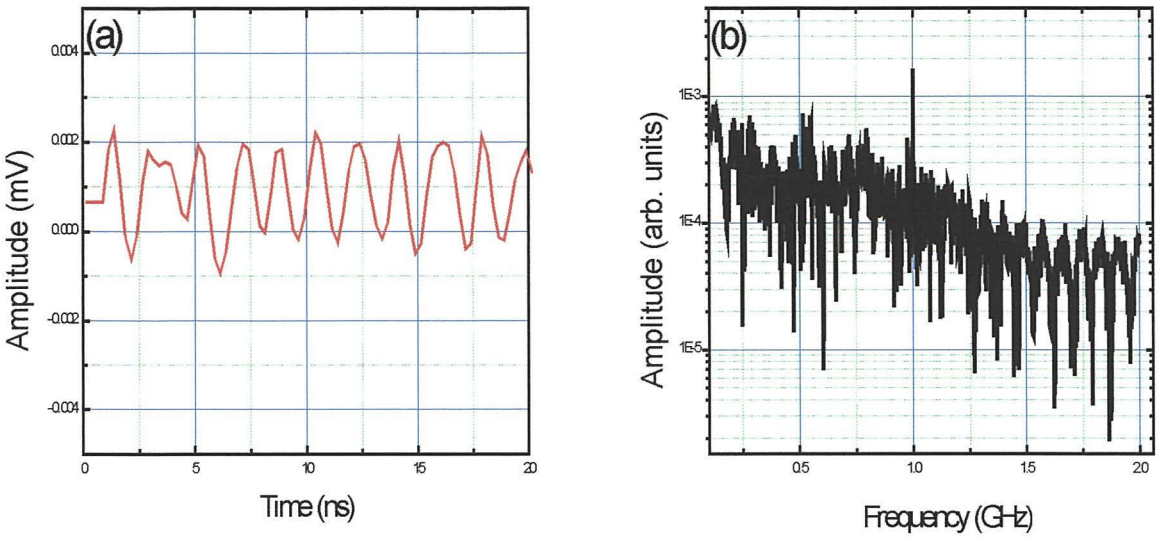

Figure 4.5: *(a) Recovered message and (b) its power spectrum*

It has thus been shown experimentally that it is possible to encode, transmit and decode a 1 GHz bandwidth signal using chaotic external-cavity diode lasers.

4.4 Closed-loop vs. open-loop receivers

The experimental arrangement used in [11] is shown schematically in figure 4.6. The message laser drive current is modulated by a 1 GHz sine-waveform. BS1 is used to couple the message laser and the transmitter laser. BS2 and BS4 are used to couple the transmitter laser to the receiver laser. The outputs of the transmitter laser and receiver laser are coupled to PD1 and PD2 via BS3 and BS5 respectively. The coupling strength between the message and transmitter lasers is controlled by CA1. Likewise, the coupling strength between the transmitter and receiver lasers is controlled by CA2.

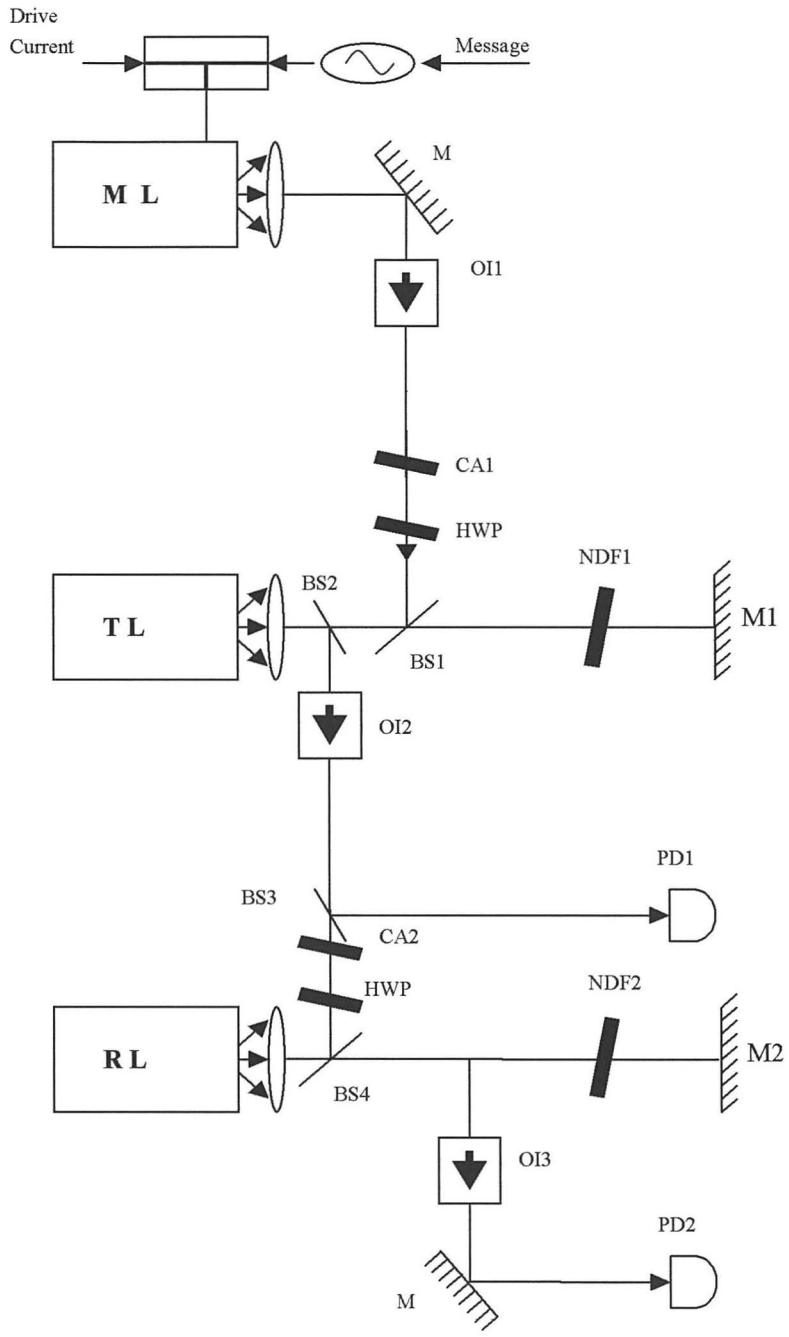

Figure 4.6: *Schematic representation of the experimental arrangement ML: Message Laser; TL: Transmitter Laser; RL: Receiver Laser; BS: Beam Splitter; M: Mirror; OI: Optical Isolator; CA: Coupling Attenuator; NDF: Neutral Density Filter; HWP: Half-Wave Plate; PD: Photodetector*

The transmitter laser is subjected to optical feedback from an external-cavity mirror M1 placed at a distance of 70 cm. In the closed-loop scheme, M2 is adjusted such that the receiver has the same external-cavity length as the transmitter and in the open-loop scheme, M2 is removed. The optical feedback levels of the transmitter and receiver in the closed-loop scheme are varied by using NDF1 and NDF2 so that the lasers can be rendered chaotic. OI1-3 ensure that the lasers are free from parasitic feedback. Each isolator introduces a change of polarisation by 45^0. Two half wave plates (HWP) are used to correct the polarisation change introduced by OI1 and OI2. Large bandwidth (6 GHz) photodetectors (PD1, PD2) are used in the experiments to ensure high frequency operation of the chaotic system.

In this experiment, the most critical parameter to match is the centre wavelength of all three lasers. The temperature and current of the message laser and transmitter laser (22.10 ^{0}C and 34.74 mA) are adjusted such that they operate at same wavelength. For the receiver laser, the temperature and current are adjusted to 25.78 ^{0}C and 28.10 mA in the case of the closed-loop scheme, and 25.78 ^{0}C and 28.80 mA in the case of the open-loop scheme. 20 % of the modulated output power from the message laser is injected into the transmitter via CA1 constituting a 10 dB chaos-to-signal ratio for good message encoding. The transmitter has an external-cavity round trip time which is 4.67 ns and an external-cavity mirror which provides –38 dB optical feedback driving the transmitter laser into the LFF (low frequency fluctuation) regime. The system generates chaotic signals with a bandwidth up to 5 GHz which allows encoding of high frequency messages. In the closed-loop configuration, 0.7 % of the transmitter output power and 0.3 % of the receiver feedback intensity are injected into the receiver. Thus, the total receiver input power is 1%. In the open-loop configuration, 3 % of the transmitter output power is injected into the receiver.

Measurements of the quality of chaotic synchronisation without a message were made for both closed-loop and open-loop configurations. Intensity synchronisation of the transmitter and receiver lasers is obtained and figure 4.7 shows its synchronisation diagrams. The quality of the synchronisation is determined (as explained in chapter 3). The correlation would be unity for perfect synchronisation and zero for two independent systems. The system shows a good synchronisation with correlation factor of 0.942 in the closed-loop case and 0.949 in the open-loop case. The open-loop scheme shows a higher synchronisation quality than the closed-loop scheme. When the transmitter and receiver are decoupled in the closed-loop scheme, the chaotic

outputs of the transmitter and receiver have a correlation factor of less than 0.06. Hence, as expected, they are completely independent chaos generators when they are decoupled.

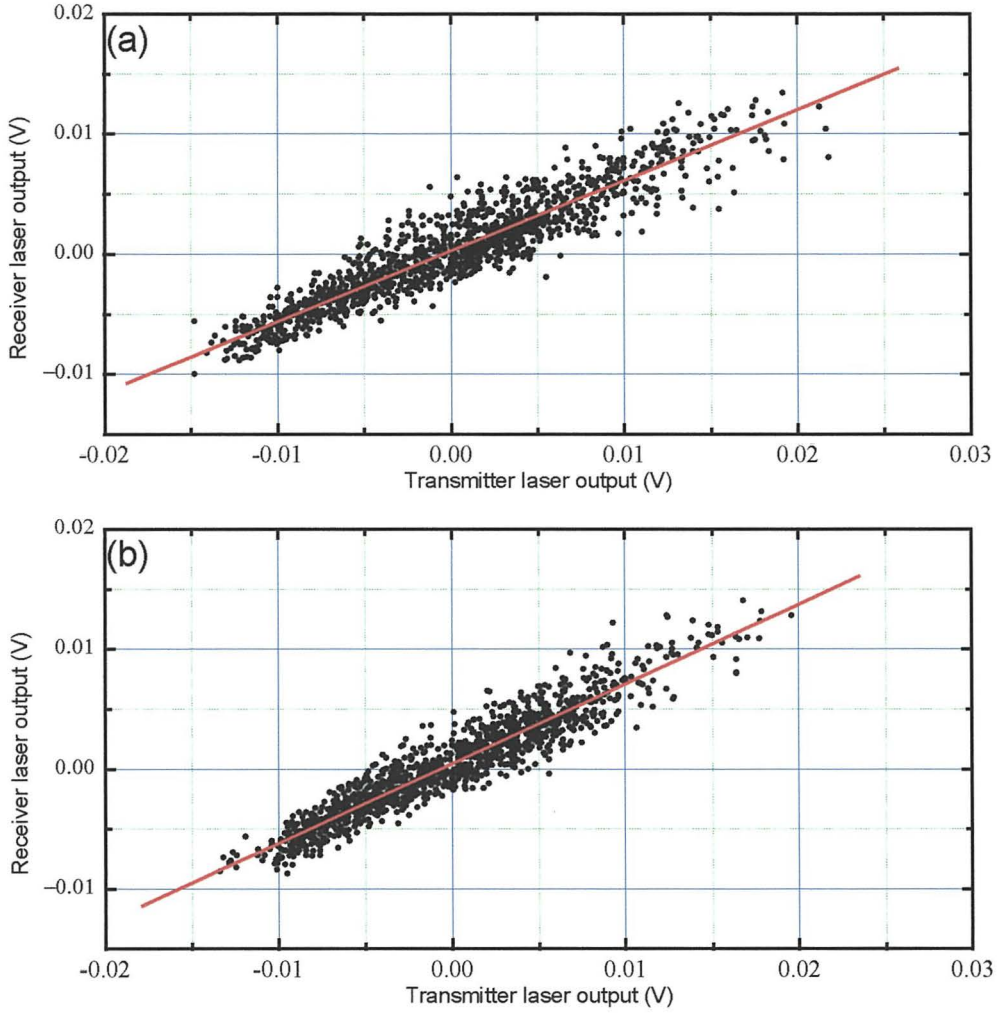

Figure 4.7: *Synchronisation diagram of the transmitter and receiver outputs without message. (a) Closed-loop case. (b) Open-loop*

To measure the synchronisation quality as a function of current, the receiver laser current was scanned from 23 mA to 33 mA whilst fixing the laser operating temperature. The current and the temperature of the message and transmitter lasers were held constant. Figure 4.8 shows the correlation factors as a function of the receiver laser current for the closed-loop and open-loop configurations.

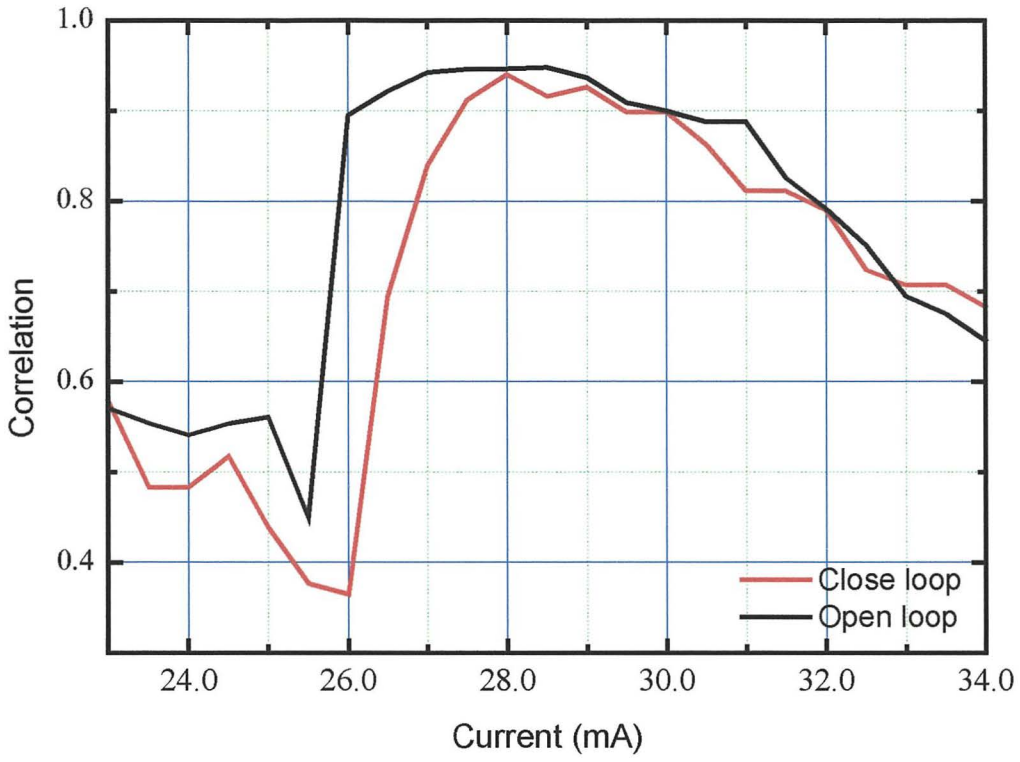

Figure 4.8: *Correlation factor as a function of the receiver laser current*

The synchronisation quality of the open-loop configuration remains higher than that of the closed-loop configuration. The coupling rate and feedback level of the transmitter were found not to have a significant effect on this result. Moreover, the near constant value of the synchronisation quality around the drive current of 28 mA, indicates that the synchronisation in the open-loop scheme is more stable than in the closed-loop scheme. For currents between 23 and 25 mA, the correlation factor is high, but this does not imply good synchronisation, because the slope of synchronisation plot is due to the low output intensity of the laser below threshold.

Synchronisation was implemented with a 1 GHz message being transmitted to the receiver. Figure 4.9 shows the synchronisation between the transmitter and receiver in both the closed-loop and open-loop schemes. The correlation factors, again obtained by fitting the synchronisation plot to a straight line, are 0.937 for the closed-loop scheme and 0.953 for the open-loop scheme. Even with the message, the synchronisation performance of the open-loop scheme is better than that of the closed-

loop scheme. Finally, message decoding has been performed in both the schemes. The technique used for message subtraction is that used by VanWiggeren [3].

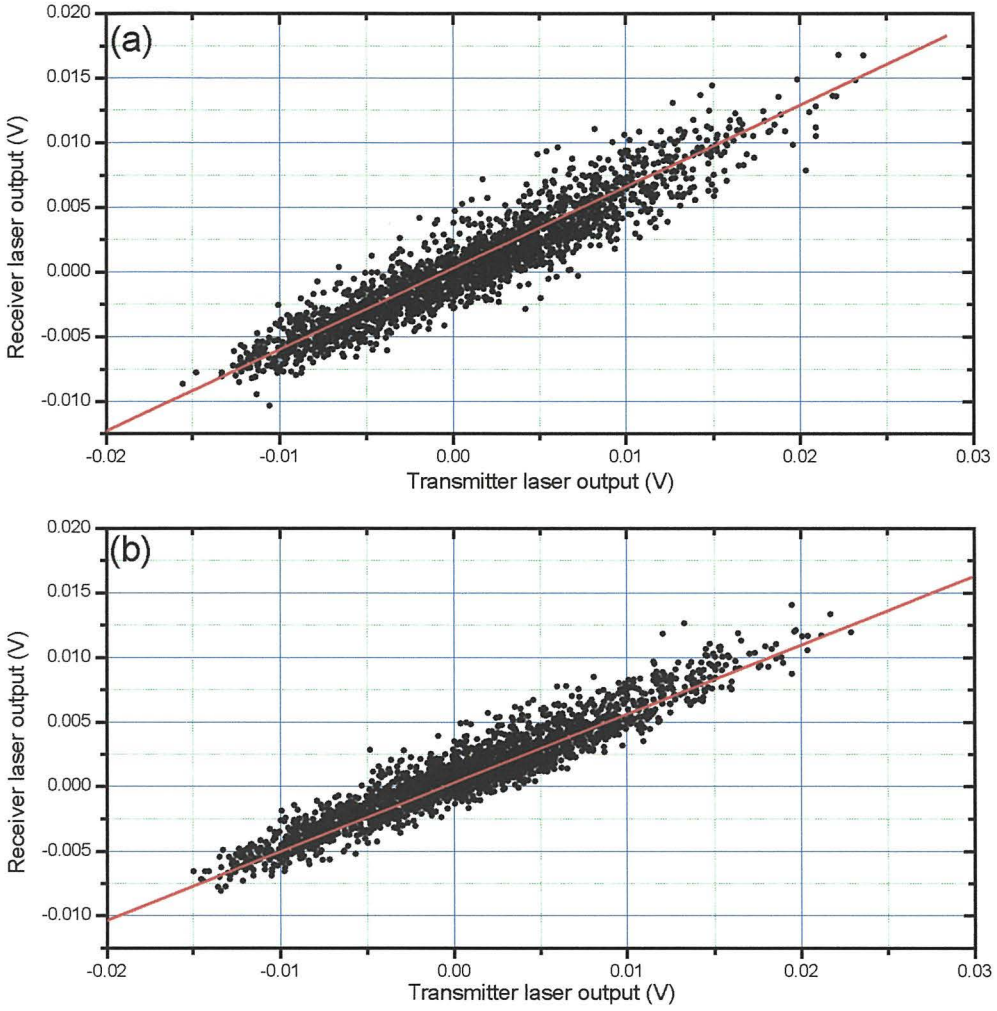

Figure 4.9: *Synchronisation diagram of the transmitter and receiver outputs with message. (a) Closed-loop case. (b) Open-loop case*

The message laser supplies the message to the chaotic transmitter laser, where the message is encoded into the chaotic output of the laser and then transmitted to the receiver. A part of the transmitted signal is coupled to the PD1. The receiver laser output is coupled to the photodetector PD2. The message is recovered by a simple subtraction between the electronic output from PD1 and from PD2. The results of message encoding and decoding are shown in figure 4.10.

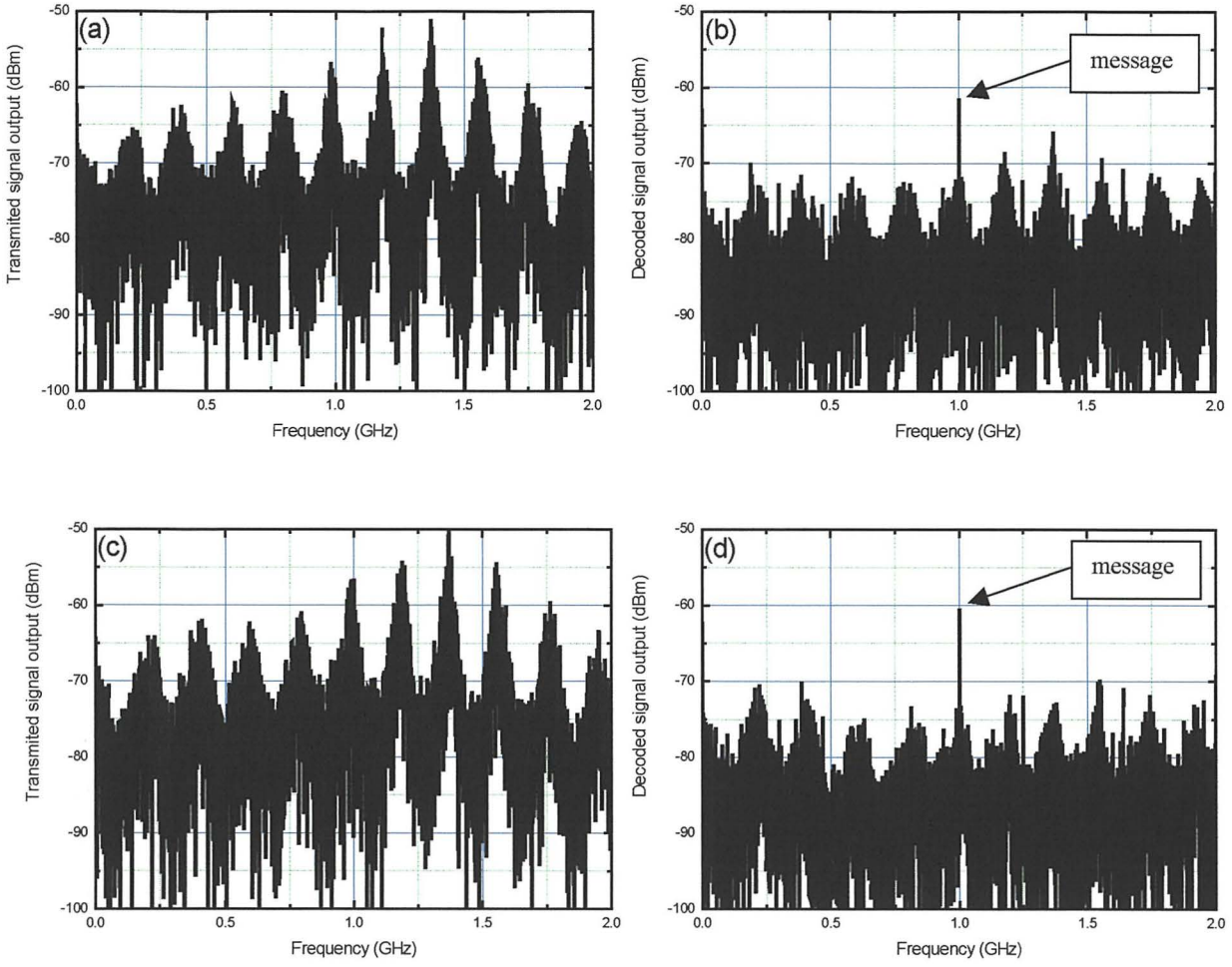

Figure 4.10: *FFT of encoded and decoded message showing (a) the transmitted signal in closed-loop scheme, (b) the recovered message in closed-loop scheme, (c) the transmitted signal in open-loop scheme and (d) the recovered message in open-loop scheme*

Figure 4.10(a) shows the power spectra of the transmitted chaotic signal in which the message is masked for the closed-loop case. The 5 GHz bandwidth chaotic output is able to mask the message. Figure 4.10(b) shows the power spectra of the recovered message where a strong peak indicates the detection of the message at 1 GHz. The decoded message shows about 13 dB of signal-to-noise ratio. It is apparent from figure 4.10(c), that in the open-loop case the message is masked as effectively as in the closed-loop case. Figure 4.10(d) shows the decoded message in the open-loop

scheme where the signal-to-noise ratio of the message is about 16 dB. This value is higher than that of the closed-loop scheme. Thus, even the message decoding quality in the open-loop scheme is better than that in the closed-loop.

4.5 Conclusion

Chaotic message encoding and decoding using external-cavity semiconductor lasers has been experimentally demonstrated. A 1 GHz sinusoidal message was included in the transmitter laser output by direct modulation of its drive current. The message was transmitted through free-space to a receiver laser, which was identical to the transmitter laser and therefore synchronised with the chaotic dynamics but not with the message. By comparing the input and the output of the receiver laser good quality message-recovery was demonstrated. Also a comparison has been undertaken of the qualities of synchronisation and message decoding using closed-loop and open-loop schemes. In the open-loop scheme the receiver laser is subjected only to optical injection from the transmitter laser, while in the closed-loop scheme it also has external-cavity optical feedback. From the results, it was shown that the open-loop scheme has a better performance in terms of synchronisation and message recovery quality than the closed-loop scheme. This conclusion is not affected by changes in the optical feedback level and coupling rate. However, In this case the feedback is incoherent and the result may be different if the feedback is cohrent, this could be verified with by performing the same experiment with lasers that have a long coherence length. The next chapter examines the effects of external-cavity length on the security of the system.

4.6 References

[1] K. M. Cuomo and A. V. Oppenheim, "Circuit implementation of synchronised chaos with applications to communications," Phys. Rev. Lett., vol. 71, pp. 65-68, 1993

[2] J. Ohtsubo, "Chaos synchronisation and chaotic signal masking in semiconductor lasers with optical feedback," IEEE J. Quant. Elec., vol. **38**, pp. 1141-1153, 2002

[3] G. D. VanWiggeren and R. Roy, "Communication with synchronised chaotic lasers," Science, vol. **279**, pp. 1198-1200, 1998

[4] L. Larger, J. Goedgebuer and F. Delorme, "Optical encryption system using hyperchaos generated by an optoelectronic wavelength oscillator," Phys. Rev. E, vol. **57**, pp. 6618-6624, 1998

[5] S. Sivaprakasam and K. A. Shore, "Signal masking for chaotic optical communications using external-cavity diode lasers," Opt. Lett., vol. **24**, pp. 1200-1202, 1999

[6] S. Sivaprakasam and K. A. Shore, "Message encoding and decoding using chaotic external-cavity diode lasers," IEEE J. Quant. Elec., vol. **36**, pp. 35-39, 2000

[7] A. Uchida and S. Yoshimori, "Chaotic on-off keying for secure communications", Opt. Lett., vol. **26**, pp. 866-868, 2001

[8] J. B. Cuenot, L. Larger, J. Goedgebuer and W. T. Rhodes, "Chaos shift keying with an optoelectronic encryption system using chaos in wavelength," IEEE J. Quant. Elec., vol. **37**, pp. 849-855, 2001

[9] J. Paul, S. Sivaprakasam, P. S. Spencer, P. Rees and K. A. Shore, "GHz bandwidth message transmission using chaotic diode lasers," Elec. Lett., vol. **38**, pp. 28-29, 2002

[10] S. Tang and J. M. Liu, "Message encoding-decoding at 2.5gbits/s through synchronisation of chaotic pulsing semiconductor lasers," Opt. Lett., vol. **26**, pp. 1843-1845, 2001

[11] M. W. Lee, J. Paul, S. Sivaprakasam and K. A. Shore, "Comparison of closed-loop and open-loop feedback schemes of message decoding using chaotic laser diodes," Opt. Lett., vol **28**, pp. 2168-2170, 2003

[12] J. Paul, S. Sivaprakasam, P. S. Spencer and K. A. Shore, "Optically modulated chaotic communication scheme with external-cavity length as a key to security," J. Opt. Soc. Am. B., vol. **20**, pp. 497-503, 2003

Chapter 5

Effects of external-cavity length on system security

5.0 Introduction

Having described the method used to encrypt and decrypt a message and also compared the merits of an open loop receiver and a closed loop receiver, this chapter is devoted to the role of the external-cavity length in determining the security of the system. This chapter also describes how it is possible to recover a low amplitude message, thus optimizing the chaos masking of the signal and further increasing the security of the optical system. This chapter is based on publication [1] that demonstrated for the first time an optically modulated chaotic communication scheme which employs the external-cavity length as a key to security. The scheme used in this chapter employs a single external-cavity to drive the transmitter laser to chaos. It is known that with such a configuration an FFT of the transmitter output dynamics can be used to discover the external-cavity length. Recent work [2] that uses two transmitter laser external-cavities of different lengths has identified a regime of operation that prevents an eavesdropper from estimating the external-cavity lengths that are used. This can be achieved by setting one external-cavity length to be a fraction of the other. With two external-cavities the chaotic dynamics output of the transmitter laser are more complex than with a single external-cavity. Thus the potential security of the system is enhanced.

The idea behind the present scheme is the amplitude enhancement of selected chaotic dynamic frequencies produced in the transmitter laser. The frequency of the chaotic enhancement is selected such that either the fundamental frequency, or a harmonic frequency occurs at the same frequency as the message. The external-cavity length used in laboratory experimentation is typically in the range 0.3 to 1.2 meters. Therefore the round trip time of the external-cavity is typically 2 ns to 8 ns giving an external-cavity free spectral range of 500 MHz to 125 MHz. Thus the dynamics of the external-cavity can be enhanced at any selected frequency above 125 MHz by employing the fundamental frequency or a subsequent harmonic.

Use is made of three lasers as message, transmitter and receiver lasers. The message laser is amplitude modulated by a sinusoidal message and its output is optically coupled to the transmitter laser ensuring optical modulation of the message. The transmitter laser is rendered chaotic by application of appropriate optical feedback. The receiver laser is used to decode the message [3]. Since in this system the message is optically encoded in the laser output, it is an all-optical secure communication system. It thus offers advantages with respect to opto-electronic secure systems where the message is encoded by direct injection current modulation [4-6]. A typical communication system comprises of many combined transmission sections and this system allows encoding of a message in one section in an optical manner, without the need of going to an electronic level.

Section 5.2 details the scheme and the equipment and components used. In section 5.3 synchronisation of the transmitter and receiver lasers is demonstrated. Section 5.4 presents the possibility for utilizing the external-cavity length as a key for secure chaotic communications. Message recovery is demonstrated in section 5.5. Section 5.6 presents the possibility of masking, transmitting and recovering a weak message in an all-optical scheme.

5.1 Experimental set-up

The experimental arrangement is shown schematically in figure 5.1. The message is derived from a signal generator (Marconi Instruments – Model 2022) introduced by direct amplitude modulation of the laser drive current via a bias T connector (Mini-Circuits, model ZFBT-6GW) to the message laser. The transmitter laser is subject to optical feedback from an external-cavity mirror. A continuously variable neutral density filter NDF1 controls the feedback strength. NDF2 and NDF3 control the coupling strengths between the message laser and transmitter laser and between the transmitter laser and the receiver laser respectively. The optical isolators (OFR-IO-5-NIR-HP) ensure that the lasers are free from back reflection and the typical isolation is –41dB per isolator. Optical isolators OI1 and OI2 ensure that the message laser is isolated from the transmitter laser and OI3 and OI4 isolate the transmitter laser from

the receive laser. OI5 isolates the receive laser from photodetector PD2. The plane of polarisation of the lasers is parallel to the plane of the table. Each isolator introduces

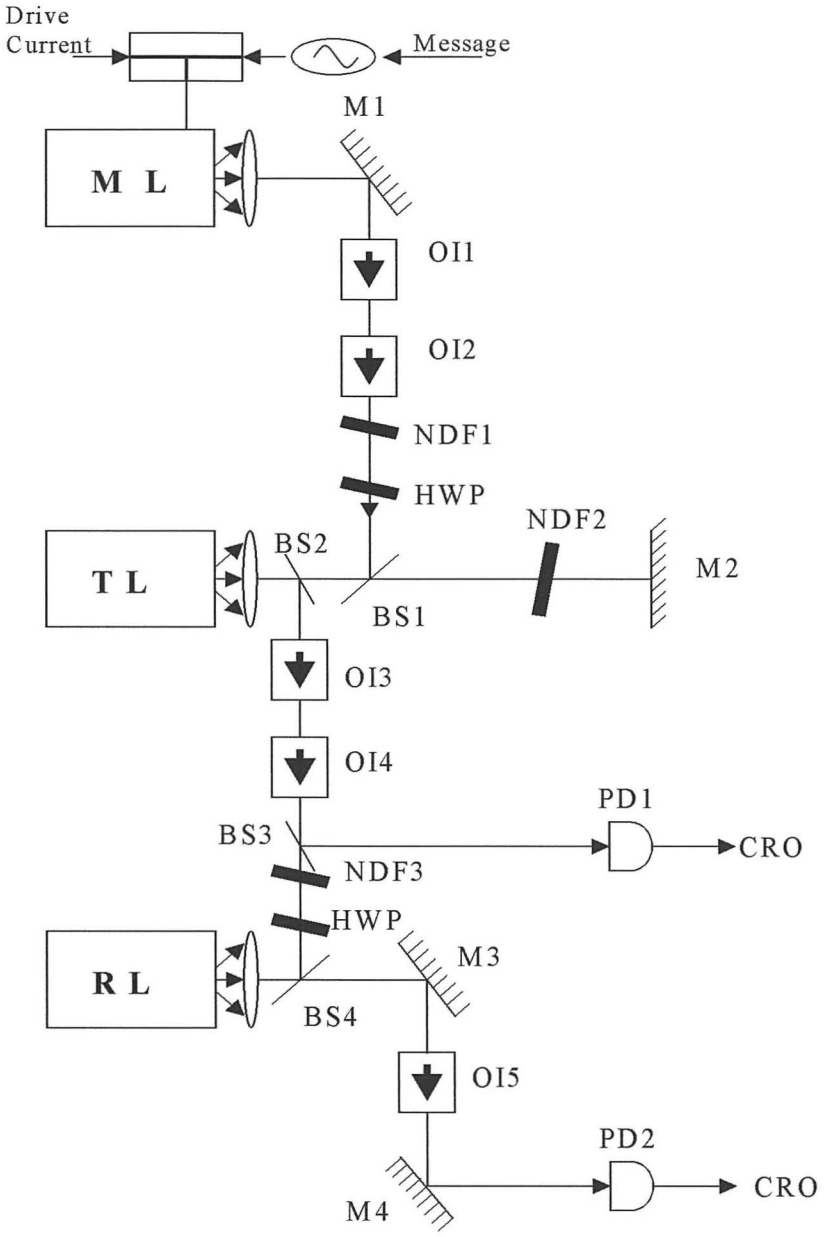

Figure 5.1: *Schematic diagram of experimental arrangement. ML: message laser; TL: transmitter laser; RL: receiver laser; BS1 - BS4: beam splitters; M1 - M4: mirrors; OI1 - OI5: optical isolators; NDF1 - NDF3: neutral density filters; HWP: half wave plates; PD1 and PD2: fast photodetectors; CRO: digital oscilloscope*

a change of polarisation by 45^0. Half wave plates (HWP) are used to correct the polarisation change introduced by IO1, IO2, IO3 and IO4. Beam splitter BS1 acts as a coupling element between the message and transmitter laser. A fraction of the message laser optical output is fed to the transmitter laser. Beam splitters BS2 and BS4 couple the message laser to the receive laser. BS3 and mirrors M3 and M4 couple the transmitter and receiver outputs to the 6 GHz bandwidth fast photodetectors (NewPort, Model no. AD-70xr). The photodetector outputs are stored in a digital storage oscilloscope (LeCroy LC564A 1GHz) and then acquired by a PC.

5.2 Synchronisation

The free-running threshold current (I_{th}) is 27mA for all three lasers. The temperature and current of the message laser (25.18^0C, 27.79mA), transmitter laser (27.15^0C, 32.73mA) and receiver laser (26.52^0C, 25.5mA) are adjusted to ensure that they operate at the same wavelength. The transmitter laser is driven into chaos by application of appropriate feedback from the external-cavity mirror. The optical feedback power for the transmitter is – 39.6 dB.

First, the external-cavity length is adjusted for a round trip time of τ = 6.67ns (L = 100cm) which corresponds to an external-cavity free spectral range of 150MHz. The message laser drive current is modulated with a 150MHz sine wave, achieving direct amplitude modulation of depth 0.6%. NDF1 is adjusted such that 21.4% of the message laser output reaches the transmitter laser. NDF3 is adjusted such that 6.1% of the transmitter laser reaches the receiver laser. The receiver laser output is plotted against the transmitter laser output to obtain the synchronisation diagram shown in figure 5.2 (a). NDF1 is varied such that message laser strengths introduced to the transmitter are 17.1%, 12.3% and 6.5% and associated synchronisation diagrams are shown in figure 5.2 (b), (c) and (d). It is seen from figure 5.2 (d) that for a relatively small signal strength, good-quality synchronisation is obtained. When the signal strength is greater [figures 5.2 (a), (b), and (c)] the synchronisation diagram exhibits a second parallel straight-line behaviour which is referred to as dual synchronisation. The same behaviour is observed if NDF1 is kept constant while the signal level from the signal generator is varied from 6dB to 0dB.

The dual synchronisation diagrams shown in figures 5.2 (a), (b) and (c) have not been observed in experiments with a directly electronically modulated external-cavity scheme. Figure 5.2 shows that it may be possible to determine if message masking has been effective by examination of the proximity of the two synchronisation traces. As the message to chaotic carrier signal strength decreases the dual synchronisation diagram is replaced by a single synchronisation trace. Thus, it can be seen that the message and chaos are separated in the transmitted signal, which is expected as the scheme employed is message masking. Thus, if the message power is kept low compared to the power of the chaos, the message will be more effectively masked.

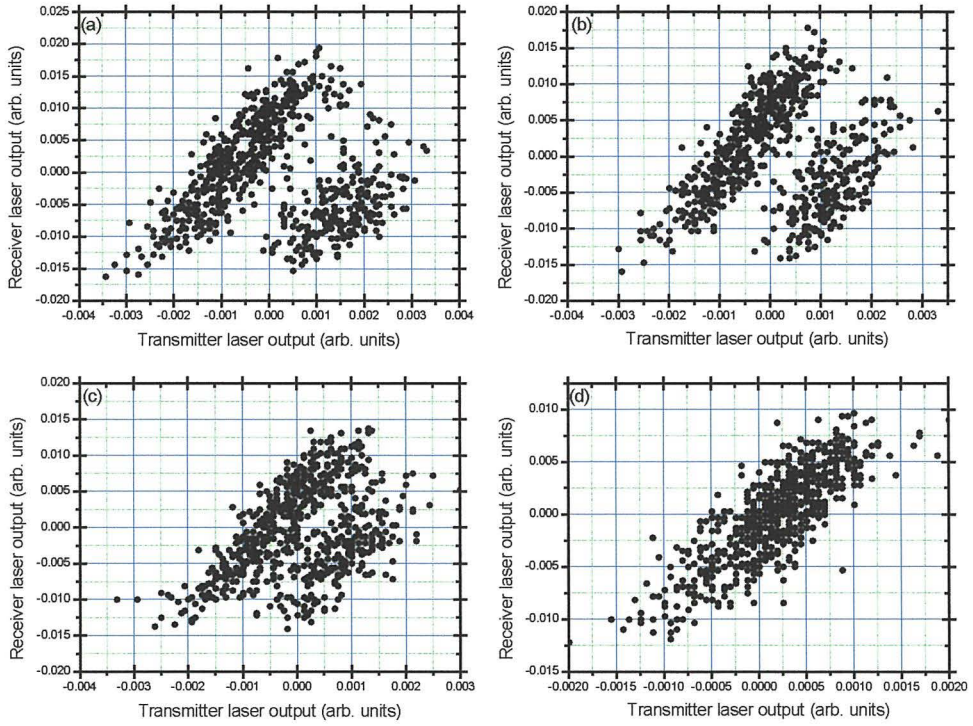

Figure 5.2: *Synchronisation diagrams of transmitter and receiver laser for message laser to transmitter laser strengths of (a) 21.4%, (b) 17.1%, (c) 12.3% and (d) 6.5%*

5.3 Cavity Length as a Key to Security

The external-cavity length is adjusted for a round trip time of τ = 4ns (L = 60cm) which corresponds to an external-cavity free spectral range of 250MHz. The message laser drive current is now modulated with a 150 MHz message of modulation depth 0.5%. NDF1 is adjusted such that the message to transmitter laser coupling is 7.2%.

Figure 5.3 shows the transmitter time trace [figure 5.3 (a)] and its corresponding power spectrum [figure 5.3 (b)]. In the power spectrum the peak (A), at 300MHz, is the first harmonic of the message. Due to the inherent nonlinearities in the system the higher harmonics of the message and the harmonics of the external-cavity free spectral range are shifted in frequency. This results in the second harmonic of the message (B) appearing at about 490MHz, instead of 450MHz as would be otherwise expected.

As can be seen from figure 5.3 (b), the message signal can be clearly observed at 150 MHz. This is due to the mismatch between the external-cavity free spectral range (250MHz) and the signal frequency (150MHz).

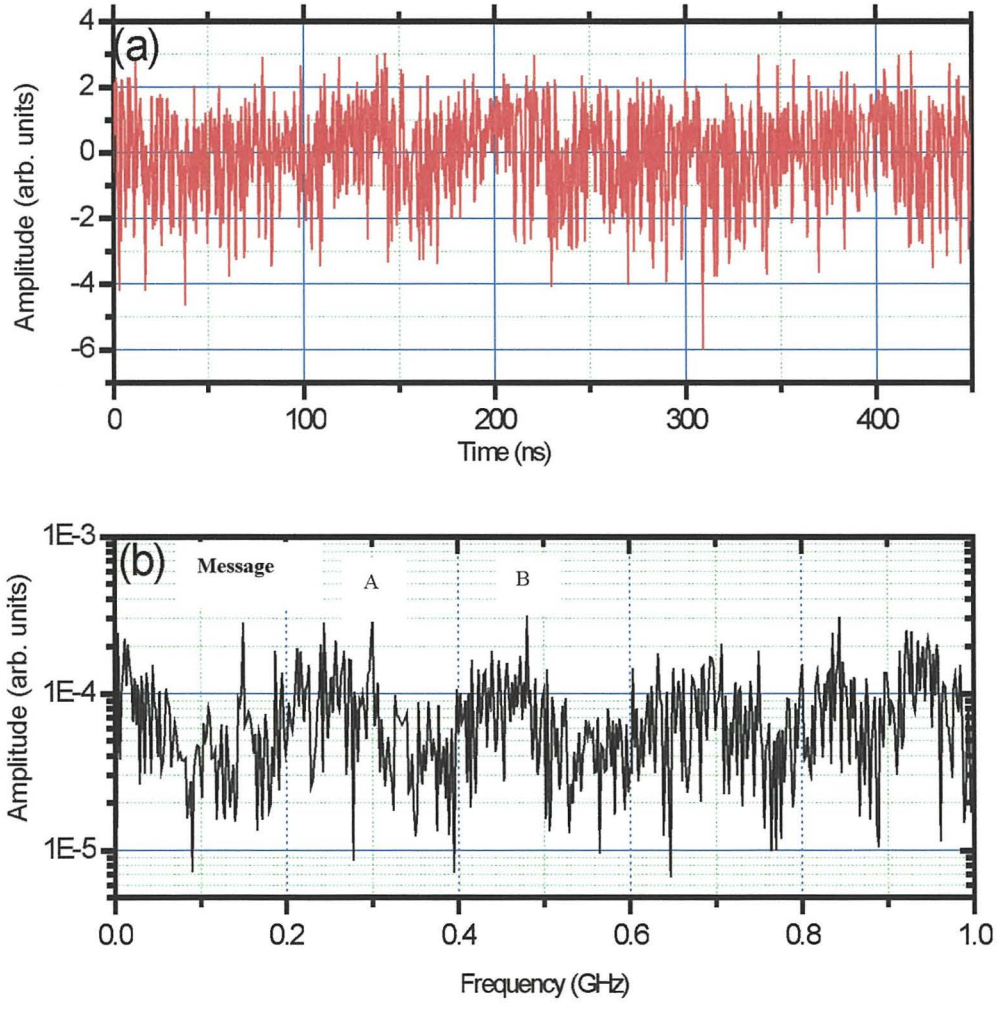

Figure 5.3: *(a) Transmitter time trace and (b) its power spectrum for a 150 MHz message with an external-cavity free spectral range of 250 MHz*

In other words, the external-cavity dynamics does not mask the message frequency. To mask the message the external-cavity length is set to L = 100cm, which give a delay time τ = 6.67ns. This corresponds to an external-cavity free spectral range of 150 MHz, which is equal to the message frequency. The transmitter time trace and its associated power spectrum are shown in figure 5.4 (a) and (b) respectively. Is clear in figure 5.4 (b) that the message signal has been effectively masked because its frequency matches that of the dynamics generated by the external-cavity.

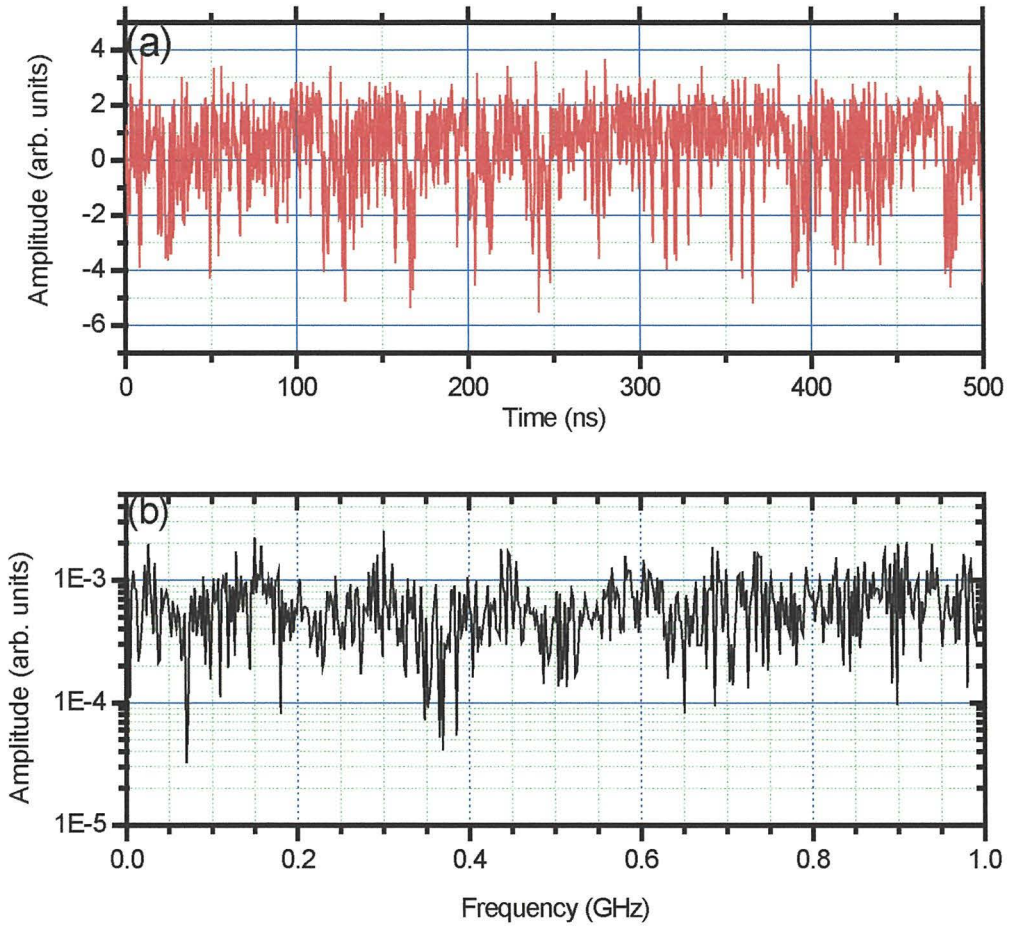

Figure 5.4: *(a) Transmitter time trace and (b) its power spectrum for a 150 MHz message with an external-cavity free spectral range of 150 MHz*

To confirm the necessity of matching the external-cavity free spectral range and message frequency for effective masking, the external-cavity length is now varied to L = 75cm (τ = 4.5ns) corresponding to a free spectral range of 200 MHz. The

message signal frequency is now set to 200 MHz, the same as the free spectral range. The time trace and power spectrum are displayed in figures 5.5 (a) and (b) respectively. The power spectrum shows that the message frequency has been masked within the chaotic dynamics generated by the external-cavity. This confirms that if the external-cavity free spectral range is commensurate with the message frequency, the signal masking is better than when they do not match. So it can be seen that the external-cavity length may be used as a key for secure optical communications. In the next section it is demonstrated that it is possible to recover the message when the free spectral range of the external-cavity equals the message frequency.

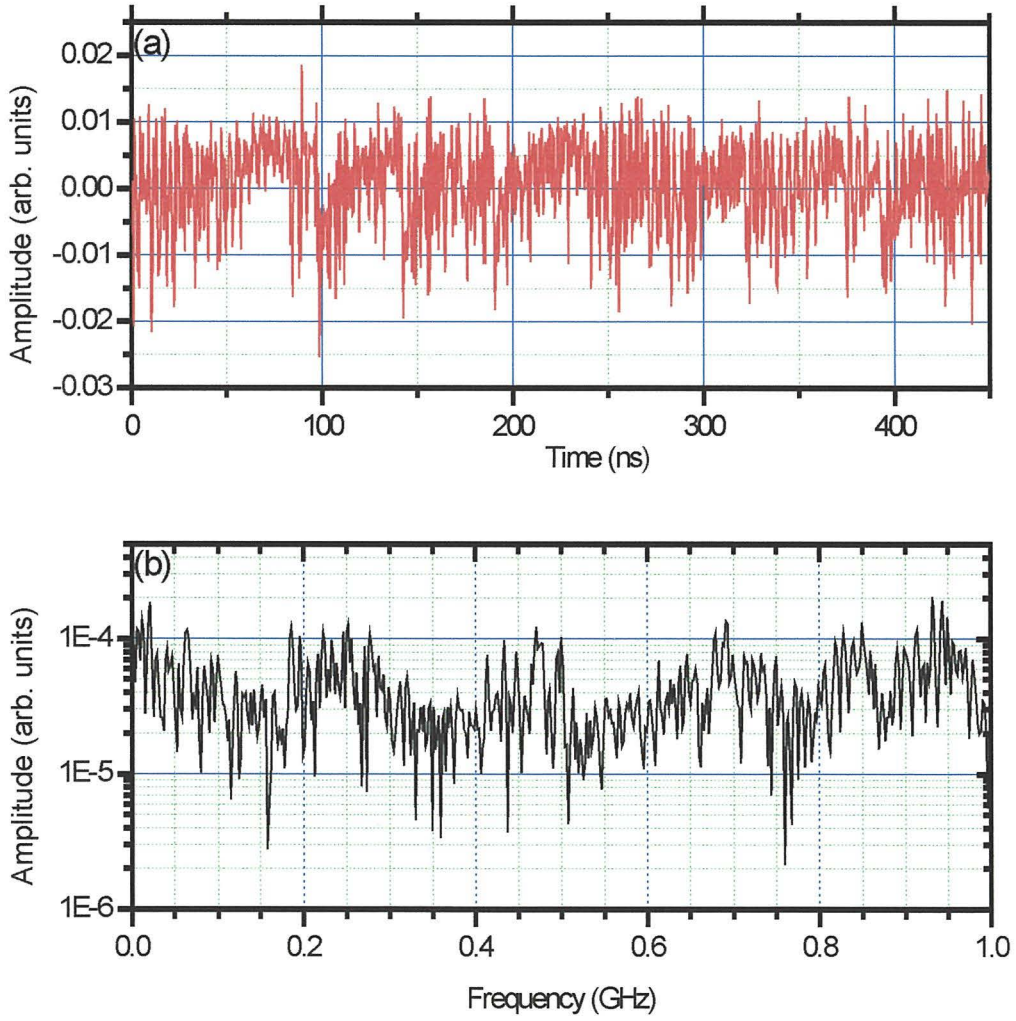

Figure 5.5: *(a) Transmitter time trace and (b) its power spectrum for a 200 MHz message with an external-cavity free spectral range of 200 MHz*

5.4 Message recovery

The technique used here to decode the message was first demonstrated by Van Wiggeren and Roy [3]. The transmitter time trace was shown in figure 5.4 (a), where a message of frequency 150 MHz was masked. The receiver time trace and its corresponding power spectrum are shown in figures 5.6 (a) and (b) respectively. To recover the message the receiver time trace is subtracted from that of the transmitter (after taking into account the time of flight between the transmitter and receiver lasers). The recovered message is then smoothed and is shown in figure 5.6 (c) along with its power spectrum [figure 5.6 (d)].

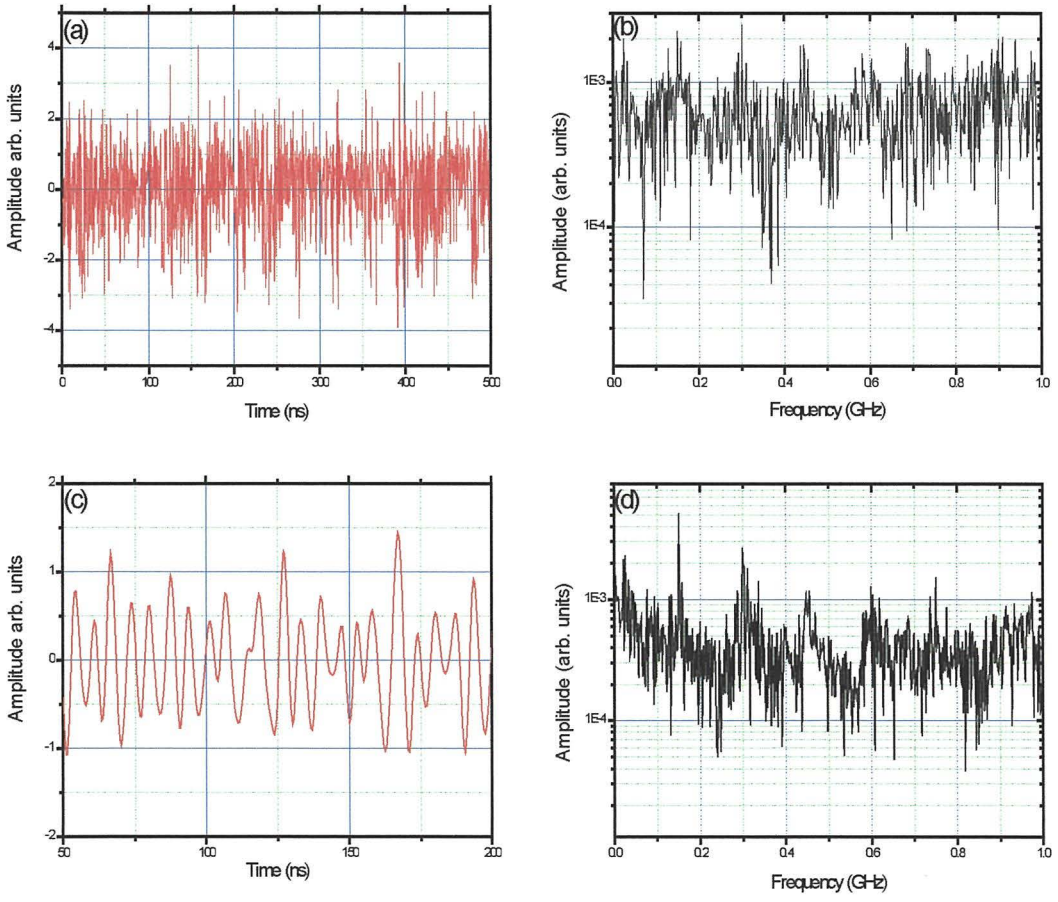

Figure 5.6: *(a) Receiver time trace, (b) receiver power spectrum, (c) recovered message and (d) its power spectrum for a 150 MHz masked message*

Figures 5.6 (c) and (d) show that good message recovery is possible. The same method of message recovery was applied to the 200 MHz message shown in figure 5.5. A successful message recovery was achieved, demonstrating that the all-optical scheme can effectively mask different frequency messages depending on the free spectral range of the external-cavity.

5.5 Weak message transmission

It is well-known that signal masking within the chaotic carrier can be effective only with the use of weak message signals [7] (weak compared to the amplitude of the chaotic oscillations of the system). If the free spectral range of the external-cavity equals the message frequency then, as shown above, the signal is most effectively masked.

In this section it is demonstrated that it is possible to encrypt, transmit, and decrypt a very weak signal, in an optimal way, selecting the external-cavity length to mask the signal.

The external-cavity length is adjusted for a round trip time of 4 ns (L = 60 cm) corresponding to an external-cavity free spectral range of 250MHz. The message laser drive current is now modulated with a 200 MHz message of very small modulation depth (0.4%). This enables the signal strength to be compared to that of the chaotic dynamics generated by the external-cavity. The techniques used for message encryption, transmission and decryption are the same as those above.

Figures 5.7 (a)-(d) display the receiver time-trace, its power spectrum, the recovered message, and its power spectrum. The message is not evident by inspection of the receiver power spectrum [figure 5.7 (b)], but the good message recovery, shown in figures 5.7 (c) and (d), demonstrates that the all-optical scheme is capable of communicating weak message signal strengths.

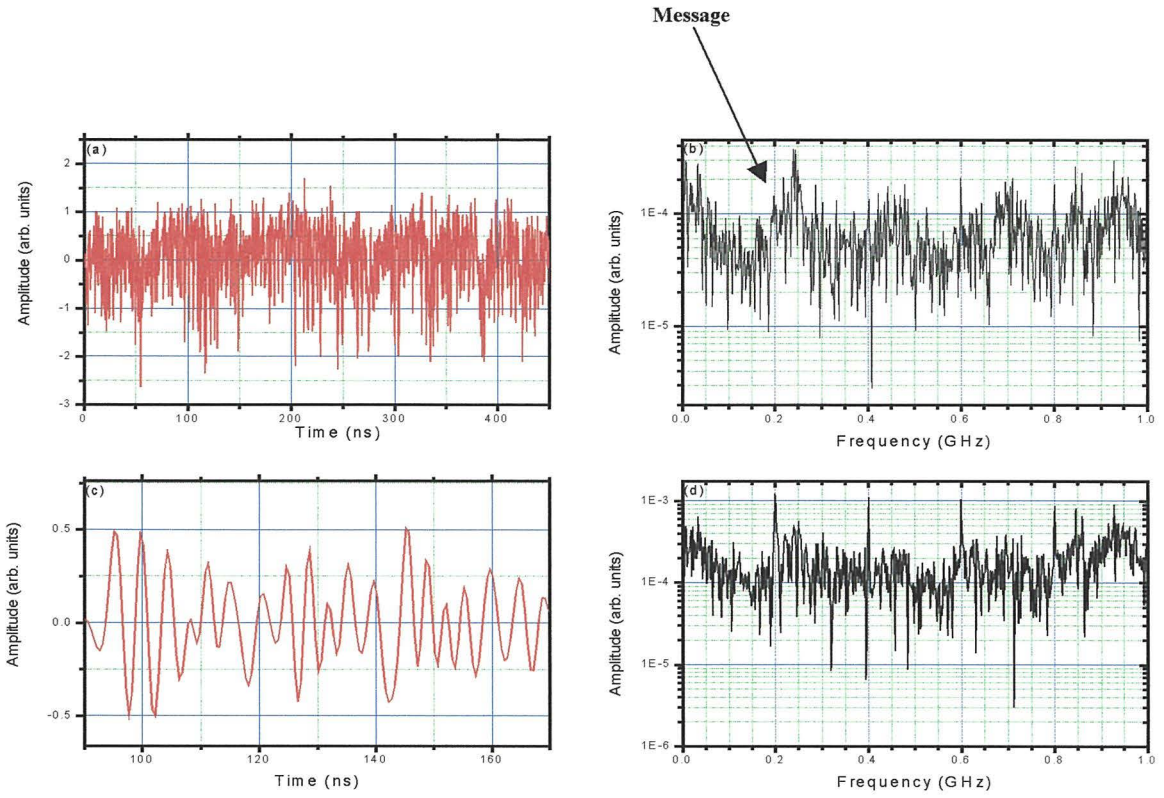

Figure 5.7: *(a) Receiver time trace, (b) receiver power spectrum, (c) recovered message and (d) its power spectrum. The arrow indicates the 200 MHz message*

5.6 Conclusion

A method for optically encoding a message into the output of a transmitter laser was demonstrated experimentally. This method has the advantage of being all-optical, with respect to the usual method to encode a message by direct current modulation. It has been shown that when the message is optically encoded it has to be of small amplitude to be effectively encoded into the chaotic output of the external-cavity transmitter laser. A large amplitude message can be detected through two lines in the synchronisation diagram (referred to as dual synchronisation). The external-cavity length was shown to be a key for increased security. This was done by carefully tuning the external-cavity length such that the chaotic dynamics generated in the transmitter laser effectively masks the frequency of the message. It has also been demonstrated that by using a message laser (rather than direct amplitude modulation of the transmitter laser) the input message into the systems transmitter can be optical rather than electronic. This technique opens the opportunity to construct a multistage

communication system incorporating all-optical repeater stations where the need to transform from an optical form to an electronic one is greatly reduced. It was also demonstrated that this all-optical scheme is capable of masking, transmitting and recovering weak signals.

5.7 References

[1] J. Paul, S. Sivaprakasam, P. S. Spencer and K. A. Shore, "Optically modulated chaotic communication scheme using external-cavity length as a key to security," J. Opt. Soc. Am. B, **20**, pp. 497-503 (2003)

[2] M. W. Lee, P. Rees and K. A. Shore, "Dynamical characterisation of a laser diode subject to double optical feedback for chaotic optical communications," submitted for publication in J. Opt. Soc. Am B.

[3] G. D. VanWiggeren and R. Roy, "Communicating with chaotic lasers," Science, **279**, pp. 1198-1200 (1998).

[4] S. Sivaprakasam and K. A. Shore, "Message encoding and decoding using chaotic external-cavity diode lasers," IEEE J. Quant. Elec. **36**, pp. 35-39 (2000)

[5] J. Paul, S. Sivaprakasam, P. S. Spencer, P. Rees and K. A. Shore, "GHz bandwidth message transmission using chaotic diode lasers," Elec. Lett., **38,** pp. 28-29 (2002).

[6] K. Kusumoto and J. Ohtsubo, "1.5-GHz message transmission based on synchronisation of chaos in semiconductor lasers," Opt. Lett., **27**, 989-991 (2002)

[7] S. Sivaprakasam and K. A. Shore, "Critical signal strength for effective decoding in diode laser chaotic optical communications," Phys. Rev. E, **61**, pp. 5997-5999 (2000)

Chapter 6

Chaotic wavelength division multiplexing

6.0 Introduction

In chapter 2, the method of experimental chaos generation in semiconductor external-cavity lasers was described. Chapter 3 proceeded to an experimental demonstration of synchronisation in two or more coupled semiconductor lasers. The methods employed for message masking and unmasking were demonstrated experimentally in chapter 4. Chapter 5 demonstrated that the external-cavity length can be varied to enhance the effects of message masking within the chaotic dynamics generated in the laser. In this chapter an experimental demonstration is given of how two optical communication channels which can be configured over a single transmission path using two chaotic external-cavity laser diodes as transmitter lasers, and a single stand-alone receiver laser. The two communication channels are shown to operate independently with little cross-talk between them. Two messages, at different modulation frequencies, generated via direct current modulation of the transmitter lasers, were masked by the chaos and were recovered at the receiver laser by the use of a fourth decoder laser. The decoder laser is used to select the channel to be unmasked. The method proposed has two advantages. First, it increases the bandwidth of the common link, overcoming any bandwidth restrictions on message transmission of a single channel (introduced by the highest frequency achievable in chaotic external-cavity laser diodes). Second, as will be explained below, each message is masked within its own chaotic signal, and by transmitting several messages through a common transmission link the complexity of the dynamics in the link is increased which also leads to an increase of the security of the system.

Synchronisation of chaos in laser arrays has been studied in the past by several authors [1-2]. In such configurations the lasers are mutually coupled to each other and therefore their dynamics are different from solitary lasers and have not been used for optical secure communications. For multiple channel chaotic secure communications use must be made of synchronisation of chaos in unidirectionally

coupled lasers. To achieve synchronisation in such systems each pair of lasers (transmitter and receiver) must have very similar parameter setting. But in order to achieve wavelength separation the parameter setting of lasers operating at one wavelength must differ from those of other lasers operating at other wavelengths. It has been shown theoretically that it is possible to synchronise pairs of chaotic oscillators [3] in a multiplexed configuration. More recent work demonstrated experimentally dual synchronisation of chaos in microchip lasers [4].

The method described in this chapter uses two communication channels composed of an external-cavity laser (transmitter laser 1) with a receiver laser; and an external-cavity laser (transmitter laser 2) with the same receiver laser. It is demonstrated that it is possible to transmit a message through each channel and recover the message with the use of a fourth laser, which is referred to as the decoder laser. Each communication channel incorporates three synchronised lasers as previously investigated in the context of cascade synchronisation [5]. As experimentally demonstrated in chapter 3, robust synchronisation is obtainable between three lasers. A demonstration that crosstalk between the two channels is very low and does not significantly affect the quality of the recovered message is also presented.

While in chapters 4 and 5 the message was extracted by comparing the injected signal in the receiver with its output (the standard procedure), here, use is made of a novel scheme to extract the message. In the present case there are two encoded messages whose extraction cannot be effected simply by comparing the signal injected into the receiver laser with its output. To achieve message extraction the decoder and receiver lasers are wavelength tuned such that they synchronise to the appropriate transmitter and comparisons are made of the signals injected into the decoder laser with its output. Thus, by tuning the decoder and receiver lasers it is possible to select which of the two messages is to be extracted. To the best of our knowledge, there is no previous experimental study that has employed this method of message recovery.

This chapter is based on [6] which reports the first experimental demonstration of WDM operation of chaotic semiconductor lasers. Section 6.2 describes the experimental set-up. Section 6.3 the synchronisation characteristics of the two communication channels. Section 6.4 describes message encoding and decoding and section 6.5 presents a conclusion of the results of this chapter.

6.1 Experimental Set-up

The experimental arrangement is shown schematically in figure 6.1.

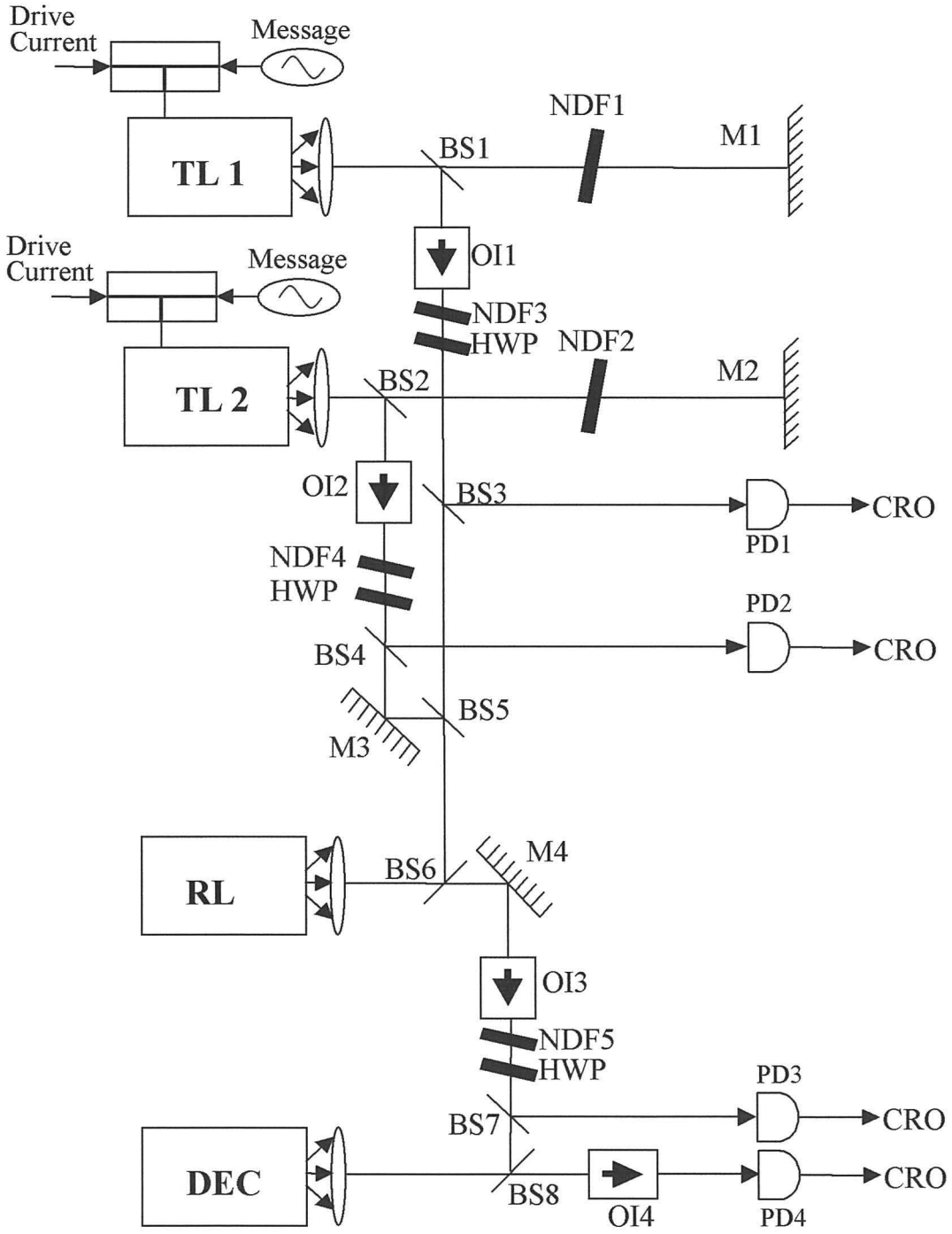

Figure 6.1: *Schematic diagram of experimental arrangement. TL 1: transmitter laser 1; TL 2: transmitter laser 2; RL: receiver laser; DEC: decoder laser; BS1 – BS8: beam splitters; M1 - M4: mirrors; OI1 - OI4: optical isolators; NDF1 - NDF5: neutral density filters; HWP: half wave plates; PD1 - PD2: fast photodetectors; CRO: digital oscilloscope*

The messages are derived from signal generators (Marconi Instruments, Model 2022) and introduced by direct amplitude modulation of the laser drive currents through bias -T connectors (Mini-Circuits, Model ZFBT-6GW). Both transmitter lasers are subject to optical feedback from external-cavity mirrors M1 and M2. Continuously variable neutral-density filters NDF1 and NDF2 control the feedback strength to transmitter 1 and transmitter 2 respectively. NDF3 controls the coupling strength between transmitter laser 1 and the receiver laser. Likewise, NDF4 controls the coupling strength between transmitter laser 2 and the receiver laser. The coupling strength between the receiver and decoder laser is controlled by NDF5. The optical isolators (OFR-IO-5-NIR-HP) ensure that the lasers are free from back reflections, the typical isolation is –41dB per isolator. OI1 and OI2 ensure that transmitter laser 1 and 2 are isolated from the receiver laser, OI3 isolates the receiver laser from the decoder laser. OI4 isolates the decoder laser from photodetector PD4. The plane of polarisation of the lasers is parallel to that of the table. Each isolator introduces a change of polarisation by 45^0. Half-wave plates (HWP) are used to correct the polarisation change introduced by IO1, IO2 and IO3. Beam splitters BS1 and BS6 couple the transmitter laser 1 to the receiver laser. Transmitter laser 2 is coupled to the receiver laser via BS2, BS5, mirror M3 and BS6. Mirror M4 and BS8 couple the receiver laser to the decoder laser. BS3 and BS4 couple the transmitter lasers outputs to PD1 and PD2, the 6-GHz-bandwidth, fast photodetectors (NewPort, Model AD-70xr). The receiver and decoder lasers are coupled to PD3 and PD4 via BS7 and BS8 respectively. The photodetector outputs from PD1, PD2, PD3 and PD4 are stored in a digital storage oscilloscope (LeCroy LC564A 1GHz). The free-running threshold current (I_{th}) is 27mA for all four lasers. The temperature and current of transmitter laser 1 (25.81^0C, 31.17mA) and receiver laser (28.02^0C, 27.78mA) are so adjusted that they operate at the same wavelength (824.837nm). This ensures that maximum coupling is achieved between transmitter laser 1 and the receiver laser and allows for stable synchronisation. The temperature and current of transmitter laser 2 (21.9^0C, 30.6mA) is adjusted so that its wavelength (824.013 nm) is 0.824nm shorter than that of transmitter laser 1 and the receiver laser, as shown in figure 6.2.

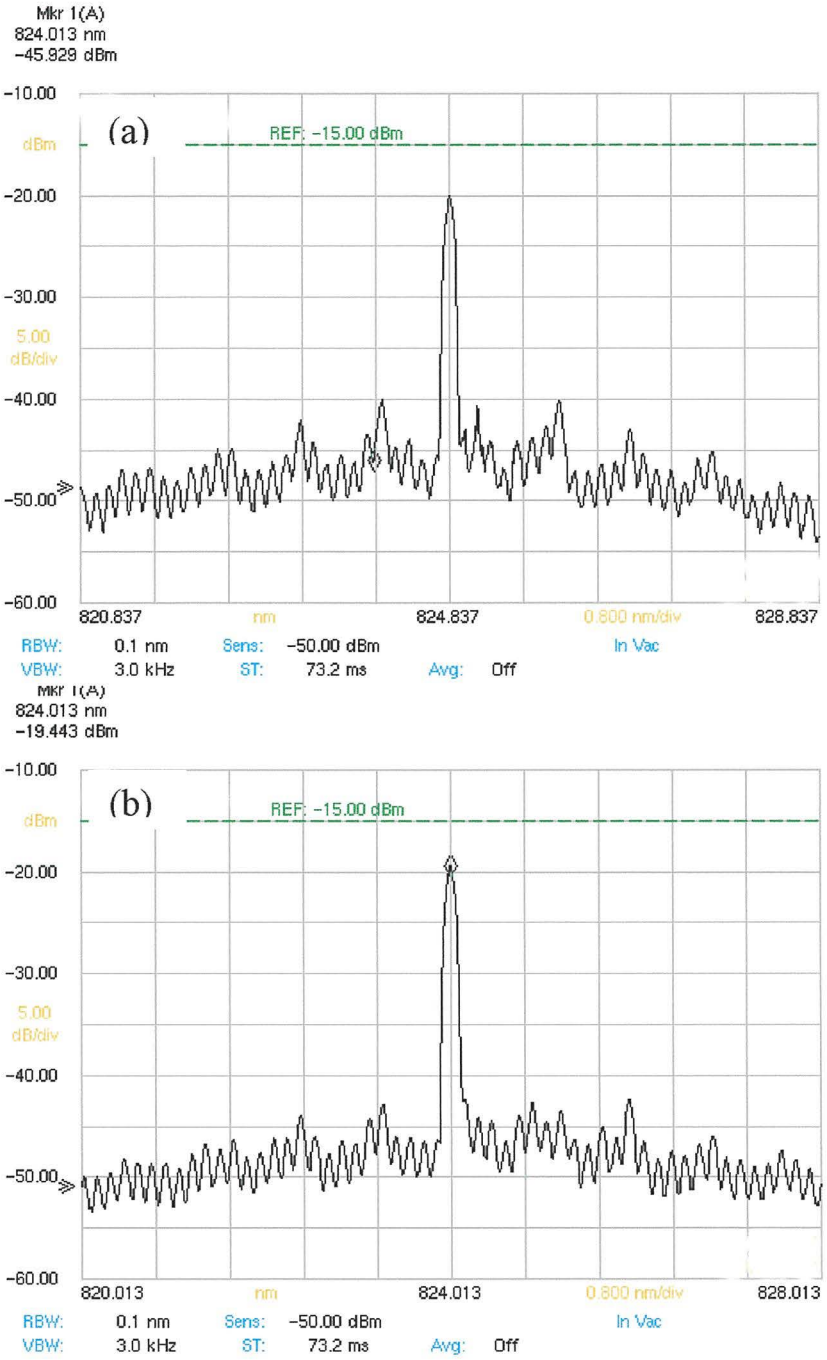

Figure 6.2: *Optical spectrum of transmitter 1 (a) and transmitter 2 (b)*

Both transmitter lasers are driven into chaos by application of appropriate feedback from the external-cavity mirrors M1 and M2. The external-cavity feedback for the transmitter lasers 1 and 2 are –39.77 dB and –39.76 dB respectively. NDF3 is adjusted such that 6.1 % of transmitter laser 1 output is coupled to the receiver. NDF4 is adjusted such that 6.2% of transmitter laser 2 is coupled to the receiver laser.

Likewise, NDF5 is adjusted such that 5.8 % of the receiver laser output is coupled to the decoder laser.

6.2 Chaos Synchronisation

In this section results of the synchronisation of transmitter laser 1, transmitter laser 2, and the receiver laser in the configuration set-up described previously are presented. Figure 6.3 displays synchronisation diagrams: the transmitter laser 1 output (Figures 6.3a, 6.3b) and the transmitter laser 2 output (Figures 6.3c, 6.3d). are plotted vs. the receiver laser output.

When the wavelength of the receiver laser is tuned to match the wavelength of the transmitter 1 laser the synchronisation diagrams shows that the receiver laser is well synchronised to the transmitter laser 1 (Figure 6.3a), but is badly synchronised to the transmitter laser 2 (Figure 6.3c).

When the temperature of the receiver laser (24.40^0C) is adjusted such that its wavelength matches that of the transmitter laser 2 (824.013 nm), the receiver laser

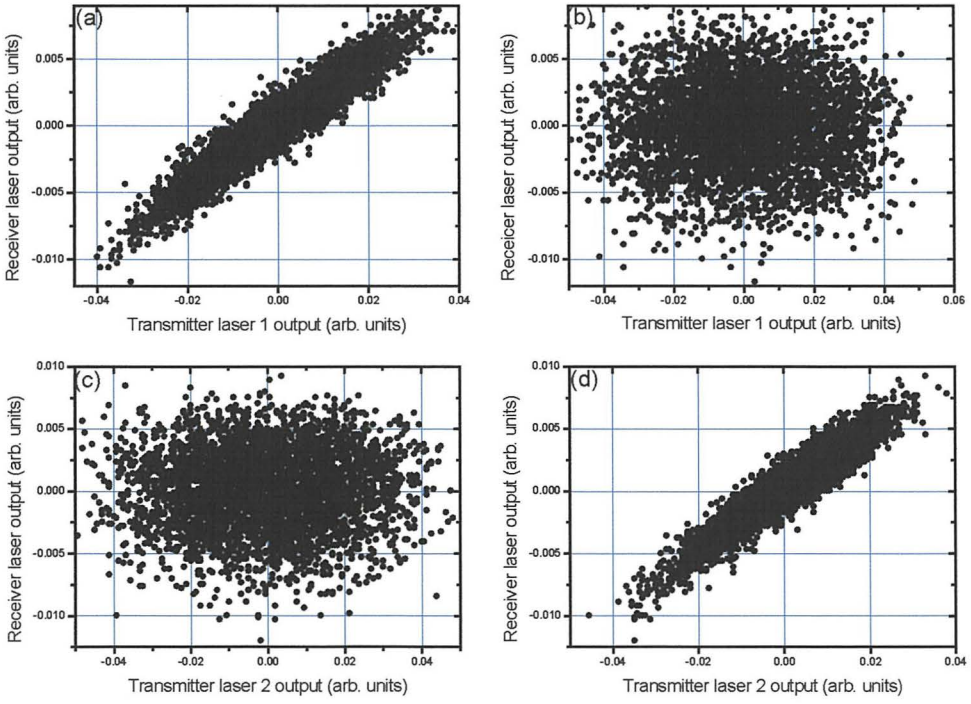

Figure 6.3: *Synchronisation diagrams. Receiver laser vs. transmitter laser 1 (Figures. 6.3a, 6.3b) and vs. transmitter laser 2 (Figures 6.3c, 6.3d)*

synchronises well to the transmitter laser 2 (Figure 6.3d) and not to the transmitter laser 1 (Figure 6.3b). This demonstrates that the chaotic output of the two transmitter lasers can be independently tuned such that they synchronise with a single receiver laser. Since the two transmitter lasers operate at different wavelengths, there are two different channels available for message transmission.

An examination of the effects of interference between the two communication channels is undertaken. The wavelengths of transmitter 2 and receiver lasers are adjusted to match, so that their outputs are synchronised, and the drive current of the transmitter laser 1 is varied (in 2mA steps from 20mA to 40mA). Figure 6.4 (a), (b) and (c) display the synchronisation diagrams between receiver laser and transmitter laser 2 for transmitter laser 1 drive currents of 20mA, 30mA and 40mA respectively.

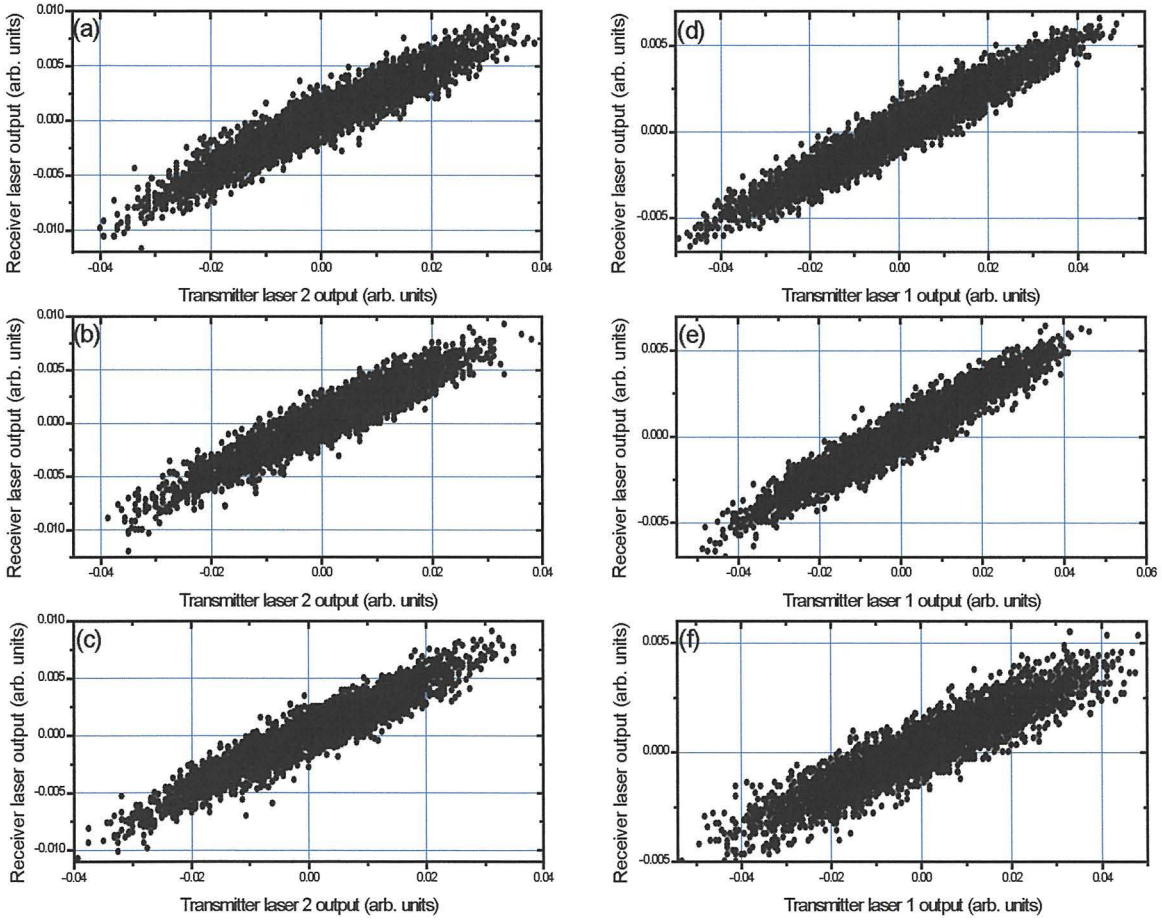

Figure 6.4: *Cross talk synchronisation diagrams. Receiver vs. transmitter laser 2 for transmitter laser 1 drive currents of 20mA (a), 30mA (b), 40mA (c) and receiver vs. transmitter laser 1 for transmitter laser 2 drive currents of 20mA (d), 30mA (e) and 40mA (f)*

The synchronisation diagram shows that the synchronisation correlation of the receiver laser and the transmitter laser 2 is nearly independent of the drive current of the transmitter laser 1. Likewise, when the temperature of the receiver laser is adjusted so that its wavelength (824.837nm) matches that of the transmitter laser 1, and the current of the transmitter laser 2 is varied (from 20mA to 40mA in 2mA steps) it is observed also that the correlation between transmitter laser 1 and the receiver laser has little dependence on the drive current of transmitter laser 2. (see Figures. 6.4 (d), (e) and (f), which show synchronisation diagrams for receiver and transmitter laser 1, with transmitter laser 2 drive currents of 20mA, 30mA and 40mA respectively).

To summarise the above results, Figure 6.5 displays the covariance of the transmitter and the receiver outputs vs. the drive current. The red (black) line shows results for the correlation of transmitter 1 (transmitter 2) and receiver lasers, when the current of transmitter 2 (transmitter 1) laser varies.

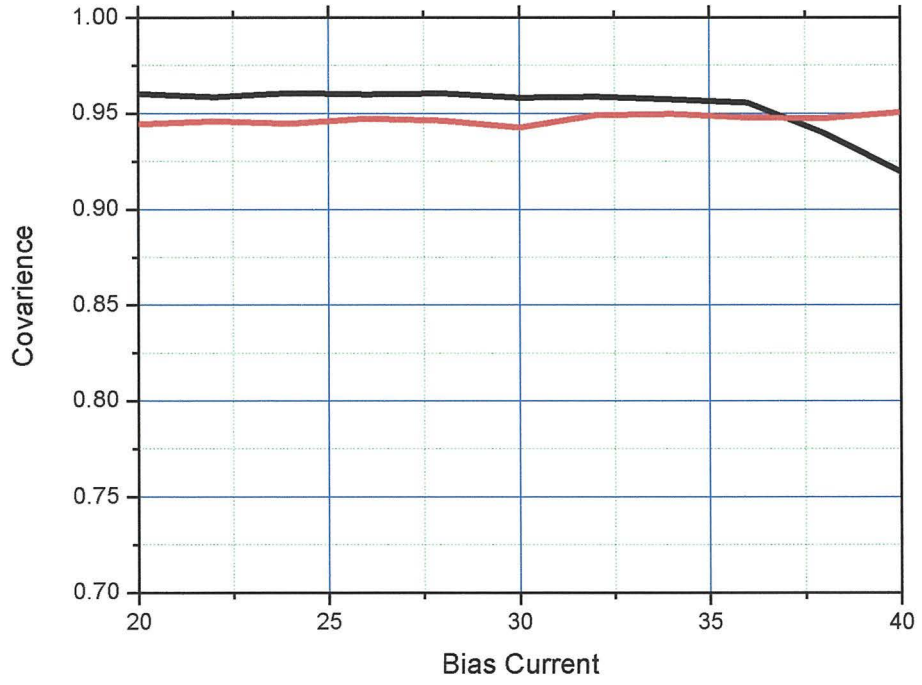

Figure 6.5: *Covariance of transmitter lasers to receiver. The red (black) line shows results for the correlation of transmitter 1 (transmitter 2) and receiver lasers, when the current of transmitter 2 (transmitter1) laser varies*

The lines show an almost constant covariance of the two synchronised lasers, independent of the bias current of the other transmitter laser, thereby showing that two

robust channels can be established. As can be seen in figure 6.5, channel 2 (black line) does show some cross talk as channel 1 transmitter reaches 36 mA, whilst channel 1 (red line) is seen to be unaffected by the bias current of channel 2 transmitter (up to 40 mA). This is due to the different operating wavelength and bias currents of the two channels.

6.3 Message transmission and recovery

In this section results are presented which show that a message can be encoded and decoded independently in the two synchronisation channels described above: transmitter laser 1 – receiver laser; transmitter laser 2 – receiver laser: The message is encoded though direct current modulation of the transmitter lasers. An experimental demonstration in chapter 5 has shown that the external-cavity length is a key parameter in determining the efficiency of message masking in this configuration [7]. In the present experiment two messages are transmitted at different modulation frequencies and a demonstration that cross-talk interference in transmission is minimal is given. For this reason appropriate external-cavity lengths are selected to enable secure transmission of the chosen messages. The message frequencies are chosen to be close to that of the second harmonic of the free spectral range of the transmitter laser external-cavities. The bias current of transmitter laser 1 is modulated with a 510 MHz message of modulation depth 0.4%. Likewise the bias current of transmitter laser 2 is modulated with a 680 MHz message of modulation depth 0.37%. The external-cavity length of transmitter laser 1 -60cm- and transmitter laser 2 -67cm- are set so that their free spectral range are 250 MHz and 225 MHz respectively. This combination ensures effective message masking.

In chapter 4 and 5 the message recovery technique employed is one that is commonly used in experimentation on secure chaotic communication systems [8]. However, in the current configuration comparing the input of the receiver laser to its output would not allow message recovery. This is because the input to the receiver laser contains both chaotic transmitter laser outputs. For the recovery of the message a fourth laser is employed - the decoder laser. The decoder laser synchronises to the receiver laser, and by subtracting the outputs of the decoder laser and the receiver laser the message

can be recovered (the time-of- light of the system is taken into account). Figure 6.6 shows the time traces of the transmitter laser 1 (Figure 6.6a), receiver laser (Figure 6.6b), decoder laser (Figure 6.6c) and recovered message (Figure 6.6d). The units in the vertical axis are arbitrary but are the same in all the figures. The temperature and current of the decoder laser (25.30^{0}C, 30.2mA) were adjusted so that its wavelength (824.837nm) matches that of transmitter laser 1 (which is synchronised to the receiver laser). It can be seen that the three lasers are well synchronised and the message (which is the difference between the time traces shown in figures 6.6c and 6.6b) is recovered.

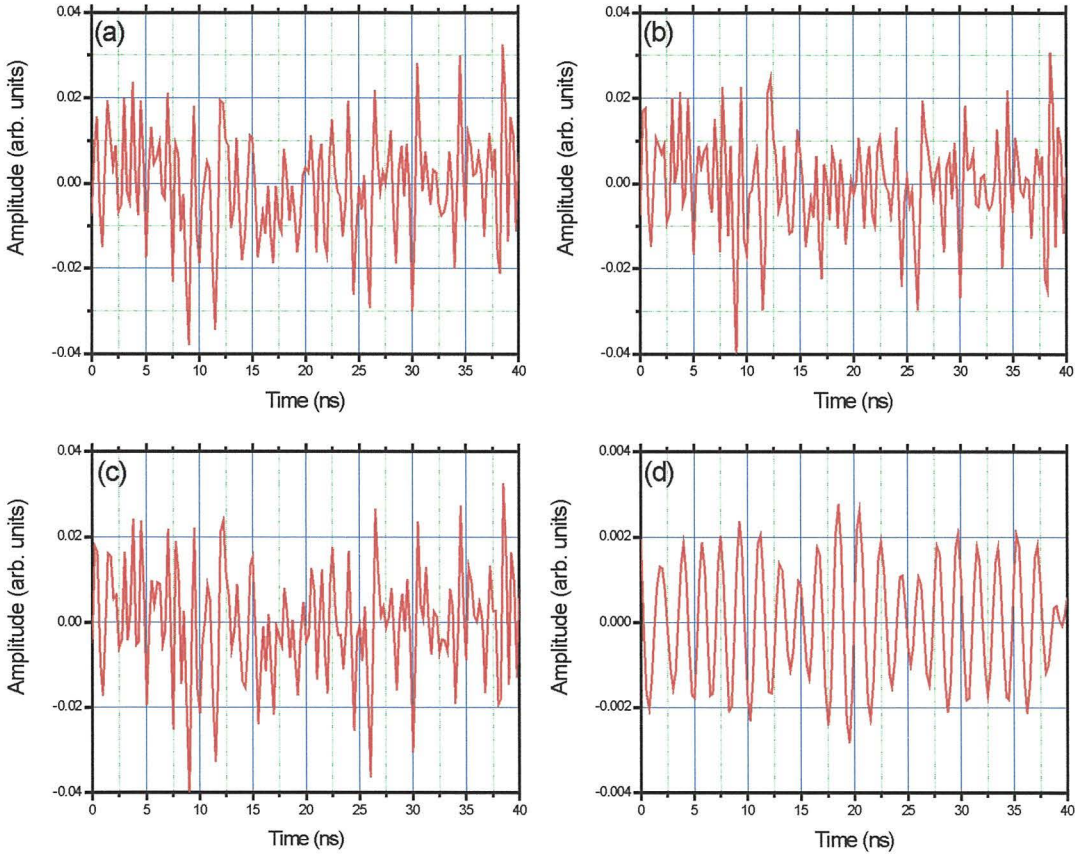

Figure 6.6: *Time traces of transmitter laser 1 (6a), receiver laser (6b), decoder laser (6c) and recovered (510 MHz) message (6d)*

Figure 6.7 displays the corresponding FFT of the transmitter laser 1 (figure 6.7a), receiver laser (figure 6.7b), decoder laser (figure 6.7c), and recovered message (figure 6.7d). The frequency of the message (510 MHz) is hidden in the chaotic background of the spectrum of the three lasers, but is clearly visible in the spectrum of the

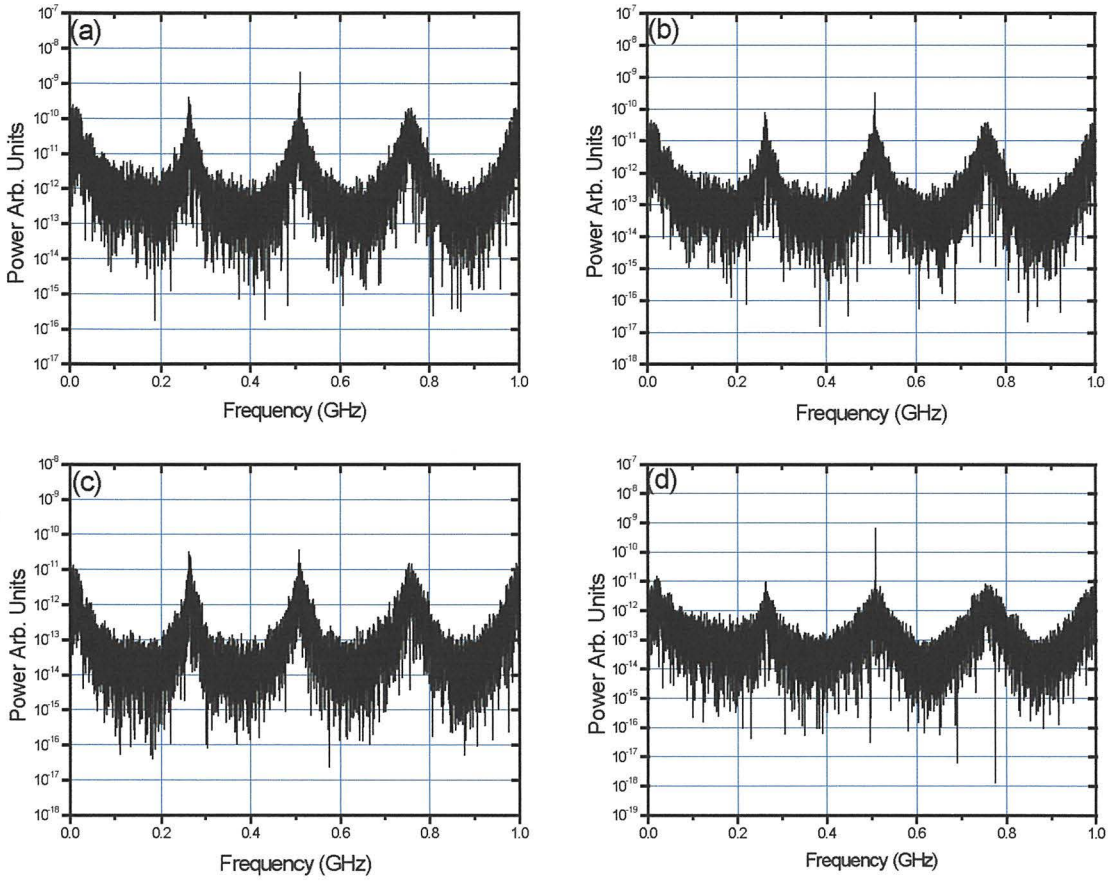

Figure 6.7: *Corresponding FFT plots for Fig. 6 showing, transmitter laser 1 (7a), receiver laser (7b), decoder laser (7c) and recovered (510 MHz) message (7d)*

recovered message. There is no crosstalk between the two communication channels because the frequency of the second message (680 MHz, hidden in the output of transmitter 2) does not appear in the spectrum of the recovered message. When the bias current and the temperature of the receiver and decode lasers are adjusted such that they synchronise with the transmitter laser 2, the messaged encoded in the chaotic output of transmitter 2 can again be recovered. Figure 6.8 shows the time traces of the transmitter laser 2 (Figure 6.8a), receiver laser (Figure 6.8b), decoder laser (Figure 6.8c) and recovered message (Figure 6.8d). The units in the vertical axis are arbitrary but are the same in all the figures. It can be seen that the three lasers are well synchronised and the message (which is the difference between the time traces shown in figures 6.8c and 6.8b) is recovered.

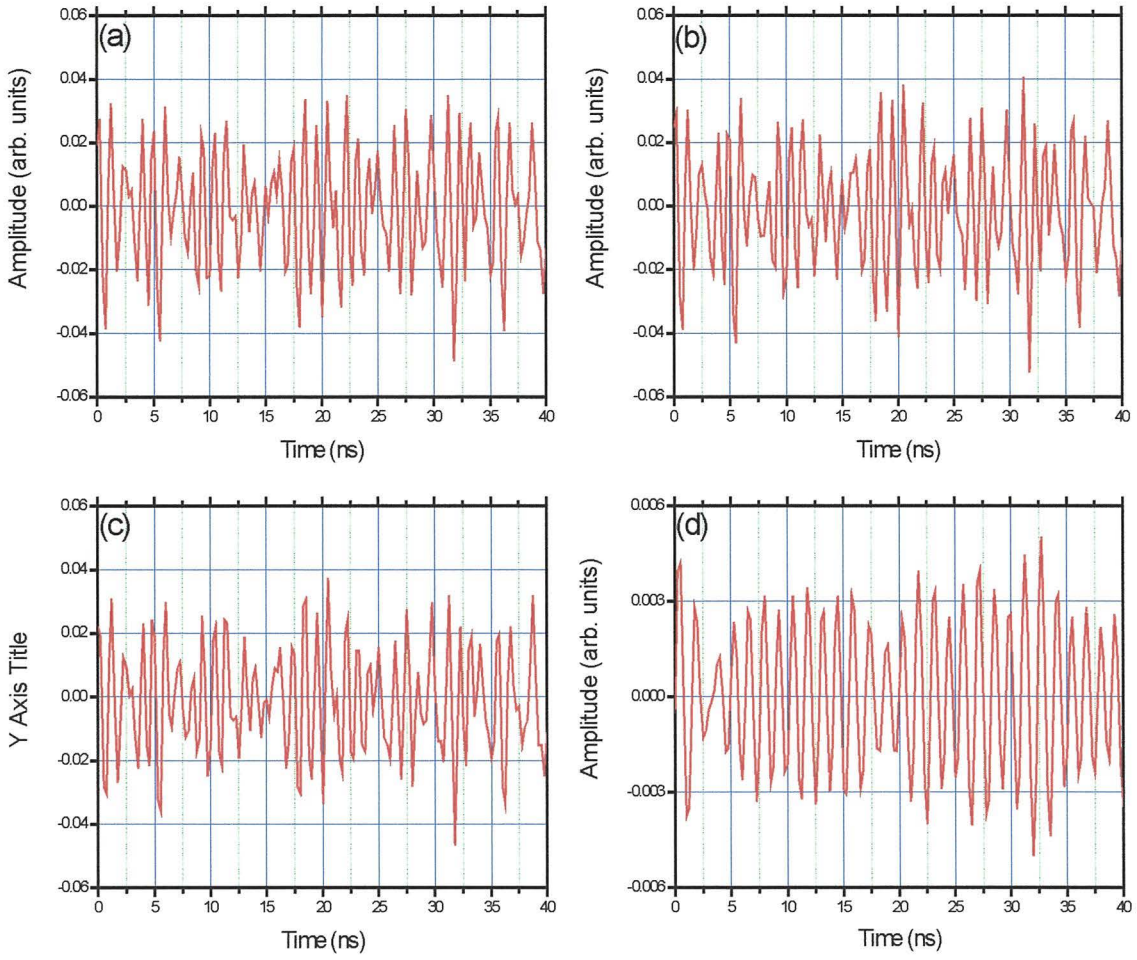

Figure 6.8: *Time traces of transmitter laser2 (6a), receiver laser (6b), decoder laser (6c) and recovered (680 MHz) message (6d)*

Figure 6.9 displays the corresponding FFT of the transmitter laser 2 (figure 6.9a), receiver laser (figure 6.9b), decoder laser (figure 6.9c), and recovered message (figure 6.9d). The frequency of the message (680 MHz) is hidden in the chaotic background of the spectrum of the three lasers, but is clearly visible in the spectrum of the recovered message. There is no crosstalk between the two communication channels because the frequency of the second message (510 MHz, hidden in the output of transmitter 1) does not appear in the spectrum of the recovered message.

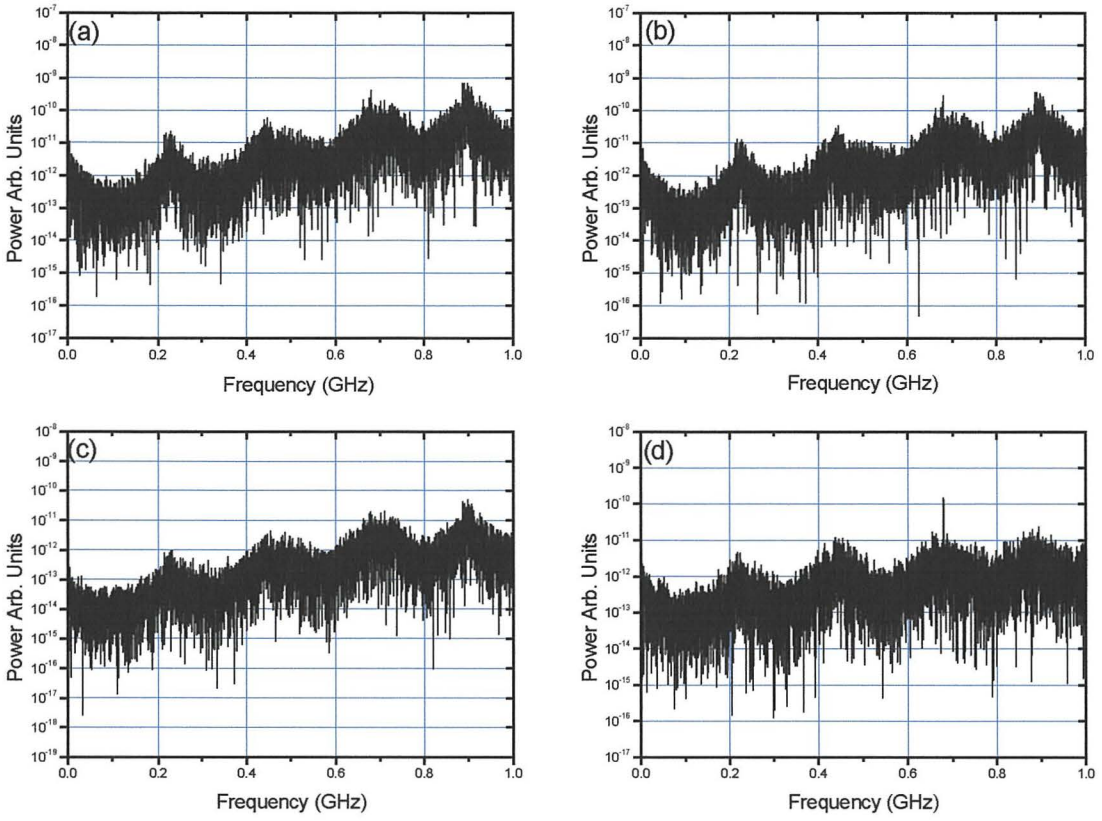

Figure 6.9: *FFT plots of transmitter laser (8a), receiver laser (8b), decoder laser (8c) and recovered (680 MHz) message (8d).*

6.4 Conclusions

It has been shown experimentally that two independent optical communication channels can be configured over a single transmission path using chaotic external-cavity diode lasers. The two channels (transmitter laser 1 – receiver laser, and transmitter laser 2 – receiver laser) are separated in wavelength, thus constituting a wavelength division multiplexing scheme. Each channel can be chaotically synchronised with virtually no interference from cross-talk between the channels. High-frequency messages can be transmitted through each channel and recovered with the use of a fourth, decoder laser. By choosing the external-cavity lengths in the

transmitter lasers related to the frequencies of the messages, the messages can be well masked by the external-cavity induced chaos.

While in previous experiments (demonstrated in chapter 4 and 5) the message is recovered by comparing the signal injected into the receiver laser and the output of the receiver laser, here use has been made of a decoder laser to extract the message. This was necessary in order to be able to extract different messages. The receiver and decoder lasers which are solitary lasers (without external-cavities) can be tuned independently to synchronise either with transmitter laser 1 or with transmitter laser 2. Comparing the output of the receiver and the decoder allows good message recovery. This result suggests that it could be possible to establish more than two chaotic channels in a single transmission path, but more work is required to determine the effects of crosstalk and the number of possible channels in such a scheme.

6.5 References

[1] H. G. Winful and L. Rahman, "Synchronized chaos and spatiotemporal chaos in arrays of coupled lasers," Phys, Rev. Lett., **65,** pp. 1575-1578 (1990)

[2] J. R. Terry, K. S. Thornburg, Jr., D. J. DeShazer, D. G. Vanwiggeren, S. Zhu, P. Ashwin, "Synchronization of Chaos in an Array of Three Lasers," Phys. Rev. E, **59**, (1999), pp. 4036-4043 (1999).

[3] Y. Liu and P. Davis, "Dual synchronisation of chaos," Phy. Rev. E, **61**, pp. R2176-R2179 (2000)

[4] A. Uchida, S. Kinugawa, T. Matsuura and S. Yoshimori, "Dual synchronisation of chaos in one-way coupled microchip lasers," Phys. Rev. E, 67, pp. 262201-262208 (2003)

[5] S. Sivaprakasam and K. A. Shore, "Cascade synchronisation of external-cavity laser diodes," Optics Lett. Vol. **26**, pp. 253-255, 2001

[6] J. Paul, S. Sivaprakasam and K. A. Shore, "Dual-channel chaotic optical communications using external-cavity semiconductor lasers," accepted for publication to J. Opt. Soc. Am

[7] J. Paul, S. Sivaprakasam, P. S. Spencer and K. A. Shore, "Optically modulated chaotic communication scheme using external-cavity length as a key to security," J. Opt. Soc. Am. B, **20**, pp. 497-503 (2003)

[8] G. D. VanWiggeren and R. Roy, "Communicating with chaotic lasers," Science, **279**, pp. 1198-1200 (1998).

Chapter 7

Conclusions and further work

7.0 Conclusions

This thesis has experimentally demonstrated the possibility of using synchronised chaotic semiconductor laser for secure optical communication systems.

In chapter 2 it was shown that optical feedback modifies the threshold and wavelength of semiconductor lasers and induces a variety of different dynamic regimes. The feedback effects depend on the external-cavity length and feedback strength (the feedback used in the experiments was incoherent and thus no phase influence was expected). It was also shown that optical feedback can induce multimode behaviour in otherwise single mode lasers. Also, it was shown that different lasers can operate at the same wavelength with similar threshold characteristics both with and without optical feedback and can be rendered chaotic with external-cavity optical feedback. The transient low-frequency-fluctuations turn-on dynamics to fully developed chaos (coherence collapse) was described in terms of the time-trace of the intensity fluctuations, and in terms of the time-resolved FFT power spectrum.

An experimental demonstration of synchronisation of chaotic semiconductor lasers was presented in chapter 3. It was shown that there are many operational parameters that affect the quality of synchronisation, such as the coupling strength, which was controlled with a coupling attenuator, and the detuning between the lasers, which was varied through the lasers drive currents and the lasers operating temperatures. Also, it was shown that there are several types of synchronisation that chaotic semiconductor lasers can experience: unidirectional synchronisation, mutual synchronisation, cascade synchronisation, and inverse synchronisation. It was shown that under certain operating conditions the receiver lasers dynamics may lead the dynamics of the transmitter laser, thereby anticipating the transmitter. This occurs when the lasers are mutually coupled and the transmitter laser is subjected to its own external-cavity feedback. A demonstration of cascade synchronisation has shown that three diode lasers may be chaotically synchronised in a cascade configuration. A particular configuration of the cascade scheme lead to nullified time of flight

synchronisation, in which the intensities of the transmitter and receiver lasers synchronise with no lag-time between them, due to a mediator laser that anticipates the transmitter. The work on nullified time of flight is based on a publication arising from the present research.

The possibility of encoding and decoding a message using chaotic transmitter and receiver lasers was demonstrated experimentally in chapter 4. Also the quality of message recovery for two different receiver set-up configurations was determined. A 1 GHz sinusoidal message was included in the transmitter laser output by direct modulation of its drive current. The message was transmitted through free-space to a receiver laser, which was identical to the transmitter laser and therefore synchronised with the chaotic dynamics but not with the message. By comparing the input and the output of the receiver laser good quality message-recovery was demonstrated. That work is based on a publication arising from the present research. Also a comparison was undertaken of the qualities of synchronisation and message decoding using closed-loop and open-loop schemes. In the open-loop scheme the receiver laser is subjected only to optical injection from the transmitter laser, while in the closed-loop scheme it also has external-cavity optical feedback. From the results, it was shown that the open-loop scheme has a better performance in terms of synchronisation and message recovery quality than the closed-loop scheme. The work on open-loop and closed-lop receivers is based on a publication arising from the present research

An experimental demonstration of the possibility of using the external-cavity length as a key to security was presented in chapter 5, which is based on a publication arising from the present research. It was shown that when the message is optically encoded it has to be of small amplitude to be effectively encoded into the chaotic output of the external-cavity transmitter laser. A large amplitude message can be detected through two lines in the synchronisation diagram (referred to as dual synchronisation). The external-cavity length was shown to be a key for increased security. This was done by carefully tuning the external-cavity length such that the chaotic dynamics generated in the transmitter laser effectively masks the frequency of the message. It was demonstrated by using a message laser rather than direct amplitude modulation of the transmitter laser that the input message into the systems transmitter can be optical rather than electronic. It was also demonstrated that this all-optical scheme is capable of masking, transmitting and recovering weak signals.

In chapter 6 an experimental demonstration of wavelength division multiplexing of chaotic lasers was presented. The chapter is based on a paper accepted for publication arising from the present research. In that research it was shown that two independent optical communication channels can be configured over a single transmission path using chaotic external-cavity diode lasers. The two channels (transmitter laser 1 – receiver laser, and transmitter laser 2 – receiver laser) are separated in wavelength, thus constituting a wavelength division multiplexing scheme. Each channel can be chaotically synchronised with virtually no interference from cross-talk between the channels. High-frequency messages can be transmitted through each channel and recovered with the use of a fourth, decoder laser.

7.1 Further work

This thesis opens many interesting lines of research for future work. A central issue is that of system security. It was shown in this thesis that the external-cavity length is a security key for the transmission of a sinusoidal message, however, the system security when a more realistic message (such as a high bit rate pseudo random bit stream) is transmitted requires further investigation. A second interesting line of future research is the analysis of the number of channels the system is capable of transmitting simultaneously in a wavelength division multiplexing scheme.

The wavelength division multiplexing scheme could be extended to include two masked message transmissions at the same frequency, but with a 90 degree difference in the plane of polarisation of their electric field. The two receiver lasers would be configured with their polarisation 90 degrees apart such that the plane of polarisation would allow individual chaotic synchronisation of each of the transmitter lasers.

This work could be extended to include experiments to determine the performance of VCSELs in a secure chaotic optical communications system.

Appendix A

Publications

Journal papers

[1] J. Paul, S. Sivaprakasam and K. A. Shore, "Dual-channel chaotic optical communications using external-cavity semiconductor lasers," J. Opt. Soc. America B, accepted for publication 2003

[2] M. W. Lee, J. Paul, S. Sivaprakasam and K. A. Shore, "Experimental determination of message decoding quality in optical chaos communications using laser diode transmitters," Optics Letters, accepted for publication 2003

[3] S. Sivaprakasam, J. Paul, P. S. Spencer, P. Rees and K. A. Shore, "Nullified time-of-flight lead-lag in synchronisation of chaotic external cavity laser diodes," Optics Letters, **28**, pp. 1397-1399, 2003

[4] J. Paul, S. Sivaprakasam, P. S. Spencer and K. A. Shore, "Optically modulated chaotic communication scheme using external-cavity length as a key to security," J. Opt. Soc. America B, **20**, pp. 497-503,2003

[5] J. Paul, S. Sivaprakasam, P. S. Spencer, P. Rees and K. A. Shore, "GHz bandwidth message transmission using chaotic diode lasers," Electron. Letts., **38**, pp. 28-29, 2002

Conference papers

[1] J. Paul, S. Sivaprakasam and K. A. Shore, "Wavelength division multiplexing of external-cavity chaotic semiconductor lasers," First 'Rio de la Plata' Workshop on Noise, Chaos and Complexity in Lasers and Nonlinear Optics Colonia del acramento, Uruguay, 1-5 December, 2003

[2] M. W. Lee, J. Paul and K. A. Shore, "Chaotic message broadcasting using DFB laser diodes," First 'Rio de la Plata' Workshop on Noise, Chaos and Complexity in Lasers and Nonlinear Optics Colonia del acramento, Uruguay, 1-5 December, 2003

[3] M. W. Lee, J. Paul, S. Sivaprakasam and K. A. Shore, "Experimental determination of message decoding quality in optical chaos communications using laser diode transmitters," First International Meeting on Applied Physics, (aphys2003), Badajoz, Spain, 14 October 2003

[4] M. W. Lee, J. Paul, S. Sivaprakasam and K. A. Shore, "Experimental determination of message decoding quality in optical chaos communications using laser diode transmitters," paper CEP1-6-THU (Postdeadline Paper) CLEO/EQEC, Munich , Germany, 23-27 June 2003

[5] S. Sivaprakasam, J. Paul, P. S. Spencer, P. Rees and K. A. Shore, "Concurrent synchronisation of chaotic external cavity laser diodes," SIOE'03, Cardiff, April 2003

[6] P. Rees, S. Sivaprakasam, P. S. Spencer, J. Paul, I. Pierce and K. A. Shore, "Chaotic data encryption using semiconductor laser diodes," SPIE, Photonics West, San Jose, CA, USA, paper 4995, 27 January 2003

[7] P. Rees, P. S. Spencer, I. Pierce, S. Sivaprakasam, J. Paul and K. A. Shore, "Bandwidth limitations of chaotic data encryption," SPIE, Opto-Ireland, Galway, Ireland, paper 4876-25, September 2002

[8] P. Rees, P. S. Spencer, I. Pierce, S. Sivaprakasam, J. Paul and K. A. Shore, "Bandwidth limitations of chaotic data encryption," SIOE 02, Cardiff, April 2002

[9] J. Paul, S. Sivaprakasam, P. S. Spencer and K. A. Shore, "Cavity length as a key to security in an all-optical external cavity chaotic communication scheme," SIOE 02, Cardiff, April 2002

[10] J. Paul, S. Sivaprakasam, P. S. Spencer and K. A. Shore, "Cavity length as a key to security in a chaotic optical communications system," paper 4283-45, Photonics West 2002, San Jose CA, USA, January 2002

[11] K. A. Shore, S. Sivaprakasam, E. M. Shahverdiev, P. S. Spencer, J. Paul, I. Pierce and P. Rees, " Synchronization regimes in chaotic semiconductor lasers," Indian Science Congress, Lucknow, India, January 2002 (Invited)

[12] J. Paul, S. Sivaprakasam, P. S. Spencer, P. Rees and K. A. Shore, "GHz bandwidth message transmission using chaotic diode lasers," paper K3, Experimental Chaos 2001, Potsdam, Germany, July 2001

[13] S. Sivaprakasam, J. Paul, P. S. Spencer and K. A. Shore, "Integrity of all-optical data encryption using chaotic external-cavity diode lasers," paper P38, Experimental Chaos 2001, Potsdam, Germany, July 2001

[14] S. Sivaprakasam, J. Paul, P. S. Spencer and K. A. Shore, "Eavesdropping in all-optical data encryption using chaotic external-cavity diode lasers," CLEO (Pacific Rim) Tokyo , Japan , July 2001

[15] S. Sivaprakasam, J. Paul, P. S. Spencer and K. A. Shore, "Integrity of all-optical data encryption using chaotic external-cavity diode lasers," SIOE 01, Cardiff April 2001

[16] J. Paul, S. Sivaprakasam, P. S. Spencer, P. Rees and K. A. Shore, "GHz bandwidth message transmission using chaotic diode lasers,", SIOE 01, Cardiff April 2001